Decadal White Papers on X-ray Science
DRAFT COMPILATION

Astro2010 Science White Paper (GCT)
Fundamental Accretion and Ejection Astrophysics

J. Miller, M. Nowak, P. Nandra, N. Brandt, G. Matt, M. Cappi, G. Risaliti, S. Kitamoto, F. Paerels. M. Watson, R. Smith, M. Weisskopf, Y. Terashima, Y. Ueda

Accretion Disks, Winds, and Jets

Disk accretion may be *the* fundamental astrophysical process. Stars and planets form through the accretion of gas in a disk. Black holes and galaxies co-evolve through efficient disk accretion onto the central supermassive black hole. Indeed, approximately 20% of the ionizing radiation in the universe is supplied by disk accretion onto black holes. And large-scale structures – galaxy clusters – are dramatically affected by the relativistic jets that result from accretion onto black holes. Yet, we are still searching for *observational* answers to some very basic questions that underlie all aspects of the feedback between black holes and their host galaxies:

- **How do disks transfer angular momentum to deliver gas onto compact objects?**
- **How do accretion disks launch winds and jets?**

X-rays probe disk accretion directly, in the region closest to the black hole itself. Leveraging this advantage into strong physical tests of accretion mechanisms, however, requires the ability to obtain excellent spectra on relevant orbital and even sub-orbital timescales. This, in turn, requires a combination of high spectral resolution and a large collecting area – the X-ray equivalent of the Keck telescopes or ESO Very Large Telescope. The jump in collecting area for high resolution spectroscopy from *Chandra* to IXO exceeds the jump from 2-4 meter to 8-10 meter optical telescopes. *With IXO, astrophysicists will be able to study the physics that drives disk accretion, and connections between disks, winds, and jets.*

Optical spectroscopy reveals that disks around pre-main sequence stars transfer matter onto the star, and angular momentum outward, partially though a magneto-centrifugal wind (Blandford & Payne 1982; Calvet, Hartmann, & Kenyon 1993). This means that poloidal magnetic field lines extend from the accretion disk, and that gas escapes along the field lines as the disk rotates. Far from the disk, such magneto-centrifugal winds may collimate into a jet (Blandford & Payne 1982). Moreover, the basic field structure necessary for such winds is essential for tapping the spin energy of the black hole itself to power Poynting jets (Blandford & Znajek 1977). There is strong *theoretical* support for common physics driving accretion onto pre-main sequence stars, and onto compact objects. At present, however, there are only tantalizing observational hints of this commonality (Mauche & Raymond 2000; Kraemer et al. 2005; Miller et al. 2006).

Chandra observations of Seyfert AGN and some quasars reveal disk winds in X-ray absorption, sometimes called "warm absorbers" (see, e.g., Kaspi et al. 2002, Blustin et al. 2005, Krongold et al. 2007). Observations of NGC 1365 have already sampled one distinct transit event (Risaliti et al. 2005, 2009). With IXO, absorption due to orbiting material will be seen to change as an absorber transits the face of the central engine. For instance, an absorber in a Keplerian orbit at 1000 GM/c^2 will take more than 30 ksec to cross the face of a central engine with a radius of 20 GM/c^2, for a 10^7 solar mass black hole. During the transit, absorption lines will shift by 400 km/s in total. Based on the X-ray absorption currently observed, IXO will detect a typical H-like O VIII line (for instance) and determine its velocity shift to high accuracy in just 5 ksec (see Figure 1), thus revealing the orbital transit. *The ability to observe orbital motion in disk-driven outflows will be revolutionary, placing black hole accretion on the same footing as stellar accretion and revealing details of angular momentum transfer, wind and jet production.*

To understand disk accretion is to understand a core aspect of feedback and the co-evolution of black holes and their host galaxies (e.g. Begelman, de Kool, & Sikora 1991, Silk & Rees 1998, Ciotti & Ostriker 2007). The disk winds seen in Seyfert AGN and some quasars are expected to move up to 10^8 solar masses of material during their active lifetimes (Blustin et al. 2005), and the main component of the mass and kinetic luminosity is only visible in the X-ray band. This gas amounts to the dominant source of hot interstellar material in many galactic bulges. Moreover, surveys show that AGN tend to show evidence for recent episodes of star formation (Kauffmann et al. 2003), and outflows from AGN may contribute to this process through shocks (Crenshaw & Kraemer 2000).

Accretion onto stellar-mass black holes and neutron stars provides an important point of comparison. Although single transits cannot be observed with IXO, for sources as bright as 10^{-9} erg/cm^2/s, detailed absorption spectra can be obtained on timescales corresponding to Keplerian orbits at just 200 GM/c^2. Changes in disk winds can be tracked precisely in stellar-mass systems, including black holes and neutron stars. Lines are stronger in some white dwarf systems, meaning that lower flux levels can be reached.

The fundamental accretion exploration described here can be conducted in at least 20 AGN. Generous integrations of 100 ksec each will only require 2 Msec – a low fraction of the IXO observing budget over 5 years. (This work can be done *simultaneously* with explorations of General Relativity using relativistic disk lines.) In a 5-year mission, 5 transient stellar-mass black holes, 5 transient neutron stars, 30 persistent neutron stars, and 30 white dwarfs can be studied. With modest integrations of 30 ksec, only 2.1 Msec will be required to build a stellar-mass sample for comparison with AGN and optical/IR observations of pre-main sequence stars.

It is worth noting that accretion studies with IXO will tap a deep discovery space, fortuitously supported by a golden age in accretion theory. Simulations of accretion disks and outflows are advancing rapidly, as computational power grows and becomes widely available. Around the world, a rapidly increasing number of research groups are producing disk simulations that will test analytical work and make new predictions (see, e.g., Balbus & Hawley 1991, Miller & Stone 2000, Proga 2003, Gammie 2004, Anderson et al. 2005, Blaes et al. 2006, Hawley, Beckwith, & Krolik 2007, McKinney & Blandford 2008). The crystal spectrometer that flew aboard *Einstein* inspired the calculation of X-ray line parameters (see, e.g., Kallman & McCray 1982) that later provided a rich and essential resource when *Chandra* and *XMM-Newton* launched with the first dispersive X-ray spectrometers. Current accretion disk simulations - and those conducted in the next 10 years - will provide a similar framework for understanding IXO observations of disk accretion onto compact objects.

Starving Black Holes

Active accretion phases are short-lived (e.g. Martini 2003, Hopkins et al. 2005; see Figure 2). A full understanding of the co-evolution of black holes and galaxies, then, requires that we understand how black holes interact with their local environments when mass only accretes at low fractions of the Eddington limit (10^{-4}, and below). Advanced theoretical studies of galaxy evolution suggest that *even within such "quiet" phases, feedback from black holes is required to match the observed colors of galaxies* (e.g. Croton et al. 2006). Robust physical arguments and simple observations show that a standard thin accretion disk cannot be the driving force when rates of mass transfer are very low. However, owing to the low luminosity of inefficient accretion and to the limited mirror area of current missions, astrophysicists are left to ask:

- **What is the fate of gas falling onto a black hole at a low rate?**

In the simplest terms, we do not know if gas remains bound to a black hole at low accretion rates. The paradigm for accretion onto black holes at low rates of mass transfer is that radiation is trapped within the flow, and *advected* across the event horizon with the gas (see, e.g., Narayan & Yi 1994). However, an independent treatment of the problem gives a very different answer: most accreting gas *must* be driven away in a wind due to viscous heating (Blandford & Begelman 1999). Winds are detected through line spectroscopy, and the temperatures and sizes of advective flows are revealed through emission lines. Current missions lack the sensitivity needed to detect lines. The high collecting area of IXO, its energy broad energy range, and superior instrumental capacities mean that astrophysicists will finally be able to make paradigm-testing observations of the accretion modes that dominate the lifetimes of black holes and their host galaxies.

The specific example of a modest survey can help to illustrate the major progress that improved spectroscopy will make. Stellar dynamics and gas dynamics have been used to constrain the mass of black holes in approximately 40 nearby galaxies. These black holes are the basis of the well-known M-sigma relationship between black hole mass and velocity dispersion (see, e.g., Tremaine et al. 2002). These galaxies generally lie within 30 Mpc, and most of the black holes have X-ray luminosities of 10^{40} erg/s or less. Investigating black holes with known masses would be particularly expedient, as accretion flow properties can be studied as a function of Eddington luminosity.

In exposures of 100 ksec or less, IXO can detect line spectra from each of these black holes, even if the plasma is extremely hot (up to 10^9 Kelvin) and line-poor (see Figure 3). A wealth of physical information will be available for the first time: line ratios can be used to measure plasma temperatures, line strengths can be used to estimate the size of the accretion flow (Narayan & Raymond 1999), and line shifts will indicate whether gas is bound to the black hole. Within the context of this example survey, the nature of the flows can be determined as a function of black hole mass, mass accretion rate, and a host of feedback parameters such as the star formation rate.

Galactic compact objects will provide an important point of comparison. Transient Galactic sources evolve through orders of magnitude in mass accretion rate and luminosity. If, for instance, gas is bound to black holes at low accretion rates but mostly lost in a wind at *very* low accretion rates, this evolution can be revealed through IXO observations of transient Galactic sources. In a given year, several stellar-mass black hole and one neutron star transients can be expected to go into outburst and then decay. By also observing neutron star transients, the role of a hard stellar surface (versus an event horizon) in shaping accretion and outflows can also be addressed. For both black holes and neutron stars at typical distances, a 100 ksec IXO observation can detect line spectra at source luminosities of 10^{-6} Eddington, and below.

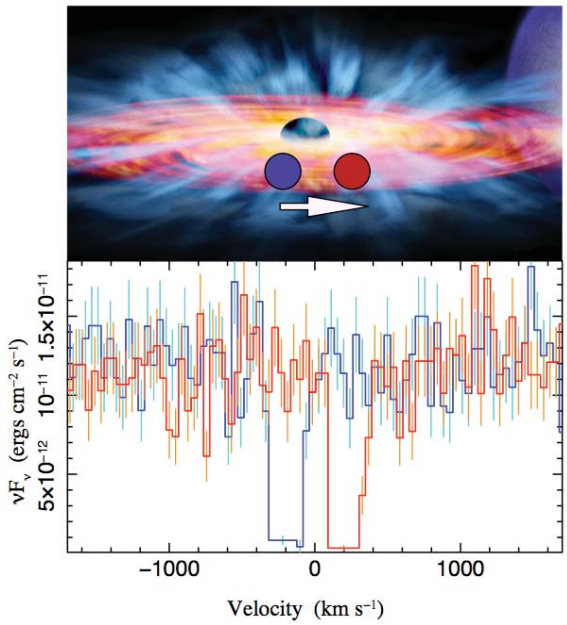

Figure 1: Strong tests of accretion physics become possible when orbital motion can be detected. IXO has the sensitivity to detect Doppler shifts in orbiting winds that can carry away angular momentum and permit disk accretion in Seyfert AGN. The figure above shows O VIII absorption lines with expected Doppler shifts from simulated 5 ksec observations of a transit with IXO.

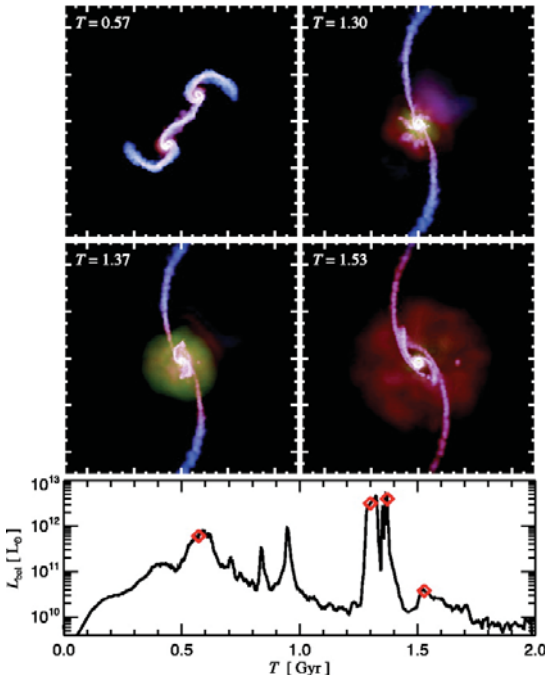

Figure 2: New simulations of galaxy mergers show that merger activity drives episodes of active accretion onto supermassive black holes. As shown above, active episodes are brief (Hopkins et al. 2005). To match the galaxy colors, however, the black hole must still exert influence on its host galaxy during inactive periods. The superior spectral resolution and collecting area of IXO will make it possible to reveal the physics of accretion onto supermassive black holes at low rates of mass transfer.

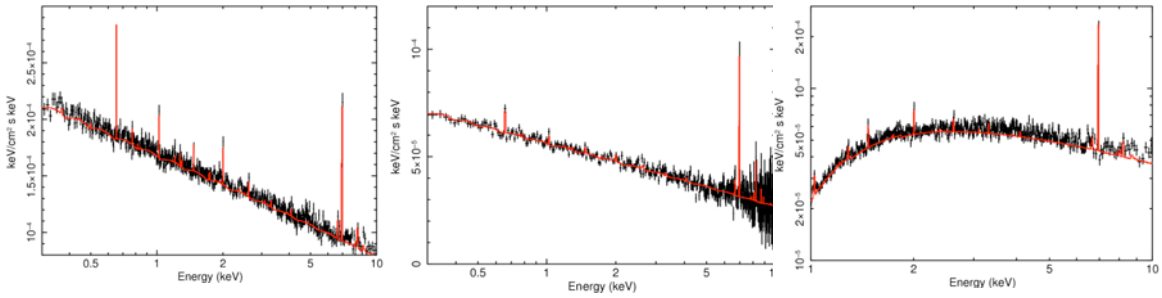

Figure 3: IXO will be able to detect lines from hot (50-100 keV) plasmas in a broad range of black holes, including those in nearby galaxies such as M87 (left), NGC 4143 (center), and stellar-mass black holes in the Milky Way such as V404 Cyg (right). With line spectra, paradigms for accretion onto black holes at low mass transfer rates can finally be tested.

References

Anderson, J. M., et al., 2005, ApJ, 630, 945
Balbus, S. A., & Hawley, J. F., 1991, ApJ, 376, 214
Begelman, M., de Kool, M., & Sikora, M., 1991, ApJ, 382, 416
Blaes, O. M., et al., 2006, ApJ, 645, 1402
Blandford, R. D., & Begelman, M., 1999, MNRAS, 303, L1
Blandford, R. D., & Payne, 1982, MNRAS, 199, 833
Blandford, R. D., & Znajek, R. L., 1977, MNRAS, 179, 433
Blustin, A., et al., 2005, A&A, 431, 111
Calvet, N., Hartmann, L., & Kenyon, S., 1993, ApJ, 402, 623
Ciotti, L., & Ostriker, J. P., 2007, ApJ, 665, 1038
Crenshaw, D., & Kraemer, S., 2000, ApJ, 542, 247
Croton, D. J., et al., 2006, MNRAS, 365, 11
Gammie, C. F., 2004, ApJ, 614, 309
Hawley, J. F., Beckwith, K., & Krolik, J. H., 2007, Ap&SS, 311, 117
Hopkins, P. F., et al., 2005, ApJ, 630, 705
Kallman, T. R., & McCray, R., 1982, ApJS, 50, 263
Kaspi, S., et al., 2002, ApJ, 574, 643
Kauffmann, G., et al., 2003, MNRAS, 346, 1055
Kraemer, S. B., et al., 2005, ApJ, 633, 693
Krongold, Y., et al., 2007, ApJ, 659, 1022
Martini, P., 2003, in "The Coevolution of Black Holes and Galaxies", ed. L. Ho, Cambridge Press
Mauche, C. W., & Raymond, J. C., 2000, ApJ, 541, 924
McKinney, J. C., & Blandford, R. D., 2009, MNRAS, submitted.
Miller, J. M., et al., 2006, Nature, 441, 953
Miller, K. A., & Stone, J. M., 2000, 534, 938
Narayan, R., & Yi, I., 1994, ApJ, 428, L13
Narayan, R., & Raymond, J. C., 1999, ApJ, 515, L69
Proga, D., 2003, ApJ, 585, 406
Risaliti, G., et al., 2005, ApJ, 630, L129
Risaliti, G., et al., 2009, ApJ, in press, arxiv:0901:4809
Silk, J., & Rees, M., 1998, A&A, 331, 1
Tremaine, S., et al., 2002, ApJ, 574, 740

Astro2010 Science White Paper (SSE)
Stellar-Mass Black Holes and Their Progenitors

J. Miller, Uttley, Nandra, Barret, Matt, Paerels, Mendez, Diaz, Cappi, Kitamoto, Nowak, Wilms, Rothschild, Smith, Weisskopf, Terashima, Ueda

If a black hole has a low spin value, it must double its mass to reach a high spin parameter (Volonteri et al. 2005). Although this is easily accomplished through mergers or accretion in the case of supermassive black holes in galactic centers, it is impossible for stellar-mass black holes in X-ray binaries. Thus, the spin distribution of stellar-mass black holes is almost pristine, largely reflective of the angular momentum imparted at the time of their creation. This fact can help provide insights into fundamental questions:

- **What is the nature of the central engine in supernovae and gamma-ray bursts?**
- **What was the spin distribution of the first black holes in the universe?**

Optical depth effects make it difficult to directly probe the central engines in supernovae (SNe) and gamma-ray bursts (GRBs). Especially in the case of GRBs, we only see the surface of last scattering in a highly relativistic jet, far from the black hole that is created through the collapse of a massive star, the merger of two neutron stars, or the merger of a neutron star and a black hole. However, the angular momentum of the black hole remnant is an important clue that can greatly aid in efforts to reverse-engineer the most powerful explosions in the universe (Heger et al. 2002, Nomoto et al. 2003, Gammie et al. 2004, Woosley & Heger 2006). **Do all explosions put equal energy into black hole spin? Does spin power the jets in GRBs?**

Similarly, understanding the spin of natal black holes in the early universe is extremely important. Spinning black holes convert accretion energy into radiation more efficiently, for instance, and would have supplied young host galaxies with more ionizing radiation that could impact star formation. While it is presently unclear whether a single massive black hole formed in early galaxies, or if a supermassive black hole was built out of the merger of many intermediate-mass black holes resulting from Population III stars, ***stellar-mass black holes represent our best opportunity for understanding the distribution of spins that result from a single collapse event.***

It is possible that many factors play into determining how much angular momentum is imparted to a black hole formed in a SNe or GRB. However, fundamental properties such as the mass and and the angular momentum of the progenitor star must be important (Heger et al. 2002, Woosley & Heger 2006). The most sophisticated treatment of this problem suggests that single collapse events should create black hole with spins of a = 0.75-0.90 (Gammie et al. 2004), where $a = cJ/GM^2$. Presently, only a limited number of observations have obtained data that can be used to constrain the spin of stellar-mass black holes. The most complete study to-date only includes eight black holes (Miller et al. 2009); Figure 1 plots the resulting distribution, and includes two additional results. This modest histogram is the result of using relativistic disk lines and disk reflection spectra to constrain black hole spin. Clearly, to make a strong test of the theoretical prediction above, to provide a strong observational grounding for the nature of SNe/GRB central engines, and to understand the first black holes, the number of spin measurements must increase by an order of magnitude.

IXO represents the best means of obtaining the greatest number of new black hole spins because it offers 5 independent means of measuring spin: relativistic disk lines, the disk continuum, high frequency quasi-periodic oscillations, polarimetry, and studies of X-ray reverberation.

Relativistic Disk Lines

Irradiation of the accretion disk by hard X-rays produces emission lines and a characteristic disk reflection spectrum (for a review, see Miller 2007). The most prominent line is typically Fe K, due to the abundance and fluorescence yield of iron. The disk reflection spectrum is typified by an apparent flux excess peaking between 20-30 keV, which is actually due to Compton back-scattering. Relativistic Doppler shifts and gravitational red shifts endemic to the inner disk around black holes act to skew the shape of disk lines and the reflection spectrum. The shifts grow more extreme with increasing black hole spin, as the innermost stable circular orbit (ISCO) extends closer to the black hole. The clear imprints of special and general relativity on the line profile are thus used to measure black hole spin. Because the line shifts scale with gravitational radii (GM/c^2), the mass of a given black hole and its distance are not needed to measure its spin using this technique.

Relativistic disk lines are common in Seyfert AGN (e.g. Brenneman & Reynolds 2006, Miniutti et al. 2007), in stellar-mass black holes (Miller 2007; Miller et al. 2009), and even in the spectra of accreting neutron stars (Bhattacharyya & Strohmayer 2007, Cackett et al. 2008). A separate white paper describes how IXO spectroscopy can measure spin in 300 AGN and thereby constrain galaxy merger and accretion histories – important aspects of the coevolution of black holes and host galaxies. ***The commonality of disk lines permits comparisons of the relativistic regime around compact objects across a factor of 10^6 in mass.***

IXO is ideally suited to measuring spin in stellar-mass black holes using relativistic disk lines and disk reflection, owing to the spectral resolution of the X-ray microcalorimeter spectrometer (XMS) and the flux and timing capabilities of the high time resolution spectrometer (HTRS). Figure 2 illustrates the relationship between spin, the ISCO, and relativistic disk lines.

The Accretion Disk Continuum

Thermal continuum emission from the accretion disk may be used to measure the spin of stellar-mass black holes. An accretion disk around a spinning black hole is expected to be hotter and more luminous than a disk around a hole with low spin, because the ISCO is deeper within the gravitational potential (see Figure 3). New spectral models have recently been developed that exploit these changes in the shape of the continuum to measure spin (Davis et al. 2005, Li et al. 2005). If the mass and distance to a black hole are known, these models may be applied to spectra in order to measure the spin of a stellar-mass black hole (see, e.g., McClintock et al. 2006, Shafee et al. 2006). By virtue of their sensitivity and spectral resolution, the XMS and HTRS aboard IXO are both well suited to measuring black hole spins using the disk continuum.

X-ray Quasi-Periodic Oscillations

The X-ray flux observed from black hole X-ray binaries is sometimes modulated at a frequency commensurate with Keplerian motion at the ISCO. The oscillations are not pure, but rather have a small width due to small variations in frequency and phase jumps – as expected for gas orbiting in a real fluid disk with internal viscosity. Observed frequencies follow a 1/M scaling (Remillard & McClintock 2006; see Figure 4), strongly suggesting a relativistic origin. Indeed, frequencies are sometimes observed in a 3:2 frequency ratio, consistent with parametric resonances in GR (Abramowicz & Kluzniak).

A few models are able to account for the frequencies observed; all of them require GR and each points to a high spin value when QPOs are observed in a 3:2 frequency ratio (see Figure 4). The

large collecting area of IXO, combined with the energy range and time resolution of the HTRS, make IXO an apt next-generation X-ray timing mission. New detections of X-ray QPOs in black holes will yield new spin measurements and will elucidate the details of the modulations.

X-ray Polarimetry

Thermal X-ray emission from the accretion disc is likely to be significantly polarized. In the case of Newtonian gravitation, symmetry considerations demand that disk emission can only be parallel or perpendicular to the disk. Strong gravity effects distinctively modify the polarization properties, causing the polarization angle to appear rotated to the distant observer. The rotation is larger at smaller radii, where the disc temperature is higher, giving a unique energy dependence of the polarization angle (Stark & Connors 1977; Dovciak et al. 2008; Li et al. 2009). The degree of this dependence is related to the spin of the black hole. The plots in Figure 5 illustrate how IXO can measure black hole spin based on the polarization of thermal emission from the disk.

X-ray Reverberation

Measuring the light travel time between flux variations in the hard X-ray continuum and the lines that it excites in the accretion disk provides a model-independent way to measure black hole spin. The time delay simply translates into distance for a given geometry. If a black hole has a low spin parameter, iron emission lines in the 6.4-6.97 keV range should have a characteristic lag of approximately 6 GM/c^3; if the black hole is rapidly spinning, lags can be as short as 1 GM/c^3.

Close to spinning black holes, the path light takes will be strongly impacted by spacetime curvature. When very close to the black hole, an otherwise isotropic source of hard X-ray emission will have its flux bent downward onto the disk. An observable consequence of these light-bending effects is a particular non-linear relationship between hard X-ray emission and iron emission lines (Miniutti & Fabian 2004). At present, there is tantalizing evidence for this effect in some Seyfert AGN (e.g. Miniutti, & Fabian 2004, Ponti et al. 2006) and stellar-mass black holes (e.g. Rossi et al. 2005).

The IXO HTRS has the time resolution, broad energy range, energy resolution, and flux tolerance needed to make careful studies of lags that can lead to spin measurements and clear detections of gravitational light bending. A study of the lags that can be detected with the HTRS is shown in Figure 6. The extraordinary sensitivity of this instrument will enable errors of less than 1 GM/c^3 for fluxes of approximately 1 Crab.

Extending Our Reach with IXO

The distribution of stellar-mass black hole spins represents a rare and vital window on the central engines in SNe and GRBs and the first black holes in the universe. Is it the degree of angular momentum imparted to the black hole that separates SNe and GRBs? How much ionizing flux were the first black holes able to supply to young host galaxies? Current X-ray observatories are beginning to measure spin parameters in a small number of sources. The variety of techniques open to observers with IXO provides the best means of obtaining the greatest possible number of spin measurements. Moreover, the sensitivity of IXO will make it possible to obtain spin measurements in faint Galactic sources that are beyond the reach of current missions, and make it possible to obtain spin measurements in bright stellar-mass black holes in nearby galaxies. IXO will increase the number of current spin measurements by an order of magnitude, revealing the nature of the central engine in GRBs and SNe, and the nature of the first black holes to inhabit young galaxies at high redshift.

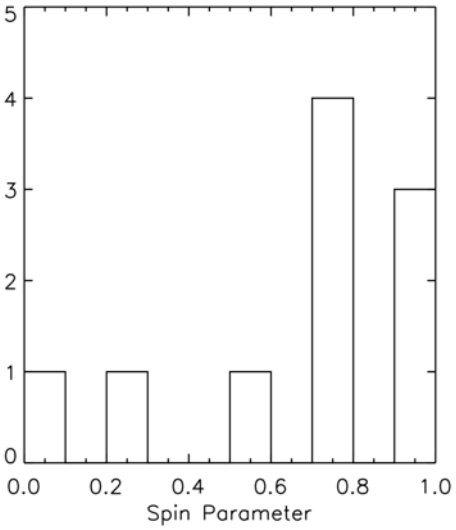

Figure 1: The histogram above shows a distribution of 10 black hole spins, measured using relativistic iron emission lines from the accretion disk (Miller et al. 2009, Reis et al. 2009, Blum et al. 2009). IXO will increase the number of stellar-mass black hole spin measurements by an order of magnitude, providing a unique window on the central engine in SNe and GRBs.

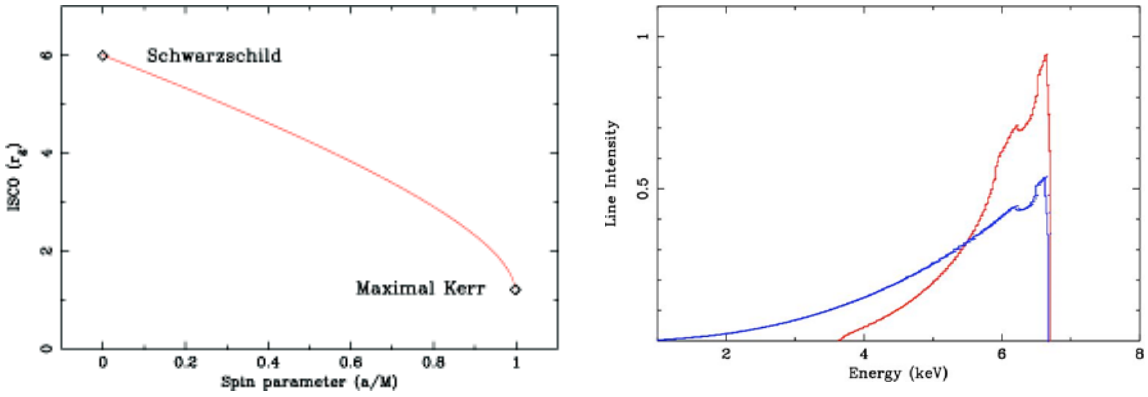

Figure 2: *Left*: Black hole spin can be measured by determining the innermost stable circular orbit of an orbiting accretion disk. All methods of determining spin that utilize the disk rely on this relation shown here. *Right*: the line profile in red is expected around a zero-spin Schwarzschild black hole; the more skewed line in blue is expected around a maximal-spin Kerr black hole. IXO will be able to reveal relativistic imprints on lines in sharp detail.

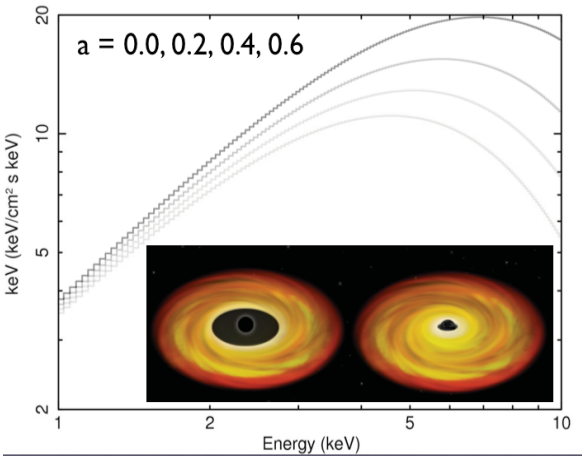

Figure 3: With increasing spin, thermal continuum emission from an accretion disk will become hotter and more luminous, because the ISCO moves closer to the black hole. The IXO XMS and HTRS are extremely well suited to measuring stellar-mass black hole spins using disk continua.

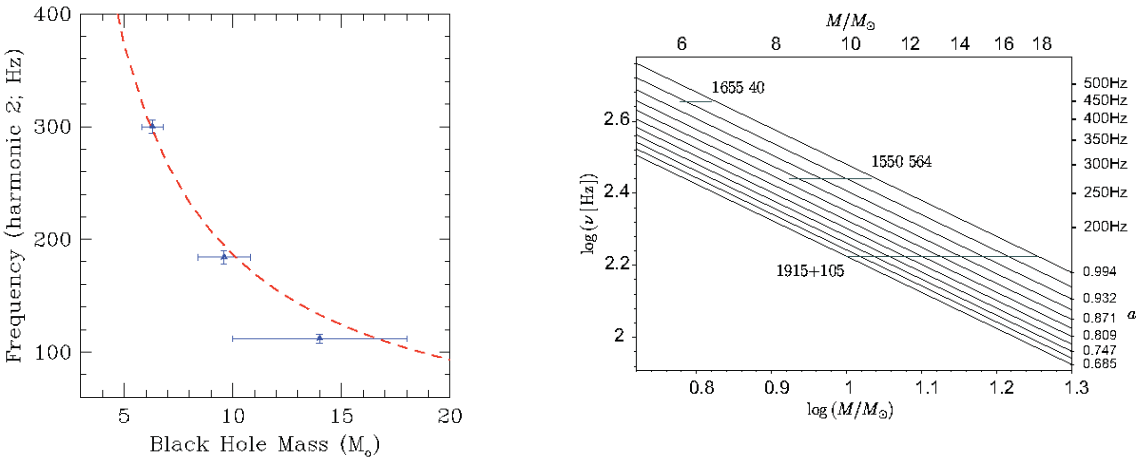

Figure 4: *Left*: High frequency QPOs in black hole X-ray binaries are consistent with a 1/M scaling, indicating a relativistic origin (Remillard & McClintock 2006). *Right*: The plot shown depicts QPO frequency (the upper frequency in a 3:2 resonance ratio) versus black hole mass. Parametric resonance models for the QPOs seen in a 3:2 frequency ratio are plotted over the data (Abramowicz & Kluzniak 2004). The IXO HTRS is designed to detect high frequency signals like these.

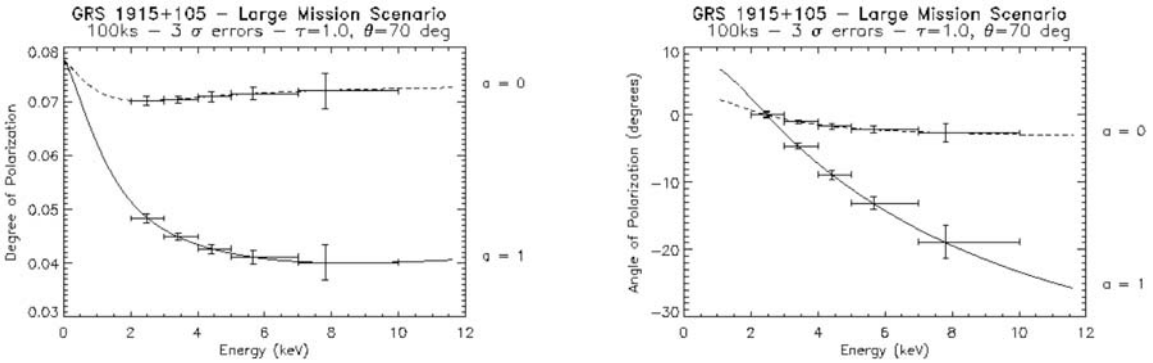

Figure 5: The plots above illustrate how the degree of polarization and angle of polarization differ for disks around a non-spinning (a=0) and maximally spinning (a = 1) black hole (Dovciak et al. 2008). IXO will fly a sensitive X-ray polarimeter that can use these signatures to measure spin in stellar-mass black holes. The plots above depict the results expected from a 100 ksec observation.

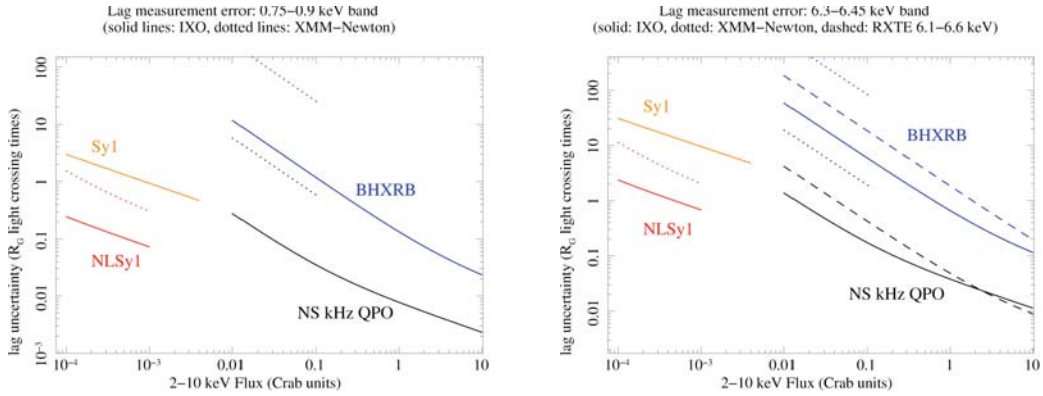

Figure 6: The IXO HTRS will be able to detect lags commensurate with the very shortest length scales around compact objects of all masses. This ability will provide another means of measuring black hole spin parameters. The left panel shows figures of merit for the Fe L range, and the right panel shows figures of merit for the Fe K band. In each plot, the uncertainty in the lag between the continuum and band of interest (in units of GM/c^3) is plotted versus source flux, for a variety of source types.

References

Abramowicz, M., Kluzniak, W., 2004, AIPC, 714, 21
Bhattacharyya, S., & Strohmayer, T., 2007, ApJ, 666, L85
Blum, J. L., et al., 2009, ApJ, subm.
Brenneman, L., & Reynolds, C. S., 2006, ApJ, 652, 1028
Cackett, E., et al., 2008, ApJ, 674, 415
Davis, S., et al., 2005, ApJ, 621, 372
Dovciak, M., et al., 2008, MNRAS, 391, 32
Gammie, C. F., Shapiro, S. L., & McKinney, J. C., 2004, ApJ, 602, 312
Heger, A., Woosley, S., Baraffe, I., & Abel, T., 2002, in "Lighthouses of the Universe", ed. M. … Gilfanov, R. Sunyaev, E. Churazov, Springer-Verlag
Li, L., et al., 2005, ApJS, 157, 335
Li, L., Narayan, R., & McClintock, J., 2009, ApJ, 691, 847
McClintock, J., et al., 2006, ApJ, 652, 518
Miller, J. M., 2007, ARA&A, 45, 441
Miller, J. M., et al., 2009, ApJ, in press
Miniutti, G., & Fabian, A. C., 2004, MNRAS, 349, 1435
Miniutti, G., et al., 2007, PASJ, 59, S315
Nomoto, K., et al., 2003, in "Stellar Collapse", ed. C. L. Fryer, Kluwer Press
Ponti, G., et al., 2006, AN, 327, 1055
Reis, R. C., et al., 2009, MNRAS, in press
Remillard, R., & McClintock, J., ARA&A, 44, 49
Rossi, S., et al., 2005, MNRAS, 360, 763
Shafee, R., et al., 2006, ApJ, 636, L113
Stark, R., & Connors, P., 1977, Nature, 266, 429
Volonteri, M., Madau, P., Quataert, E., & Rees, M. J., 2005, ApJ, 620, 69
Woosley, S., & Heger, A., 2006, ApJ, 637, 914

Astro2010 White Paper

Formation of the Elements

Primary Author:

John P. Hughes
Rutgers University
Phone: 732-445-5500 x 0980
e-mail: jph@physics.rutgers.edu

Contributing Authors and Supporters:

Carlos Badenes	Princeton University
Aya Bamba	ISAS, Japan
William Blair	Johns Hopkins University
Anne Decourchelle	CEA, Saclay, France
Daniel Dewey	Massachusetts Institute of Technology
Christopher Fryer	Los Alamos National Lab
Una Hwang	NASA/Goddard Space Flight Center
J. Martin Laming	Naval Research Lab
Ken'ichi Nomoto	University of Tokyo
Sangwook Park	Pennsylvania State University
Daniel Patnaude	Harvard-Smithsonian Center for Astrophysics
Paul Plucinsky	Harvard-Smithsonian Center for Astrophysics
Lawrence Rudnick	University of Minnesota
Patrick Slane	Harvard-Smithsonian Center for Astrophysics
F-K. Thielemann	University of Basel
Jacco Vink	Utrecht University
P. Frank Winkler	Middlebury College

Submitted to the Stars and Stellar Evolution and The Galactic Neighborhood panels

February 2009

Overview

The theoretical understanding of cosmic nucleosynthesis obtained by astrophysicists over the last century surely ranks as one of the great accomplishments of science. In general, however, this theory has been tested largely against ensemble-averaged measurements, such as the relative abundance distribution of the elements in various environments (e.g., solar), the atmospheres of stars, and so on. Nucleosynthesis is a rich, complex field that involves many disparate processes operating in different environments and at different phases of stellar evolution. Observational tests of specific model components, especially of the most energetic processes, are woefully lacking. In particular, the processes that produce Fe and Fe-group elements and eject them into the interstellar medium during the explosions of both core collapse and thermonuclear supernovae (SNe) are among the most poorly tested parts of the entire nucleosynthesis picture. X-ray studies of young supernova remnants (SNRs) can provide critical tests of the nucleosynthesis picture especially as regards the production of Fe and Fe-group elements in specific individual examples of core-collapse and thermonuclear SNe. In addition since the production of Fe and Fe-group elements is at the heart of these explosions, they offer critical insights into the explosion processes in SNe. The key astrophysical question that this white paper addresses is

How do supernovae explode and create the iron group elements?

In the following we first describe the state-of-the-art in this research area based on *Chandra*, *XMM-Newton*, and other existing X-ray facilities, before moving on to demonstrate the enormous potential of the *International X-ray Observatory* (IXO) to enable compelling science across a broad range of core questions in nucleosynthesis and SN physics.

Background

Core collapse (CC) SNe make up roughly three-quarters of all observed SNe. They come from stars more massive than $8M_{\odot}$ and from a nucleosynthetic point of view are the dominant producers of O, Ne, and Mg, although they do produce a broad spectrum of elemental species including the Fe-group. They leave compact remnants in the form of neutron stars or black holes, while their gaseous remnants tend to be highly structured with dense optically-emitting knots and typically more diffuse X-ray features. It is known that the precipitating event for a CC SNe is the collapse of a stellar core, but the process whereby the core rebounds and ejects the rest of the star is still poorly understood with at least two competing ideas currently in vogue: neutrino-driven convection (e.g., Herant et al. 1994; Burrows, Hayes, & Fryxell 1995; Kifonidis et al. 2000), including in its latest development the instability of the stalled shock (e.g., Blondin & Mezzacappa 2006; Foglizzo, Scheck & Janka 2006; Burrows et al. 2007; Scheck et al. 2008); and jet-induction (e.g., Khokhlov et al. 1999). It is also the case that at present nucleosynthesis predictions still rely on spherically symmetric models with an assumed neutron star/black hole "mass cut" (e.g., Woosley & Heger 2007).

The other main class of SNe are the thermonuclear or Type Ia SN (SN Ia). These make up roughly one-quarter of all SNe and are widely believed to result from the total incineration of a carbon-oxygen white dwarf that grows close to the Chandrasekhar mass.

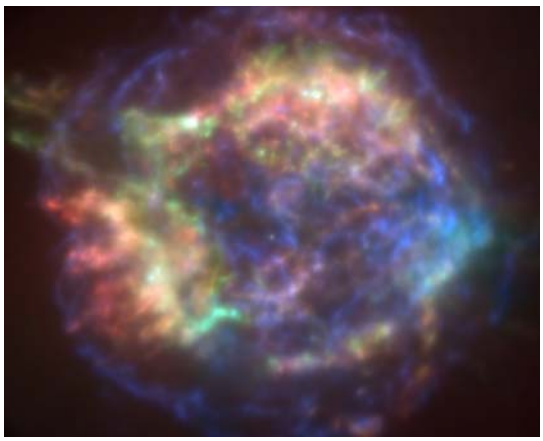

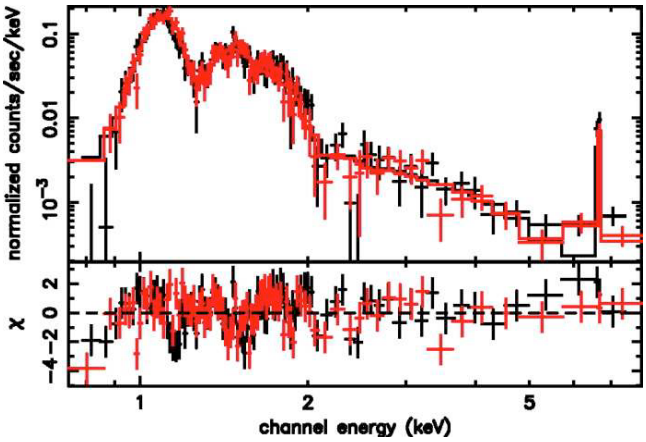

Figure 1–(Left) Color-coded X-ray image of Cas A: red corresponds to Fe L emission, green to Si K emission, and blue to 4-6 keV continuum emission. This is derived from the *Chandra* observations after smoothing with the IXO point-spread-function.
Figure 2–(Right) *Chandra* spectrum of a nearly pure Fe knot from the eastern limb of Cas A. The broad bumps at energies between 1 and 2 keV are the unresolved complex of Fe L-shell lines; the Fe K-shell emission appears at 6.5 keV. No lines from lower-Z species are present.

How the star increases its mass is unknown; single degenerate scenarios where the white dwarf accretes matter from a normal-star companion in a binary and double degenerate scenarios where two white dwarfs coalesce are the two favored possibilities. During the explosion about half of the star's mass is converted to ^{56}Ni which decays to stable ^{56}Fe. Even with hundreds of well-observed type Ia SNe and the intense focus of the theoretical community over the past 15 years, the SN Ia explosion process, i.e., how nuclear ignition occurs and the subsequent burning proceeds, remains an unsolved problem (e.g., Röpke & Bruckschen 2008; Jordan et al. 2008). Models that most successfully reproduce optical spectra of SNe Ia essentially parameterize the speed of the burning front through the star (e.g., Iwamoto et al. 1999).

We submit that understanding the synthesis of the Fe-group elements in SNe is the key to understanding these explosions. In CC SNe, Fe comes from the innermost parts of the exploding star; it is the ejected matter that has been subjected to the highest temperatures and the most extreme conditions in the rebounding core. In SN Ia, nucleosynthesis *is* the explosion (i.e., it provides the energy to unbind the star). Indeed since the optical light from these SNe has its origin in the radioactive species produced by the explosive nuclear burning, the cosmologically relevant observations of optical light curves of SN Ia rest directly on the amount and composition of the Fe-group ejecta.

X-ray studies of SNRs are an essential part of this scientific investigation. X-ray emission is optically thin (except, possibly, for a few of the strongest resonance lines) so the gaseous remnants of SNe offer a comprehensive three-dimensional view of the ejecta; this is impossible to obtain on any individual SN event, for which we sample a single line-of-sight. Light echoes (now detected from Cas A, Tycho, and SNR 0509−69.0 in the LMC) provide definitive SN typing and in some cases sub-typing, so that individual SNRs become as useful as any individual SN to probe nucleosynthesis and explosion mechanisms. Of course a nearby SN, like SN 1987A, will offer a wealth of new opportunities for scientific

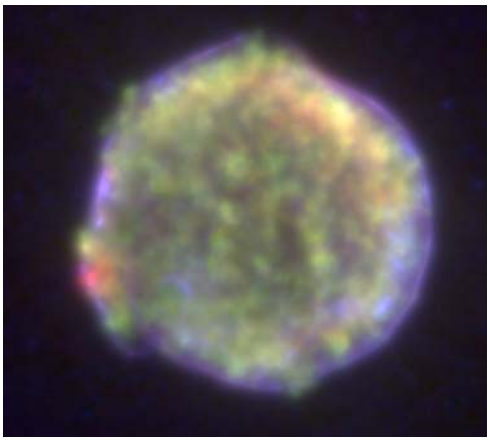

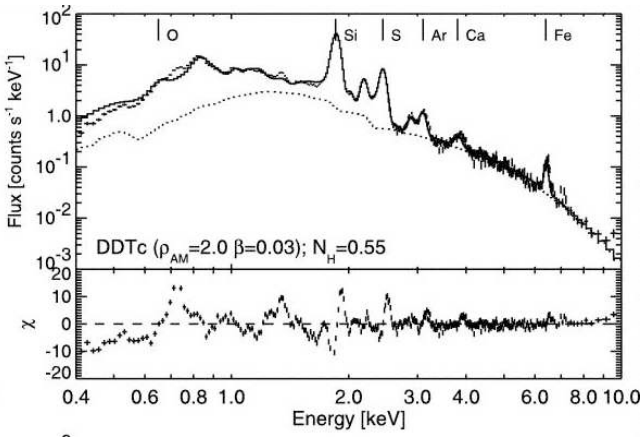

Figure 3–(Left) Color-coded X-ray image of the Tycho SNR: red corresponds to Fe L emission, green to Si K emission, and blue to 4-6 keV continuum emission. This is derived from the *Chandra* observations after smoothing with the IXO point-spread-function.
Figure 4–(Right) Spatially integrated *XMM-Newton* spectrum of the Tycho SNR with best fit ejecta model.

studies, but why wait when we have the potential to study the twenty to thirty nearest Galactic SNRs?

Results from Current Observatories

Chandra and *XMM-Newton* imaging with low-resolution spectroscopy has already shown the power of X-ray studies to illuminate the processes that occur in the hottest parts of the interiors of exploding stars. In the case of the core collapse SN Cas A (Fig. 1) the spatial distribution of the main nucleosynthetic products (Fe, Si, O) are seen to vary widely in the reverse-shock-heated ejecta. Large bulk velocities (of order $\pm$2000 km s^{-1}) are inferred from Doppler shifts of Si and Fe lines (Hwang et al. 2001; Willingale et al. 2002). One of the earliest *Chandra* results was the discovery that Fe-rich ejecta lie at the outermost edge of the remnant (Hughes et al. 2000), establishing that violent processes must have operated on the core of the SN during the explosion. These Fe-rich knots vary in precise composition including some that are nearly pure Fe (see Fig. 2, Hwang & Laming 2003), possibly from α-rich freeze out, while other knots appear to come from explosive complete Si-burning under varying conditions. **Because of the limited spectral resolution and modest effective area of current instruments, it is not possible to detect any of the lower abundance Fe-group species in these small spatial-scale features.**

Significant advances in studies of remnants of thermonuclear SNe Ia have been made using current X-ray instruments. In two cases we have now established consistency between the X-ray properties of a remnant and the optical light of its originating SN, observed through spectroscopy of light echos. The first case where this was done was the LMC SNR 0509−69.0: both the optical light (Rest et al. 2008a) and the X-ray spectrum and dynamics (Badenes et al. 2008) require a bright, highly energetic Type Ia explosion, similar to SN 1991T. More recently the spectral subtype of the Tycho SNR (Fig. 3) was determined, again based on light echo spectra (Rest et al. 2008b, Krause et al. 2008), to be consistent with the majority class of normal type Ia supernovae. Previously it had been shown that

the X-ray properties of the remnant were consistent with the hypothesis that SN1572 was a normal SN Ia (Badenes et al. 2006). Fig. 4 (taken from this paper) shows the excellent agreement between the observed *XMM-Newton* spectrum spatially integrated over the remnant and the best fit ejecta model appropriate to a normal SN Ia.

One of the great promises of future high spectral resolution studies of SNRs is the possibility to detect and measure spectral lines from trace elements, that is species other than the most abundant ones (e.g., O, Ne, C, Si, S, Fe) that are now commonly studied at CCD spectral resolution. As an example of the scientific value of this work, we point to the recent paper by Badenes, Bravo, & Hughes (2008) on using the Mn to Cr ratio in SN Ia remnants to constrain the initial metallicity of the progenitor. The basic idea is that the mass ratio of Mn to Cr produced though nuclear burning during the explosion depends sensitively on the electron-to-nucleon fraction (Y_e) in the white dwarf. Timmes et al. (2003) have already shown that Y_e is linearly proportional to the metallicity of the white dwarf progenitor. Thus from the observed Mn/Cr ratio in the remnant we learn about the metallicity and therefore the age of the original progenitor system. Applying this technique to the recent *Suzaku* spectrum of the Tycho SNR where Mn and Cr were both detected (Tamagawa et al. 2009), Badenes, Bravo, & Hughes (2008) were able to show that the metallicity of Tycho's progenitor star was supersolar. Although the errors were large, values of metallicities much below solar can be rejected.

Future Advances

Improvement in numerical calculations will be an important component in advancing this research field. Full 3D hydro calculations of the collapse, rebound, and explosion of core collapse SNe are only now at the beginning stages and detailed predictions of the nucleosynthetic yields of the resulting ejecta are not yet available. However, it seems likely that differences in the temperature, density and Y_e in the zones undergoing explosive nucleosynthesis will be imprinted on the relative composition of the Fe-group elements in the ejected matter. As shown above, this is also the case for thermonuclear SNe. By measuring the composition of Fe-rich ejecta in young SNRs, including the trace species, we will provide critical constraints on the temperatures and conditions under which the nuclear burning occurred. This will put strong constraints on the allowed models for the explosions.

Observational results obtained to date, as important and relevant as they are, suffer, fundamentally, from a lack of precision. CCD-type spectral resolution is unable to provide accurate measurements of even the most basic thermodynamic quantities that characterize the plasma, i.e., electron temperature and the charge states of the relevant ions. This introduces large errors in relative abundance measurements. Studies of dynamics are limited to only the most extreme speeds (1000's of km s^{-1}). Significant advances require improved spectral resolution and considerably more effective area than provided by current X-ray satellites or missions under development, such as *Astro-H*. The *International X-ray Observatory* offers vastly improved spectral resolution over current CCD devices (ΔE of 2.5 eV vs. 150 eV at the Fe K-shell line near 6.5 keV), coupled with a large increase in effective area (6500 cm^2 vs. 800 cm^2 for *XMM-Newton* or 300 cm^2 for *Astro-H*, at 6 keV). These

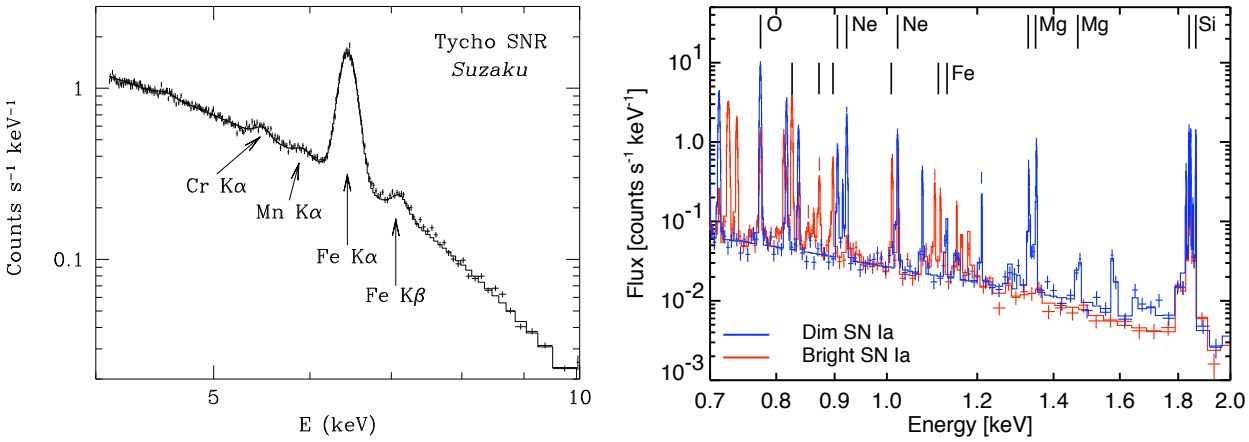

Figure 5–(Left) Spatially integrated *Suzaku* spectrum of the Tycho SNR showing the detections of faint lines from the trace Fe-group elements Cr and Mn.
Figure 6–(Right) Simulated IXO spectrum of the spatially integrated X-ray emission from 400-year-old remnants of dim (blue curve) and bright (red curve) SN Ia in the Local Group galaxy M33 observed for 100 ks each.

are the essential next steps in the observational domain. We note that the planned angular resolution of IXO (5″) is sufficient to address many of the important science goals in this subject area. Figures 1 and 3 (where the *Chandra* images have been convolved with the expected IXO beam) show that IXO can resolve many individual spectrally-distinct features in young SNRs.

Many IXO investigations of SNRs are possible. For example, in the case of radioactive ^{44}Ti in Cas A, the measured fluxes from INTEGRAL/IBIS (Renaud et al. 2006) predict an IXO count rate of ∼0.25 cts s^{-1} for the innershell Kα lines of each of the daughter products ^{44}Sc and ^{44}Ca. This is sufficient to allow for a complete census, including mapping both the spatial extent and dynamics (i.e., radial velocities), of the ^{44}Ti in Cas A. This is critical information pertinent to the unsolved question of where the neutron star/black hole mass cut lies in core collapse SNe.

IXO will map the intensities and Doppler velocity shifts of the Fe-group lines (most importantly from Mn, Cr, and Ni) as well as the much brighter lines from lighter species across the Tycho SNR as well as the half-dozen or so other Galactic SN Ia remnants. As Fig. 3 indicates, the Tycho SNR shows a distinct asymmetry in the ejecta distribution, namely, Si- and Fe-rich ejecta knots along the southeast limb. The key to understanding type Ia SN (SN Ia) lies in understanding how they produce the large quantities of Fe-group elements they do. This is what IXO is ideally suited to do.

Chandra and *XMM-Newton* surveys of the Local Group galaxies M33 and M31 (which are at distances of roughly 800 kpc) have generated catalogs of hundreds of X-ray sources, a number of which are going to be young SNRs (although none have yet been found). Once young SNRs are identified in these galaxies, IXO will be able to carry out follow-up spectroscopy. One exciting project will be to discriminate between remnants of core collapse and Type Ia SNe and relate the properties of the remnants to their local environments. In particular for SNe Ia, there is growing evidence that bright and dim SNe Ia have different kinds of progenitors (Scannapieco & Bildsten 2005). This could introduce systematic

errors that compromise the role of SN Ia in the forthcoming era of precision cosmology with the JDEM candidate missions (Aldering 2005). Type Ia SNe at high redshift are relatively common, but they are too far away to study their environments (stellar populations, metallicities, etc.) with enough detail to constrain the nature of the progenitors. IXO observations of young remnants of SN Ia in the Local Group could represent a breakthrough in this field. The X-ray spectra of young SNRs are sufficiently well understood to (a) identify the Type Ia objects (Hughes et al. 1995) and (b) discriminate the SNRs from bright and dim Type Ia SNe (Badenes et al. 2006, 2008). IXO would observe enough Type Ia SNRs (several dozens) to allow a statistical study of their progenitor properties in relation to the well-characterized stellar populations of M33 and M31.

In Fig. 6, we present the simulated spectra of two 400 yr old Type Ia SNRs at the distance of M33, with exposures of 100 ks. One spectrum was generated from a bright SN Ia model ($\sim$1 $M_\odot$ of ^{56}Ni), the other from a dim SN Ia model ($\sim$0.3 $M_\odot$ of ^{56}Ni). The X-ray spectra of the SNRs are instantly distinguishable: one is dominated by Fe L lines (red curve), and the other by lines from intermediate mass elements like Ne and Mg (blue curve). Similar studies are possible in M31 as well.

We close this white paper with two final IXO spectral simulations. Fig. 7 shows the IXO spectra of two Cas A Fe-rich knots, including the pure Fe one discussed above (c.f., Fig. 2) from alpha-rich freeze-out and another from explosive incomplete Si-burning. Fig. 8 shows the IXO spectra for the Si-rich and Fe-rich knots along the southeastern limb of Tycho. The richness of these spectra graphically demonstrate the power of the *International X-ray Observatory* to usher in a new era of precision studies of nucleosynthesis and SN explosion physics.

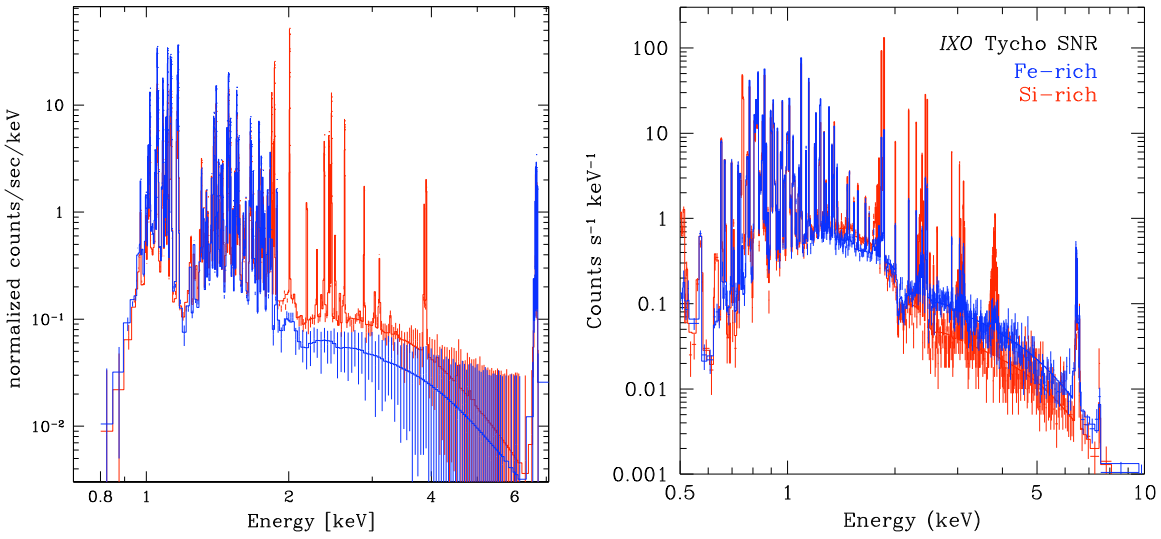

Figure 7–(Left) Simulated IXO spectrum of Fe-rich knots in Cas A for exposures of 50 ks. The blue spectrum is pure Fe, while the red spectrum contains an admixture of Si, S, Ar, and Ca in addition to Fe. *Figure 8*–(Right) Simulated IXO spectra (50 ks) of the Si-rich (red) and Fe-rich (blue) knots along the southeastern limb of the Tycho SNR.

References

Aldering, G. 2005, New Astronomy Review, 49, 346

Badenes, C., Bravo, E., & Hughes, J. P. 2008, ApJ, 680, L33

Badenes, C., Borkowski, K. J., Hughes, J. P., Hwang, U., & Bravo, E. 2006, ApJ, 645, 1373

Badenes, C., Hughes, J. P., Cassam-Chenaï, G., & Bravo, E. 2008, ApJ, 680, 1149

Blondin, J. M., & Mezzacappa, A. 2006, ApJ, 642, 401

Burrows, A., Dessart, L., Ott, C. D., & Livne, E. 2007, Phys. Rep, 442, 23

Burrows, A., Hayes, J., & Fryxell, B. A. 1995, ApJ, 450, 830

Foglizzo, T., Scheck, L., & Janka, H.-Th. 2006, ApJ, 652, 1436

Herant, M., Benz, W., Hix, W. R., Fryer, C. L., & Colgate, S. A. 1994, ApJ, 435, 339

Hughes, J. P., et al. 1995, ApJ, 444, L81

Hughes, J. P., Rakowski, C. E., Burrows, D. N., & Slane, P. O. 2000, ApJ (Letters), 528, L109

Hwang, U., & Laming, J. M. 2003, ApJ, 597, 362

Hwang, U., Szymkowiak, A. E., Petre, R., & Holt, S. S. 2001, ApJ (Letters), 560, L175

Iwamoto, K., Brachwitz, F., Nomoto, K., Kishimoto, N., Umeda, H., Hix, W. R., & Thielemann, F.-K. 1999, ApJS, 125, 439

Jordan, G. C., IV, Fisher, R. T., Townsley, D. M., Calder, A. C., Graziani, C., Asida, S., Lamb, D. Q., & Truran, J. W. 2008, ApJ, 681, 1448

Khokhlov, A. M., Höflich, P. A., Oran, E. S., Wheeler, J. C., Wang, L., & Chtchelkanova, A. Y. 1999, ApJ, 524, L107

Kifonidis, K., Plewa, T., Janka, H.-T., Müller, E. 2000, ApJ, 531, L123

Krause, O., Tanaka, M., Usuda, T., Hattori, T., Goto, M., Birkmann, S., & Nomoto, K. 2008, Nature, 456, 617

Renaud, M., et al. 2006, ApJ, 647, L41

Rest, A., et al. 2008a, ApJ, 680, 1137

Rest, A., et al. 2008b, ApJ, 681, L81

Röpke, F. K., & Bruckschen, R. 2008, New Journal of Physics, 10, 125009

Scannapieco, E., & Bildsten, L. 2005, ApJ, 629, L85

Scheck, L., Janka, H.-Th, Foglizzo, T., & Kifonidis, K. 2008, A&A, 477, 931

Tamagawa, T., et al. 2009, PASJ, 61, S155

Timmes, F. X., Brown, E. F., & Truran, J. W. 2003, ApJ, 590, L83

Willingale, R., Bleeker, J. A. M., van der Heyden, K. J., Kaastra, J. S., & Vink, J. 2002, A&A, 381, 1039

Woosley, S. E., & Heger, A. 2007, Phys. Rep., 442, 269

Cosmic Feedback from Supermassive Black Holes

Andrew C. Fabian[1,2,3]

[1] Institute of Astronomy, University of Cambridge, Madingley Road, Cambridge CB3 0HA, United Kingdom

[2] Phone: +011-44-01223-37509

[3] E-mail: acf@ast.cam.ac.uk

E. Churazov[4], M. Donahue[5], W. R. Forman[6], M. R. Garcia[6], S. Heinz[7], B. R. McNamara[8], K. Nandra[9], P. Nulsen[6], P. Ogle[10], E. S. Perlman[11], D. Proga[12], M. J. Rees[1], C. L. Sarazin[13], R. A. Sunyaev[4], G. B. Taylor[14], S. D. M. White[4], A. Vikhlinin[6], D. M. Worrall[15]

[4)] Max-Planck-Institut für Astrophysik, Karl Schwarzschild Str. 1, Garching, Germany

[5)] Department of Physics and Astronomy, Michigan State University, East Lansing, MI 48824

[6)] Harvard-Smithsonian Center for Astrophysics, 60 Garden St., Cambridge MA, 02138

[7)] Department of Astronomy, University of Wisconsin-Madison, 475 N. Charter St., Madison, WI 53706-1582

[8)] University of Waterloo, Physics & Astronomy, 200 University Avenue W., Waterloo, Ontario, N2L 3G1; Perimeter Institute for Theoretical Astrophysics, Waterloo, Ont.

[9)] Astrophysics group, Imperial College, Prince Consort Road London SW7 2AZ, United Kingdom

[10)] Spitzer Science Center, California Institute of Technology, Pasadena, CA 91125

[11)] Department of Physics and Space Science, Florida Institute of Technology, 150 W. University Blvd, Melbourne, Florida 32901

[12)] Department of Physics and Astronomy, University of Nevada-Las Vegas, 4505 Maryland Parkway, Las Vegas, NV 89154-4002

[13)] Department of Astronomy, University of Virginia, P.O. Box 400325, Charlottesville, VA 22904

[14)] Department of Physics and Astronomy, University of New Mexico, MSC 07 4220, Albuquerque, NM 87131

[15)] Department of Physics, University of Bristol, Tyndall Ave., Bristol BS8 1TL, United Kingdom

Cosmic Feedback from Supermassive Black Holes

An extraordinary recent development in astrophysics was the discovery of the fossil relationship between central black hole mass and the stellar mass of galactic bulges. The physical process underpinning this relationship has become known as feedback. The *Chandra* X-ray Observatory was instrumental in realizing the physical basis for feedback, by demonstrating a tight coupling between the energy released by supermassive black holes and the gaseous structures surrounding them. A great leap forward in X-ray collecting area and spectral resolution is now required to address the following question:

How did feedback from black holes influence the growth of structure?

Feedback and galaxy formation

Every massive galaxy appears to have a massive black hole at its center whose mass is about 0.2% of the mass of the galaxy's bulge (Tremaine et al. 2002). It is now widely considered that the black hole may have brought about this correlation by regulating the amount of gas available for star formation in the galaxy. Massive black holes thereby have a profound influence on the evolution of galaxies, and possibly on their formation. Several puzzling aspects of galaxy formation, including the early quenching of star formation in galactic bulges and the galaxy mass function at both high and low ends, have been attributed to black hole "feedback" (Croton et al. 2006).

In size, a black hole is to a galaxy roughly as a person is to the Earth. Something very small is determining the growth of something very large. This is possible because the gravitational potential energy acquired by an object approaching a black hole is a million times larger than the energy of an object orbiting in the potential of a typical galaxy. As a black hole grows to 0.2% of the bulge mass through accreting matter, it releases nearly 100 times the gravitational binding energy of its host galaxy.

There is no question that a growing black hole *could* drastically affect its host galaxy. Whether and how it *does* so, however, is an open question that depends on how much of the energy released actually interacts with the matter in the galaxy. If the energy is in electromagnetic radiation and the matter largely stars, then very little interaction is expected. If the matter consists of gas, perhaps with embedded dust, the radiative output of the black hole can both heat the gas, and drive it via radiation pressure. Alternatively, if significant AGN power emerges in winds or jets, mechanical heating and pressure provide the link. Either form of interaction can be sufficiently strong that gas can be driven out of the galaxy entirely (Silk & Rees 1998).

The radiative form of feedback is most effective when the black hole is accreting close to its Eddington limit. The mechanical form associated with jets, on the other hand, operates at rates below the Eddington limit. X-ray observations are essential for studying both forms of feedback. The mechanical forms of feedback rely on dynamical

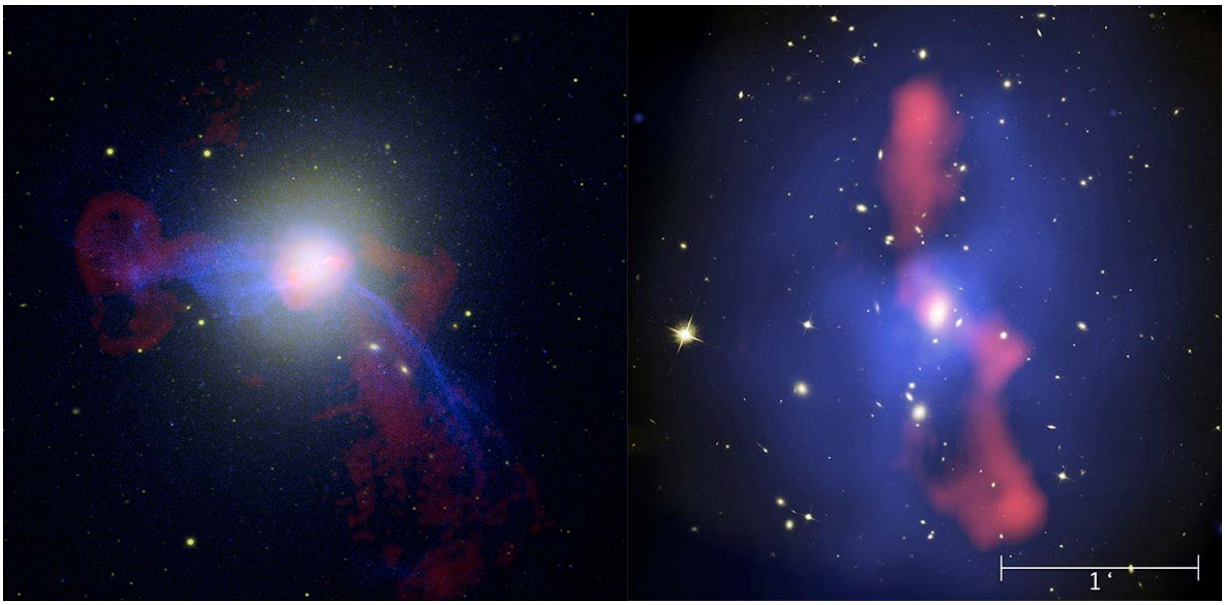

Fig. 1, Left: X-ray emission (blue), radio emission (red) superposed on an optical image of M87. The X-ray structure (shocks, bubbles) was induced by a ~10^{58} erg outburst that began 10 Myr ago (Forman et al. 2005). The persistence of the delicate, straight-edge X-ray feature indicates a lack of strong turbulence. We expect IXO to reveal ordered velocity structure. The image is 50 kpc on a side. **Right:** X-ray emission (blue), 320 MHz radio emission (red) superposed on an HST image of the z=0.21 cluster MS0735.6+7421 (McNamara et al. 2005). The image is 700 kpc on a side. Giant cavities, each 200 kpc (1 arcmin) in diameter, were excavated by the AGN. The mechanical energy is reliably measured in X-rays by multiplying the gas pressure by the volume of the cavities, and by the properties of the surrounding shock fronts. With a mechanical energy of 10^{62} erg, MS0735 is the most energetic AGN known. This figure shows that AGN can affect structures on galaxy scales of tens of kpc and on cluster-wide scales, spanning hundreds of kpc in MS0735.

(ram) pressure to accelerate gas to high speeds (Fig. 1). If this gas is initially of moderate temperature, the interaction will shock it to high temperatures where it can only be detected in X-rays. Since the efficiency of ram pressure acceleration is roughly proportional to the volume filling factor of the accelerated gas, most of the energy is probably absorbed by the hot component of the interstellar medium in any case. Gas accelerated by radiation pressure or radiative heating is likely to be cold and dusty. The interaction is therefore much more difficult to observe directly. X-ray and far infrared emission can emerge from the inner regions where the interaction occurs, revealing the Active Galactic Nucleus (AGN) itself.

Radiative acceleration appears to be particularly dramatic in the outflows from some luminous quasars. UV observations indicate that outflows reaching 0.1-0.4c may be present in most quasars. X-ray observations are required to determine the total column density and hence the kinetic energy flux. Current work on a small number of objects

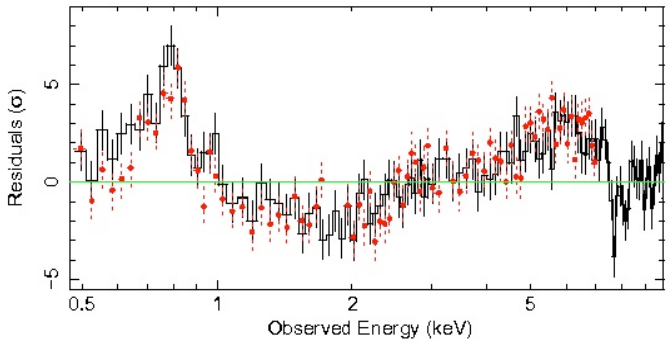

Fig. 2, Top: *Suzaku* X-ray spectrum of luminous quasar PDS456 at z=0.184. The strong iron absorption lines at 9 keV in the rest frame indicate an outflow at 0.3c and a mechanical power of 10^{47} erg s^{-1} (Reeves et al. 2009).

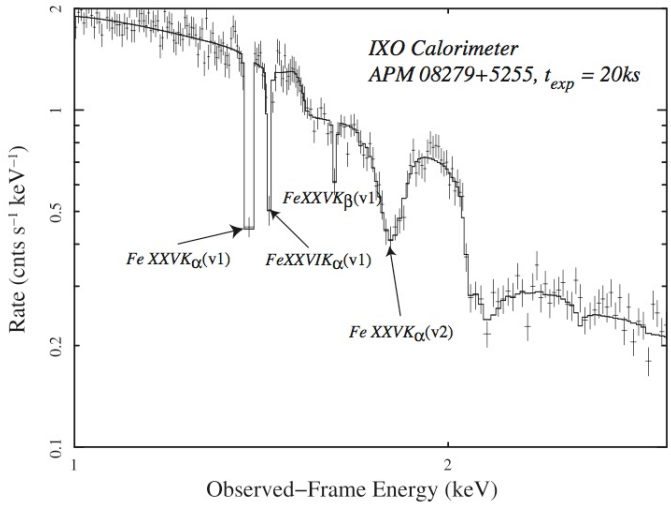

Bottom: 20 ksec simulation of an IXO spectrum of the absorption structure of the mildly relativistic outflow seen by *Chandra* in the BAL quasar APM08279 at z=3.91.

implies that this can be comparable to the radiative luminosity (Fig. 2). To diagnose the energetics of quasars we need large samples of quasars, comparing them with the less energetic (but still substantial) outflows from lower luminosity AGN, which can reach speeds of several thousand km/s.

IXO's huge spectroscopic throughput will extend this to redshifts *z*=1-3, where the majority of galaxy growth is occurring. IXO will be sensitive to all ionization states from Fe I – Fe XXVI, allowing us to study how feedback affects all phases of interstellar and intergalactic gas, from million-degree collisionally ionized plasmas to ten-thousand degree photoionized clouds. These measurements will probe over 10 decades in radial scale, from the inner accretion flow where the outflows are generated to the halos of galaxies and clusters, where the outflows deposit their energy.

Current models of galaxy evolution predict that merger-induced star formation and AGN activity proceeds under heavy obscuration, building the galaxy's bulge and black hole before the AGN blows out all of the gas and terminates star formation. Following this, an unobscured QSO is briefly revealed before the galaxy becomes much less active as a massive red elliptical. The complete census of AGN enabled by IXO will pinpoint galaxies whose black holes are undergoing all these phases of evolution, and crucially

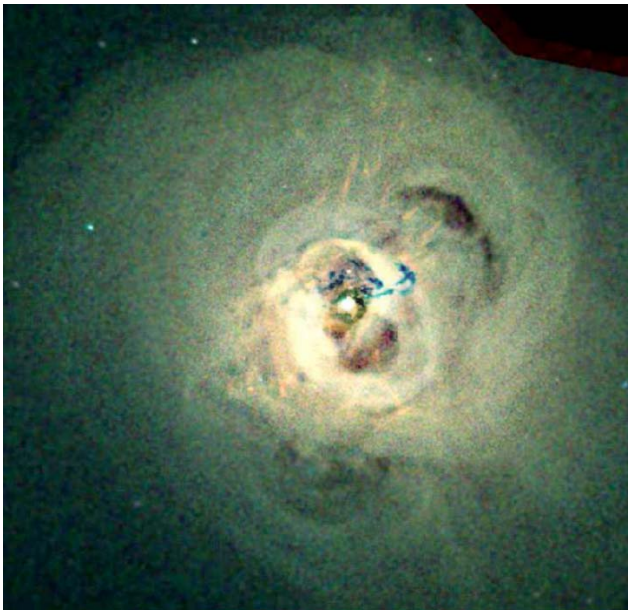

Fig. 3: How did feedback from black holes influence galaxy growth? *Chandra* X-ray observations of Perseus (left; Fabian et al. 2003) and other nearby clusters have revealed the indelible imprint of the AGN on the hot gas in the core. Radiative and mechanical heating and pressure from black holes have a profound influence not only on the hot baryons, but on the evolution of all galaxies whether or not they are in clusters.

the heavily obscured "Compton thick" phase predicted during the quenching of star formation. Observations of galaxies in the *X-ray band* are a powerful way to select accreting black holes in an unbiased fashion, and to probe the inner workings of AGN near the black hole's gravitational radius.

Thermal regulation of gas in bulges and cluster cores

Mechanical feedback dominates in galaxies, groups, and clusters at late times, as shown by X-ray observations of gas in the bulges of massive galaxies and the cores of galaxy clusters (eg., Fig. 1). The energy transfer process is surprisingly subtle. The radiative cooling time of the hot gas in these regions is often much shorter than the age of the system, so that without any additional heating, the gas would cool and flow into the center. For giant ellipticals the resulting mass cooling rates would be of order 1 solar mass per year. At the centers of clusters and groups, cooling rates range between a few to thousands of $M_{\odot}$ per year. Spectroscopic evidence from *Chandra* and *XMM* shows that some cooling occurs, but not to the extent predicted by simple cooling (Peterson & Fabian 2006). Limits on cool gas and star formation rates confirm this. Mechanical power from the central AGN acting through jets must be compensating for the energy lost by cooling across scales of tens to hundreds of kpc (McNamara & Nulsen 2007).

The gross energetics of AGN feedback in galaxies and clusters are reasonably well established (Fig. 4). Remarkably, relatively weak radio sources at the centers of clusters often have mechanical power comparable to the output of a quasar, which is sufficient to prevent hot atmospheres from cooling (McNamara & Nulsen 2007). The coupling between the mechanical power and the surrounding medium are, however,

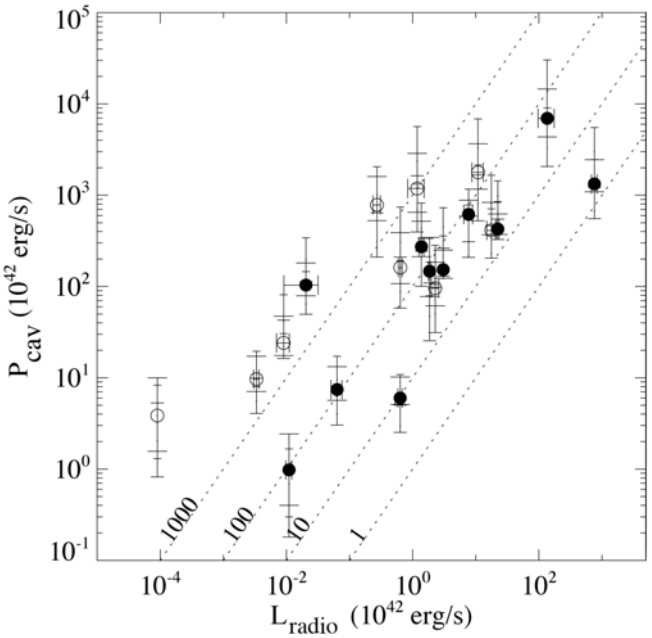

Fig. 4: Jet power inferred from X-ray cavities in clusters of galaxies (McNamara & Nulsen 2007) plotted against radio luminosity (10Mhz – 10GHz). The diagonal lines represent ratios of constant jet power to radio synchrotron power. Jet power correlates with synchrotron power but with a *very* large scatter in their ratio. Radio sources embedded in hot atmospheres are dominated by mechanical power.

poorly understood. Moreover, it is extremely hard to understand how a fine balance can be established and maintained.

The heat source – the black hole – is roughly the size of the Solar System, yet the heating rate must be tuned to conditions operating over scales 10 decades larger. The short radiative cooling time of the gas means that the feedback must be more or less continuous. How the jet power, which is highly collimated to begin with, is isotropically spread to the surrounding gas is not clear. The obvious signs of heating include bubbles blown in the intracluster gas by the jets (Figs. 1, 3) and nearly quasi-spherical ripples in the X-ray emission that are interpreted as sound waves and weak shocks. Future low-frequency radio observations of the bubbles and cavities are of great importance in determining the scale of the energy input. The disturbances found in the hot gas carry enough energy flux to offset cooling, but the microphysics of how such energy is dissipated in the gas is not understood.

The persistence of steep abundance gradients in the cluster gas, imprinted by supernovae in the central galaxy means that the feedback is gentle, in the sense that it does not rely on violent shock heating or supersonic turbulence. Long filaments of optical line-emitting gas in some objects suggest low levels of turbulence. Yet the continuous streams of radio bubbles made by the jets, the movement of member galaxies and occasional infall of subclusters must make for a complex velocity field.

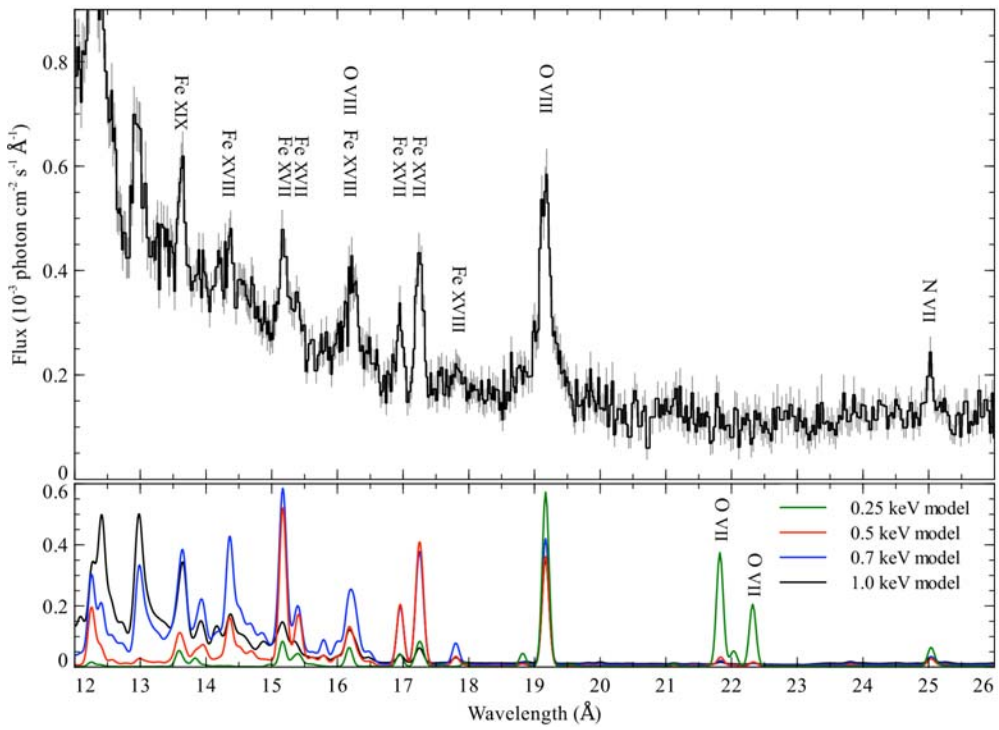

Fig. 5: *XMM-Newton* reflection grating spectrometer spectrum of the core of the Centaurus cluster (Sanders et al. 2008). This part of the spectrum shows a rich set of emission lines from oxygen, neon, and iron. The ionization states of iron show the temperature structure of the gas ranging from 0.4 keV to 4 keV.

With high resolution imaging and moderate resolution spectroscopy (Fig. 5), the *Chandra* and *XMM-Newton* observatories have established AGN feedback as a fundamental astrophysical process in nature. However, the dynamics of these powerful outflows are not understood.

This demands a leap in spectral resolution by one to two orders of magnitude above that of *Chandra* and *XMM-Newton*. The spectral resolution and sensitivity of the next generation X-ray observatory, such as IXO, is needed to understand how the bulk kinetic energy is converted to heat. Its capabilities are essential in order to measure and map the gas velocity to an accuracy of ten km/s, revealing how the mechanical energy is spread and dissipated (Fig. 6). From accurate measurements of line profiles and from the variations of the line centroid over the image it is possible to deduce the characteristic spatial scales and the velocity amplitude of large (> kpc) turbulent eddies, while the total width of the line provides a measure of the total kinetic energy stored in the stochastic gas motions at all spatial scales. Such data will provide crucial insight into the ICM heating mechanisms. Observations of the kinematics of the hot gas phase, which contains the bulk of the gaseous mass, and absorbs the bulk of the mechanical energy in massive elliptical galaxies, are only possible at X-ray wavelengths.

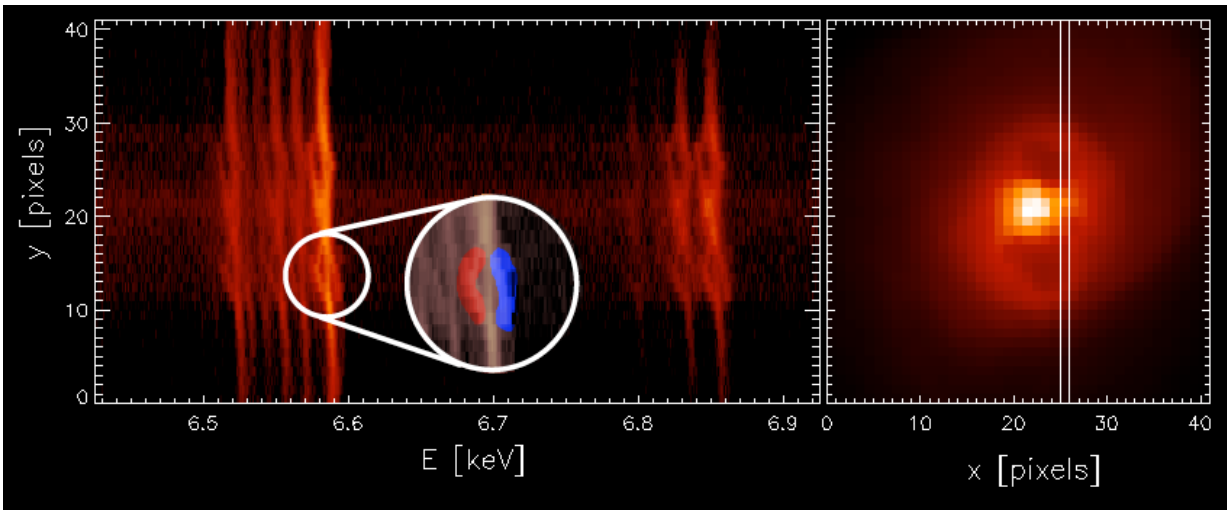

Fig. 6. Simulated high-resolution X-ray spectra from the shells and X-ray cavities in the Perseus cluster (see Fig. 3), demonstrating the power of imaging spectroscopy for AGN feedback studies. The right panel shows the X-ray image and the chosen cut (spectral slit, slicing through both cavities), while the left shows the spectrum of the K-alpha lines from Fe XXV and Fe XXVI (both lines are multiplets), as would be observed by the IXO micro calorimeter spectrograph in an exposure of 250,000 seconds. At the location of the cavities (y=10-15 and y=25-30), each of the lines splits into three components: The front wall of the cavity (blue-shifted), the rear wall of the cavity (red-shifted), and a rest-frame component from fore- and background cluster emission. The expansion velocity and thus the age of the cavity can easily be determined from the red- and blue shifts of the lines, allowing a precise determination of the jet power. The cluster/radio galaxy model used for the spectral simulations is the result of direct hydrodynamic simulations of jets in galaxy clusters with parameters appropriate for Perseus (jet power 10^{45} erg s^{-1}; Heinz et al. 2009, in preparation). See www.astro.wisc.edu/~heinzs/perseus for a movie.

References

1) Croton, D. et al. 2006, MNRAS, 365, 11
2) Fabian, A.C. et al. 2003, MNRAS, 344, L433
3) Forman, W.R. et al. 2005, ApJ, 635, 894
4) McNamara, B.R. & Nulsen, P.E.J. 2007, ARAA, 45, 117
5) McNamara, B.R. et al. 2005, Nature, 433, 45
6) Peterson, J. & Fabian, A.C. 2006, Phys Rep, 427, 1
7) Reeves, J. et al. 2009, MNRAS, submitted
8) Sanders, J. et al. 2008, MNRAS, 385, 1186
9) Silk, J. & Rees, M. 1998, A&A, 331, L1
10) Tremaine, S. et al. 2002, ApJ, 574, 740

The Growth of Supermassive Black Holes Across Cosmic Time

Kirpal Nandra

Astrophysics Group, Imperial College London, Blackett Laboratory, Prince Consort Road, London SW7 2AZ, UK. Tel: +44 207 594 5785, e-mail: k.nandra@imperial.ac.uk

J.A. Aird[1], D.M. Alexander[2], D.R. Ballantyne[3], X. Barcons[4], F.E. Bauer[5], T. Boller[6], W.N. Brandt[7], M. Brusa[6], A. Cattaneo[8], G. Chartas[7], A.L. Coil[9], A. Comastri[10], D.J. Croton[11], R. Della Ceca[12], M. Dickinson[13], A.C. Fabian[14], G.G. Fazio[15], F. Fiore[16], K.A. Flanagan[17], W.R. Forman[15], N. Gehrels[18], A. Georgakakis[19], I., Georgantopoulos[19], R. Gilli[10], G. Hasinger[20], P.F. Hopkins[21], A.E. Hornschemeier[18], R.J. Ivison[22], G. Kauffmann[23], A.R. King[24], A.M. Koekemoer[17], D.C. Koo[25], H. Kunieda[26], E.S. Laird[1], N.A. Levenson[27], Y. Li[15], P. Madau[25], T. Ohashi[28], K.A. Pounds[24], J.R. Primack[25], P. Ranall[10], G.R. Ricker[30], E.M. Rossi[31], O. Shemmer[32], R.S. Somerville[17], D. Stern[33], M. Stiavelli[17], H. Tananbaum[15], Y. Terashima[34], E. Treister[35], Y. Ueda[36], C. Vignali[10], M. Volonteri[37], M.G. Watson[26], N.E. White[18], S.D.M. White[23]

1 Astrophys cs Group Imper a Co ege London B ackett Laboratory Pr nce Consort Road London SW7 2AZ UK
2 Department of Phys cs Durham Un vers ty South Road Durham DH1 3LE UK
3 Center for Re at v st c Astrophys cs Schoo of Phys cs Georg a Inst tute of Techno ogy At anta GA 30332 USA
4 Inst tuto de Fís ca de Cantabr a (CSIC-UC) Aven da de os Castros 39005 Santander Spa n
5 Co umb a Astrophys cs Laboratory Co umb a Un vers ty 550 W 120th St Rm 1418 New York NY 10027 USA
6 Max-P anck-Inst tut für extraterrestr sche Phys k G essenbachstrasse 1 D-85478 Garch ng Germany
7 Department of Astronomy and Astrophys cs Penn State Un vers ty 525 Davey Lab Un vers ty Park PA 16802 USA
8 Astrophys ka sches Inst tut Potsdam an der Sternwarte 16 14482 Potsdam Germany
9 Department of Phys cs Un vers ty of Ca forn a San D ego CA 92093 USA
10 INAF-Osservator o Astronom co d Bo ogna v a Ranzan 1 I-40127 Bo ogna Ita y
11 Centre for Astrophys cs & Supercomput ng Sw nburne Un vers ty P O Box 218 Hawthorn VIC3122 Austra a
12 INAF - Osservator o Astronom co d Brera v a Brera 28 20121 M an Ita y
13 Nat ona Opt ca Astronomy Observatory 950 North Cherry Avenue Tucson AZ 85719 USA
14 Inst tute of Astronomy Mad ng ey Road Cambr dge CB3 0HA UK
15 Harvard-Sm thson an Center for Astrophys cs 60 Garden Street Cambr dge MA 02138 USA
16 INAF-Osservator o Astronom co d Roma v a Frascat 33 00040 Monte Porz o Catone (RM) Ita y
17 Space Te escope Sc ence Inst tute 3700 San Mart n Dr ve Ba t more MD 21218
18 NASA Goddard Space F ght Center Greenbe t MD 20771 USA
19 Nat ona Observatory of Athens Inst tute of Astronomy V Pau ou & I Metaxa Athens 15236 Greece
20 Max-P anck-Inst tute for P asma Phys cs Bo tzmannstr 2 D-85478 Garch ng Germany
21 Department of Astronomy Un vers ty of Ca forn a Berke ey Berke ey CA 94720 USA
22 UK Astronomy Techno ogy Centre Roya Observatory B ackford H Ed nburgh EH9 3HJ UK
23 Max-P anck Inst tut fuer Astrophys k Kar -Schwarzsch d Strasse 1 D-85748 Garch ng Germany
24 Un vers ty of Le cester Un vers ty Road Le cester LE1 7RH UK
25 UCO/L ck Observatory Un vers ty of Ca forn a Santa Cruz CA 95064 USA
26 Department of Phys cs Nagoya Un vers ty Furo-cho Ch kusaku Nagoya 464-8602 Japan
27 Department of Phys cs and Astronomy Un vers ty of Kentucky Lex ngton KY 40506 USA
28 Department of Phys cs Tokyo Metropo tan Un vers ty 1-1 M nam -Osawa Hach oj Tokyo 192-0397 Japan
29 RIKEN Cosm c Rad at on Laboratory H rosawa 2-1 Wakosh Sa tama 351-0198 Japan
30 Kav Inst tute for Astrophys cs and Space Research MIT Cambr dge MA 02139-4307 USA
31 Racah nst tute for Phys cs The Hebrew Un vers ty Jerusa em 91904 Israe
32 Department of Phys cs Un vers ty of North Texas Denton TX 76203 USA
33 Jet Propu s on Laboratory Ca forn a Inst tute of Techno ogy Pasadena CA 91109 USA
34 Department of Phys cs Eh me Un vers ty Matsuyama Eh me 790-8577 Japan
35 Inst tute for Astronomy 2680 Wood awn Dr ve Un vers ty of Hawa Hono u u HI 96822 USA
36 Department of Astronomy Kyoto Un vers ty Kyoto 606-8502 Japan
37 Department of Astronomy Un vers ty of M ch gan Ann Arbor MI 48109 USA

The Growth of Supermassive Black Holes Across Cosmic Time

How did feedback from supermassive black holes shape the properties of galaxies?

One of the main themes in extragalactic astronomy for the next decade will be the evolution of galaxies over cosmic time. Many future observatories, including JWST, ALMA, GMT, TMT and E-ELT will intensively observe *starlight* over a broad redshift range, out to the dawn of the modern Universe when the first galaxies formed. It has, however, become clear that the properties and evolution of galaxies are intimately linked to the growth of their central black holes. Understanding the formation of galaxies, and their subsequent evolution, will therefore be incomplete without similarly intensive observations of the *accretion light* from supermassive black holes (SMBH) in galactic nuclei. To make further progress, we need to chart the formation of typical SMBH at $z>6$, and their subsequent growth over cosmic time, which is most effectively achieved with X-ray observations. Recent technological developments in X-ray optics and instrumentation now bring this within our grasp, enabling capabilities fully matched to those expected from flagship observatories at longer wavelengths.

The co-evolution of black holes and galaxies

A major recent development in astrophysics has been the discovery of the relationship in the local Universe between the properties of galaxy bulges, and dormant black holes in their centers (Magorrian et al. 1998; Ferrarese & Merrit 2000; Gebhardt et al. 2000). These tight relationships represent definitive evidence for the co-evolution of galaxies and Active Galactic Nuclei (AGN). The remarkable implication of this is that some consequence of the accretion process on the scale of the black hole event horizon is able to influence the evolution of an entire galaxy. The main idea is that radiative and mechanical energy from the AGN regulates both star formation and accretion during periods of galaxy growth.

This kind of black-hole driven feedback is thought to be essential in shaping the first galaxies. Current models propose that mergers of small gas-rich proto-galaxies in deep potential wells at high redshift drive star formation and black hole growth (in proto-quasar active galaxies) until a luminous quasar forms. At this point, a black-hole driven wind evacuates gas from the nascent galaxy, limiting additional star formation and further black hole growth (Silk & Rees 1998; Fig. 1). Further episodes of merger-driven star formation, accretion, and feedback are expected to proceed through cosmic time. This provides a plausible origin for the M-σ relation (e.g. King 2003), and explains many outstanding problems in galaxy evolution (e.g. Croton et al. 2005; Hopkins et al. 2006). Despite the intense current interest in this topic, and its great importance, direct evidence for widespread AGN feedback at high redshift is scarce and the details of the physical processes are unclear. It is thus certain to remain one of the most active topics in astrophysics during the next decade and beyond.

The first supermassive black holes

The very first stars formed in primordial structures where gravity was able to overpower the pressure of the ambient baryons, some hundred million years after the Big Bang. The first seed black holes (~100 $M_{\odot}$) are left behind as remnants of the most massive stars. The first galaxies, hosting these first black holes in their cores, are responsible for reionizing the Universe by z~10, as shown by WMAP. Still, the highest redshift galaxies and quasars currently known are all in the range *z*=6–7. To understand the inner workings of the first luminous sources we need to bridge the gap between the few known sources at this redshift, and the information we can extract from the microwave background.

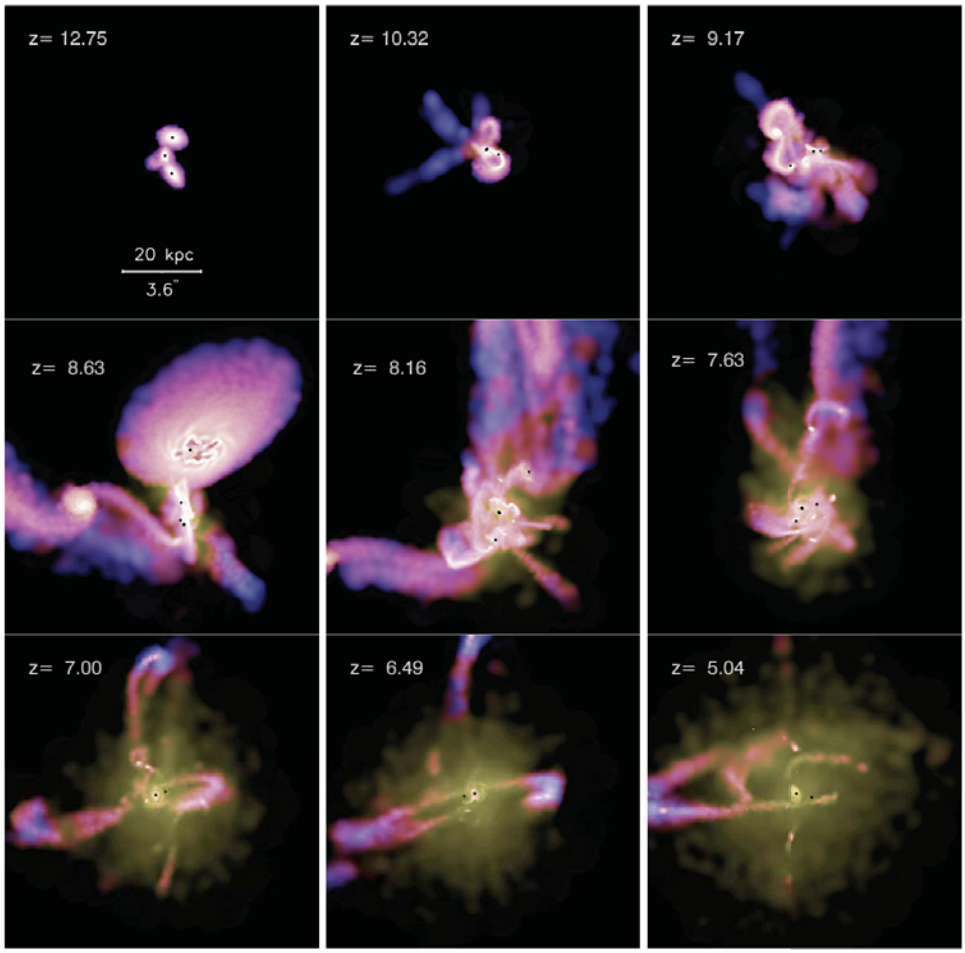

Figure 1: Formation of a high-redshift quasar from hierarchical galaxy mergers as simulated by Li et al. (2007). Color shows gas temperature, and intensity shows gas density. Black dots represent black holes. Small, gas-rich galaxies merge in the deepest potential wells at high redshift, promoting star formation and black hole growth. At z ~ 7 to z ~ 5 a luminous quasar forms, associated with the most massive black hole. It drives a wind (yellow) that evacuates gas from the nascent galaxy.

The known AGN population at *z*=6-7 consists of luminous optical quasars (e.g. Fan et al. 2003). Growing the extremely massive black holes required in <1 Gyr

represents a challenge for theoretical models, because it requires Eddington-limited accretion over many folding times. Recent gas-dynamical cosmological simulations are nevertheless able to produce quasars with ~10^9 $M_\odot$ at z=6.5 through a rapid sequence of mergers in small groups of proto-galaxies (Li et al. 2007; Fig. 1). The growth is likely to proceed in a self-regulated manner owing to feedback with the progenitor host, with a period of intense star formation and obscured accretion preceding the optically bright quasar phase. The complex physics involved in such a scenario is, however, poorly understood.

It must also be borne in mind that these luminous QSOs, hosting among the most massive black holes (>10^9 $M_\odot$) in the Universe, are extremely rare. Typical AGN, which are of lower luminosity and often obscured, remain largely undiscovered. Uncovering such objects at z=6-7, and searching for them at even higher redshift holds the key to our understanding of this crucial phase in the development of the Universe. It is very likely that SMBH as massive as 10^6 $M_\odot$ hosted by vigorously star forming galaxies, existed as early as z=10–11. X-ray observations offer a unique tool to discover and study the accretion light from moderate luminosity AGN at z=6-11, which are rendered invisible in other wavebands due to intergalactic absorption and dilution by their host galaxy.

Obscured accretion and galaxy evolution

The tight relation between galaxy bulges and black holes shows that star formation and accretion must have co-evolved throughout the history of the Universe. To understand this we need to uncover AGN over a broad range of redshifts, luminosities, and obscuration, to characterise the accretion history over the whole of cosmic time. In the theoretical framework discussed above, we expect most of the accretion at high redshift to be heavily obscured. Observational support for this comes from the deepest *Chandra* and *XMM-Newton* surveys, which are most likely missing a significant fraction of the total AGN population. At least 50% of the >6 keV background is still unresolved (e.g. Worsley et al. 2005). Population synthesis models (Comastri et al. 1995; Treister & Urry 2005; Gilli et al. 2007) predict the sources of the unresolved X-ray background to be heavily obscured, Compton-thick AGN (N_H>10^{24} cm^{-2}). While there is a sizable population of these in the local Universe (Risaliti et al. 1999), their properties are basically unknown at larger distances, and their numbers are controversial (Treister et al. 2009). It has been suggested that Compton-thick AGN at z~2 may be hiding among infrared bright, optically faint galaxies (e.g. Daddi et al. 2007; Alexander et al. 2008; Fiore et al. 2008). Their average hard X-ray flux corresponds to an intrinsic X-ray luminosity >10^{43} erg s^{-1}, so if there is a large population of such objects at cosmological redshifts, they could make a major contribution to the total accretion power (Fabian & Iwasawa 1999).

They could also radically alter our inferences regarding co-evolution scenarios. The leading hypothesis is that intense periods of star formation and black hole growth occur concurrently in the history of massive galaxies, possibly triggered

by mergers (e.g. Sanders et al. 1988; Springel et al. 2005). Eventually, feedback from the AGN terminates star formation and, eventually, extinguishes the AGN itself. To test these models, and understand the process of co-evolution, we must determine the key properties of galaxies undergoing an active black hole growth phase, such as their morphologies, star formation rates, and star formation histories. Despite much recent progress, this has proved notoriously difficult. Even with the best current data, it is very challenging to disentangle emission from the galaxy from that associated with the AGN. Furthermore, given the considerations regarding Compton thick sources discussed above, it seems likely that at present we are far from a complete census of the AGN population.

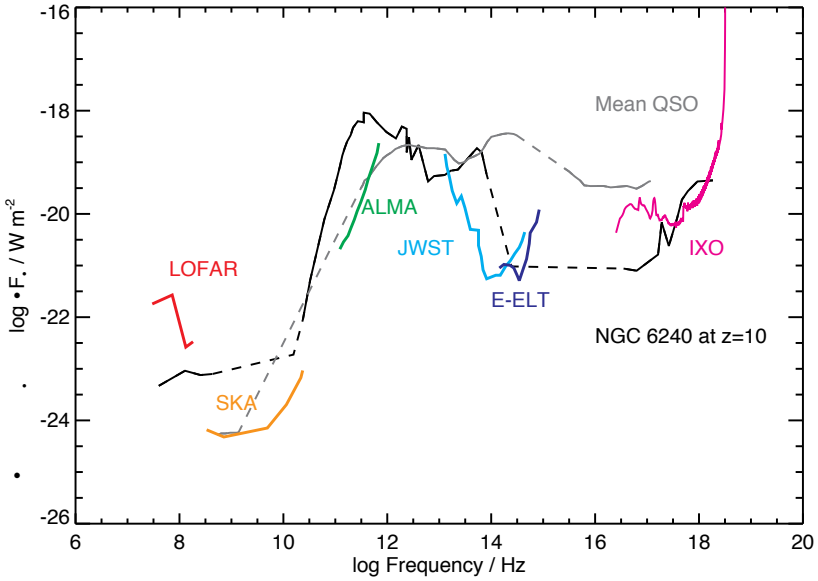

Figure 2: Sensitivity of future multiwavelength facilities to AGN at high *z*. An average QSO template, and the obscured starforming merger NGC 6240 are shown at z=10. Dashed sections indicate unobserved portions of the spectrum. Sensitivities assume 1 Ms 5σ detections for IXO and equivalent 12h 1σ detections for the other instruments. The emission of NGC 6240 is dominated by starlight in all but the X-ray band, so while the other facilities can examine the evolving galaxy, an X-ray observatory like IXO is required to reveal and characterise the AGN component.

AGN in the local Universe tend to be in massive bulges with evidence for an abundant available gas supply (Kauffmann et al. 2003). At *z*~1, the X-ray AGN population is found in largely quiescent, red, host galaxies also with undisturbed, bulge-dominated morphologies (e.g. Grogin et al. 2005; Nandra et al. 2007). There is thus little evidence either for intense, ongoing star formation or merging in the bulk of known AGN, contrary to the dominant theoretical framework. On the other hand, at higher redshifts (*z*~2) submm-selected galaxies show evidence for rapid co-eval, obscured star formation and black hole growth (Page et al. 2001; Alexander et al. 2005) and these FIR luminous galaxies are commonly mergers. These apparent contradictions can be understood if heavily obscured AGN represent a different phase of galaxy evolution. Indeed, models predict that the

Compton thick phase may be precisely at the stage where the AGN blows out gas from the galaxy, terminating star formation (Hopkins et al. 2006). Such objects are difficult to detect without extremely sensitive hard X-ray data. To understand AGN/galaxy co-evolution fully we must, therefore, complete the census of the AGN population by uncovering and characterising the properties of obscured objects at the peak of AGN and starforming activity at z=1-3.

Direct observation of feedback at high redshift: the smoking gun?

AGN feedback is seen directly in the local Universe in the cores of some clusters. The central AGN clearly influences the surrounding gas, preventing infall, cooling and star formation (McNamara et al. 2000; Fabian et al. 2003). This mode of feedback appears to solve the cooling flow problem (Peterson et al. 2001), and can explain the observed properties of massive cluster galaxies, which would be dramatically different if star formation were to proceed unabated (Croton et al. 2005). Outside these massive haloes and at high redshift, where most galaxy building occurs, alternative modes of AGN feedback involving powerful winds have been proposed (e.g. Hopkins et al. 2006). To understand these we need to design experiments to observe feedback directly at z=1-3, at the peak of starforming and AGN activity in the Universe.

X-ray observations are uniquely powerful at revealing the conditions in the immediate vicinity of SMBH, including winds. When a black-hole driven wind lies along the line of sight, it causes ionized and/or neutral X-ray absorption via metal edges and lines; perhaps surprisingly, metals are known to be abundant in AGN out to the highest redshifts. Critically, the hotter X-ray absorbing component of the wind likely carries more mass and energy than components detected at longer wavelengths such as the rest-frame UV. X-ray measurements are thus essential for assessing the level of feedback. *XMM-Newton* and *Chandra* have shown that ionized outflows are common in nearby AGN. These are typically not powerful enough to influence the galaxy scale, but there are cases where much larger velocities and mass flows are implied (e.g. Pounds et al. 2003). At higher redshifts, AGN are usually too faint for sensitive X-ray spectroscopy using current instrumentation. Using the magnifying power of gravitational lensing, however, evidence has been presented for massive, high velocity outflows in a few rare cases at high z (Chartas et al. 2002). The requirement now is to observe black hole winds in typical AGN at $z=1–3$, where the majority of galaxy growth occurs.

Tackling the problem in the next decade

Exploring galaxy evolution is an inherently multiwavelength problem. The premier current surveys (e.g. AEGIS, COSMOS, GOODS) use large investments of time from essentially all of the most sensitive space and ground-based facilities (e.g. *Chandra/XMM-Newton*, HST, Keck, SCUBA, Spitzer, VLA). Future experiments from the radio-through-optical (e.g. SKA, ALMA, JWST, E-ELT/GMT/TMT), will

reach the highest redshifts, probing the evolution of the stellar component of galaxies out to the epoch when the first objects were born. Determining the role of black hole accretion in this process requires X-ray observations of comparable sensitivity (Fig. 2). New technological developments in X-ray optics and instrumentation now make feasible the required performance, and this provides one of the main science drivers for the *International X-ray Observatory* (IXO).

The first supermassive black holes: the highest redshift QSOs known have been discovered in wide-field optical surveys (e.g. SDSS; Fan et al. 2001). These are fascinating sources, but it is crucial to bear in mind that they are among the most extreme and unusual objects in the Universe. Large area optical surveys will be continued with, e.g. PAN-STARRS, LSST, VISTA, and perhaps JDEM/EUCLID, which will discover many more high z QSOs. The optical surveys are, however, fundamentally limited to objects in which the AGN outshines the galaxy. For this reason, X-ray observations can probe much lower bolometric luminosities than the optical. Current deep X-ray surveys probe factors of 100-1000 fainter down the luminosity function than SDSS, at or around L* at z=1-3, where typical objects reside and the bulk of the accretion power is produced. We furthermore expect the majority of AGN at high redshift to be heavily obscured by gas and dust, where the accretion light is rendered invisible in the optical but detectable at X-ray energies. X-ray observations are thus absolutely essential in both the discovery and characterization of *typical* accreting black holes at high redshift.

To detect typical AGN at z≥7 and investigate their growth requires an unprecedented combination of large throughput, good angular resolution and large field-of-view in the X-ray regime. Current surveys are unable to probe to sufficient depth over a wide enough area to find such objects in significant number, but this problem will be solved with IXO. Followup of faint IXO sources with JWST and/or ALMA will provide the necessary identification of the highest z AGN. Note that even though we expect ALMA and/or JWST to be able to detect the host galaxies of these objects, sensitive X-ray observations are needed to disentangle the power associated with black hole accretion from that due to star formation. Reasonable extrapolations of the best estimates of the X-ray luminosity function at high redshift (Aird et al. 2008; Brusa et al. 2009) predict a handful of z~7 AGN in the current deepest *Chandra* surveys (CDF-N, CDF-S and AEGIS). This is consistent with observations of optically invisible X-ray sources (EXOs; Koekemoer et al. 2004; note that JWST/ALMA may confirm these as being at z>7). IXO can reach the CDF depth in <1/10th of the *Chandra* exposure time, with a slightly larger FoV, more uniform sensitivity across the field, and vastly greater X-ray photon statistics. It will thus revolutionise this field, likely yielding many 10s to 100s of moderate luminosity AGN at z≥7 and pushing to z=8-10. Semi-analytic models predict numbers of ultra-high z AGN that differ by several orders of magnitude (cf. Rhook & Haehnelt 2008; Marulli et al. 2008), based on differing evolutionary scenarios. IXO will discriminate decisively between them.

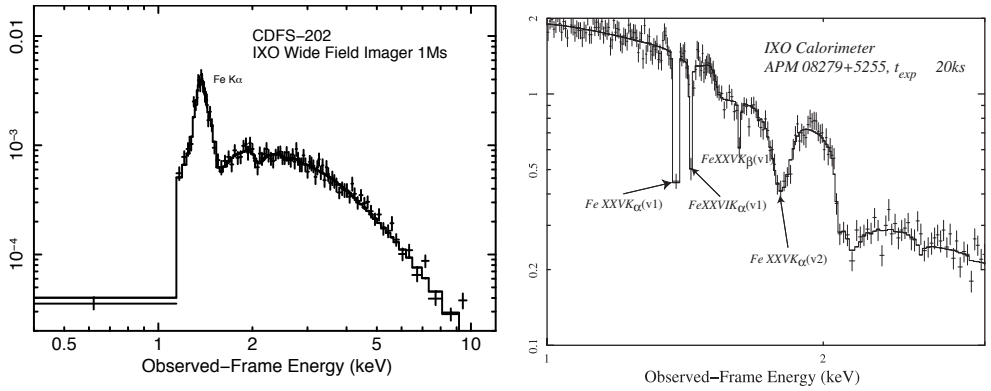

Figure 3: Simulated spectra of (left) the z=3.7 Compton thick AGN CDFS-202 (Norman et al. 2002), in a 1Ms exposure with the IXO WFI; Parameters are based on the deep XMM observation of the CDF-S (PI: Comastri) (right) the characteristic X-ray BAL signatures of the fast (~0.2c) outflow in APM 08279+5255 (Chartas et al. 2002), which may be in the "blowout phase", as seen by the IXO/XMS calorimeter in just 20ks.

Obscured accretion: X-ray selection has provided the most robust AGN samples to date, but finding the most obscured objects has proved difficult. Mid-IR selection is promising, but has not yet yielded samples that are both reliable and complete. Future hard X-ray (>10 keV) imaging (*NUSTAR*, *ASTRO-H*, *Simbol-X*) will provide a step forward in revealing AGN with column densities of ~few × 10^{24} cm^{-2}. Interestingly, hard X-ray surveys have revealed surprisingly few Compton thick AGN in the local universe (Tueller et al. 2008; Treister et al. 2009). They may be more rare than previously thought, or more heavily obscured. At the highest column densities, even the 10-40 keV light is suppressed (by a factor ~10 at N_H=10^{25} cm^{-2}), leaving the AGN visible only in scattered X-rays. The spectral sensitivity of IXO in the 2-10 keV band will reveal the telltale intense iron Kα emission characteristic of a Compton reflection dominated source (Fig. 3), and can be combined simultaneously with hard X-ray data (of unprecedented sensitivity if the goal angular resolution is achieved).

Direct observations of feedback: The same combination of unprecedented throughput and spectroscopic capability will open up the distant X-ray Universe to spectroscopy for the first time. Inter alia, this will enable the first significant samples of autonomously determined X-ray redshifts, and a detailed examination of any changes in the accretion process throughout cosmic time. For the present discussion, we highlight the extraordinary sensitivity of IXO to absorption features due to outflows, via iron Kα and many other metal species. Detection of powerful winds in AGN hosts at the major epoch of galaxy formation is the "smoking gun" of feedback, and detailed spectroscopy will reveal the velocity, column density, metallicity and ionization structure of the outflows (Fig. 3) for detailed comparison with physical models, which are at present completely unconstrained.

Reference list and further information can be found at:
http://astro.imperial.ac.uk/research/ixo/smbh_growth.shtml

Solid State Astrophysics
Probing Interstellar Dust and Gas Properties with X-rays

A White Paper Submitted to the Astro2010 Decadal Survey for Astronomy and Astrophysics

Julia C. Lee[1], Randall K. Smith[2]
C. R. Canizares[3], E. Costantini[4], C. de Vries,[4], J. Drake[2], E. Dwek[5], R. Edgar[2], A. M. Juett[5], A. Li[6], C. Lisse[7], F. Paerels[8], D. Patnaude[2], B. Ravel[9], N. S. Schulz[3], T. P. Snow[10], L. A. Valencic[11], J. Wilms[12], J. Xiang[1]

[1]*Harvard University*
[2]*Smithsonian Astrophysical Observatory*
[3]*Massachusetts Institute of Technology*
[4]*SRON-NL*
[5]*NASA/Goddard Space Flight Center*
[6]*University of Missouri*
[7]*Johns Hopkins University Applied Physics Laboratory*
[8]*Columbia University*
[9]*NIST*
[10]*University of Colorado*
[11]*Johns Hopkins University*
[12]*Universität Erlangen-Nürnberg-Germany*

Abstract

The abundances of gas and dust (solids and complex molecules) in the interstellar medium (ISM) as well as their composition and structures impact practically all of astrophysics. Fundamental processes from star formation to stellar winds to galaxy formation all scale with the number of metals. However, significant uncertainties remain in both absolute and relative abundances, as well as how these vary with environment, *e.g.* stellar photospheres versus the interstellar medium (ISM). While UV, optical, IR, and radio studies have considerably advanced our understanding of ISM gas and dust, they cannot provide uniform results over the entire range of column densities needed. In contrast, X-rays will penetrate gas and dust in the cold (3 K) to hot (10^8 K) Universe over a wide range of column densities ($N_{\rm H} \sim 10^{20-24}{\rm cm}^{-2}$), imprinting spectral signatures that reflect the individual atoms which make up the gas, molecule or solid. **X-rays therefore are a powerful and viable resource for delving into a relatively unexplored regime for determining gas abundances and dust properties such as composition, charge state, structure, and quantity via absorption studies, and distribution via scattering halos.**

Introduction

Understanding astrophysical processes, from galaxy evolution to star formation to stellar or AGN outflows, requires an understanding of the metal abundances in the surrounding medium, in gas *and* dust phases. As the primary repository of metals in the interstellar medium (ISM), dust plays a major role in the chemical evolution of stars, planets, and life. Although it makes up only ∼1% of the baryonic mass of our Galaxy, it accounts for virtually all of the UV/optical extinction, in scattering and absorption. This extinction is so efficient that only 1 in 10^{12} of the optical photons created in the Galactic Center reaches us.

In addition, ISM dust and molecules store the heavy elements needed for making Earth-like planets, while their physics and chemistry play an important role in giant molecular clouds, where dust acts as a catalyst in the formation of the organic compounds vital to the development of life (Whittet 2003). **Accurate measurements of the distribution of gas and dust phase abundances in galactic environments are therefore crucial for improving our understanding of a wide range of astrophysical processes from nucleosynthesis to planet formation.**

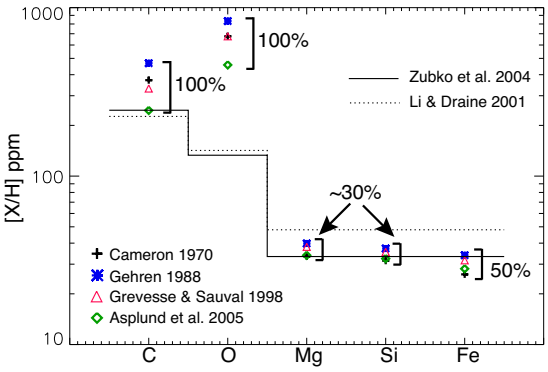

Fig. 1.— *Measured solar abundances of important metals have varied between 30-100% over the last 40 years, which has had significant effects on the range of allowable dust models.*

Despite extensive multi-wavelength studies (primarily in radio to IR bands), we have a limited understanding of dust grain size distributions, their elemental and crystalline composition, and their distribution in astrophysical environments ranging from the cold ISM to the hot disks and envelopes around young stars and compact sources. One immediate difficulty arises from our incomplete knowledge of the overall material available in the gas and dust phases (Fig. 1). Dust abundances are traditionally

inferred from the observed depletion of the gas phase relative to the assumed standard solar abundances (or some linear fraction of them), rather than directly measured. The best direct measurements of gas abundances thus far have come from optical & UV absorption-line studies of diffuse interstellar clouds (e.g. Savage & Sembach 1996). However, these results are limited to low opacity sightlines, and cannot penetrate dense molecular clouds. IR and radio spectroscopy can see into dense clouds to measure many ISM molecules and compounds (mostly polycyclic aromatic hydrocarbon or PAHs, graphites, certain silicates, and ice mantle bands). Yet, since these spectral features come from probing complex molecules as a whole through rotational or vibrational modes originating from e.g. the excitation of phonons (rather than electrons), they require sophisticated modelling efforts or matching to laboratory spectra. Reproducing the exact IR spectral features observed has proven difficult in many cases, making robust abundance and structure determinations for these molecules dependent upon assumptions about their physical properties (Draine 2003b).

The power of X-ray ISM studies of dust and gas

X-rays probe *all* ions from neutral atoms to hydrogenic ions, including H-like Fe XXVI (Fe^{+25}), thereby providing a unique window into the cold (3 K) to hot (10^8 K) Universe, over a wide range of column densities ($N_H \sim 10^{20-24} cm^{-2}$), not possible in any other waveband (see Paerels & Kahn 2003 and references therein). Detailed X-ray studies of the ISM began with Schattenburg & Canizares (1986), who first detected photoelectric edges along with a tentative detection of an atomic OI line. Fifteen years later, the Chandra and XMM gratings have facilitated stringent ISM abundance measurements of *individual* ionic species, from e.g. OI-VII (e.g. Paerels et al. 2001; Juett et al. 2004; Juett et al. 2006). To draw similar parallels, the improved spectral resolution and throughput available to future studies will allow us to routinely use X-ray spectra to determine the *quantity and composition* of dust, where such studies are now pushing the limits of extant satellite capabilities (see Lee et al. 2009a). These important studies can be facilitated as additional bonus science spawned from targeted studies of X-ray bright objects whose lines-of-sight also intersect with inter- and intra-stellar gas and dust with enough opacity to imprint their unique spectral signatures. For the remainder of this white paper, we focus on the unique means by which X-

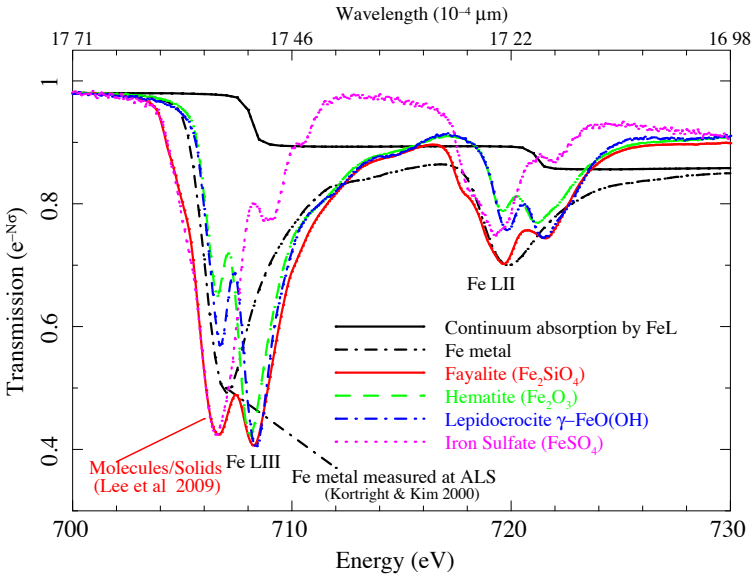

Fig. 2.— *Absorption calculated from laboratory cross section (σ) measurements for 0.7 keV FeL (Lee et al. 2009a). At this high spectral resolution (R=3000, the baseline IXO value), different molecules (color), metals (dashed-dot black) and continuum absorption (solid black), are easily distinguished.*

ray studies can be used to combine condensed matter/solid state theory and atomic physics techniques to the study of astrophysical gas (in photoionized and collisional environments), and dust (composition, quantity, structure, and distribution), that is highly complementary to other wavebands and fields (e.g. planetary science, chemistry, geology, and experimental physics, as relevant to laboratory astrophysics). As such, we can expect such studies to have relevant applications which span the Galactic to Cosmological.

An X-ray absorption method for determining gas-to-dust ratios

Both gas and dust (when $\lesssim 10\mu$m) are semi-transparent to X-rays. Therefore, these high energy photons can be used to make a *direct measurement of condensed phase chemistry via a study of element-specific atomic processes*, whereby the excitation of an electron to a higher-lying, unoccupied electron state (i.e. band/molecular resonance) will imprint signatures in X-ray spectra that reflect the individual atoms which make up the molecule or solid. In much the same way we can identify ions via their absorption or emission lines, the observed spectral modulations near photoelectric edges, known as X-ray absorption fine structure (XAFS) provide unique signatures of the condensed matter that imprinted that signature. Fig. 2 shows how XAFS signatures of different molecules and solids can be identified by their unique structure and wavelength. With high X-ray spectral resolution, and throughput, one can easily assess these details to determine astrophysical dust and molecular properties. At the current highest spectral resolution (R=1000) of the Chandra HETGS, one can discern at high confidence between e.g. Fe_2O_3 and $FeSO_4$ (Fig. 3), but not between Fe_2O_3 and FeO(OH)[‡], as would be possible at the $R = 3000$ spectral resolution of Fig. 2. Furthermore, higher throughput and spectral resolution than currently available will provide additional important knowledge about grain structure (i.e. bond lengths and charge states). Therefore, X-rays should be considered a powerful and viable resource for

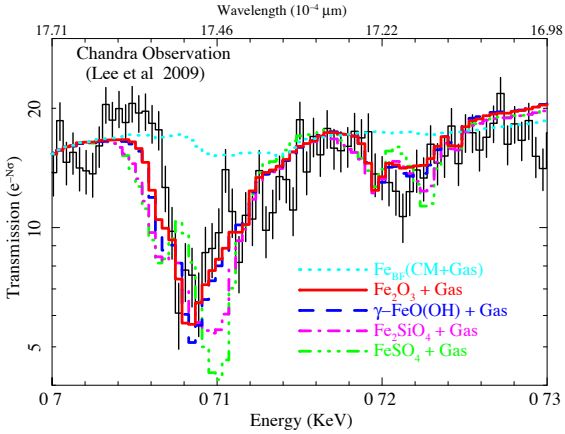

Fig. 3.— *A 15ks Chandra HETGS observation of Cygnus X-1 (black) zoomed in on the* $\sim 700eV$ *(*$\sim 17.7\AA$*) FeL spectral region shows that at the current highest available spectral resolution, we can discern at high confidence between* Fe_2O_3 *(red) and* $FeSO_4$ *(green), but not between e.g.* Fe_2O_3 *and FeO(OH) (dark blue). In light blue is continuum absorption by Fe L from both gas and solids (CM). In addition, even for a source as bright as Cyg X-1, a 15 ks integration is require to achieve a* $S/N \sim 5$ *per bin. Future missions with higher throughput will allow us to engage in such studies with more sources, and accompanying higher spectral resolution as e.g. that shown in Fig. 2 will enable more involved studies of dust structure, not currently possible.*

[‡]We note that, while XAFS theory is quite mature, the study of XAFS is still largely empirical. Therefore, the success of such a study will require that space-based measurements be compared with empirical XAFS data taken at synchrotron beamlines to determine the exact chemical state of the astrophysical dust.

delving into a relatively unexplored regime for determining dust properties: composition, charge state, structure, quantity (via absorption studies; see Lee et al. 2009a for discussion on how to determine quantity *and* composition), and distribution (via scattering halo studies; e.g. Xiang et al. 2007 and references therein; details to follow).

Chandra and XMM have begun this work but have been limited by the available effective area at high spectral resolution (e.g. Lee et al. 2001, 2002; Takei et al. 2002; Ueda et al. 2004; deVries & Costantini 2009). As such, *condensed matter astrophysics* (i.e. the merging of condensed matter and astrophysics techniques for X-ray studies of dust) is now possible, albeit difficult due primarily to the need for more S/N. As stated, for more involved studies of grain structure, higher spectral resolution than currently available is also needed.

To illustrate the complementarity of X-ray studies with those in other wavebands, consider Lee et al. (2009b)'s Spitzer IR and X-ray study of the line-of-sight toward the BH binary Cygnus X-1 which shows different grain populations: IR detections of silicates versus X-ray studies ruling out silicates. This brings to bear intriguing questions relating to grain sizes and origin: e.g. does the IR probe a population of *large* silicate grains that are opaque to the X-rays, or are we probing truly different origins, or is it something more complex? Another example arises from Spitzer IRS studies of the star HD 113766, which shows tantalizing evidence for dust associated with terrestrial planet formation (Lisse et al. 2008). Analysis of the IR spectra provided knowledge of the mineralogy, but could not determine overall abundance ratios, e.g. the amount of Mg vs Fe depleted into grains, to better than a factor of 2. This information can be extracted from X-ray studies of XAFS spectra with sufficient S/N and spectral resolution. These examples highlight the power of an orthogonal approach using X-rays to complement other wavebands: (1) by probing dust properties missed by other detection techniques, and (2) by being sensitive to the range of sub-micron to $\sim$10 μm size dust in $N_{\rm H} \sim 10^{20-24}{\rm cm}^{-2}$ environments. Such multi-wavelength studies, especially if achieved with high throughput and spectral resolution in the X-ray band, will add significantly to our knowledge of the mineralogy and distribution of nascent and interstellar dust populations and therefore the environments from which they originate, be they outflows or star forming regions.

Despite the power of using X-rays for dust studies, this energy band has not been fully exploited for spectral studies of gas, dust and molecules, due largely to the unavailability of instruments with *both* good throughput and spectral resolution ($R \gtrsim 1000$). Missions such as IXO can push the frontiers of such studies by enabling high-precision elemental abundance measurements of *gas and dust* towards hundreds of sightlines, both in our Galaxy and beyond (see Figure 4[Right]). Simulations based on IXO's target spectral resolution and area show that a S/N=10 per bin can be achieved for over 200 sources in 30 ksec or less, while the higher spectral resolution will allow us to realize the previously-discussed studies of dust structure that are not currently possible.

IXO's energy coverage will allow us to study in detail photoelectric edges near C K, O K, Fe L, Mg K, Si K, Al K, S K, Ca K, and Fe K, and therefore all gas-phase as well as molecules/grains containing these constituents, covering all the important species with

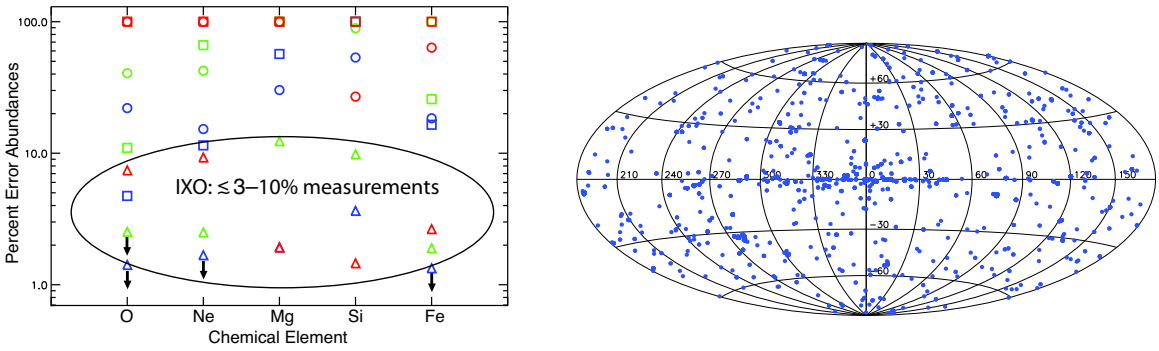

Fig. 4.— *[Left] Potential abundance measurement accuracy from spectra with 50 ksec exposures using the Chandra ACIS-S, LETG (circles), XMM-Newton RGS (squares) and IXO calorimeter (triangles) for* $N_{\rm H}$ *values of* 5×10^{20} *cm*$^{-2}$ *(green),* 5×10^{21} *cm*$^{-2}$ *(blue), and* 5×10^{22} *cm*$^{-2}$ *(red). [Right] Sightlines to bright AGN or X-ray binaries for which IXO will be able both study the source and determine abundances to better than 10%.*

high depletion rates onto dust. These studies, when applied to different astrophysical environments, Galactic or extragalactic, will enable probes of the gamut of outstanding issues ranging from NS and BH (stellar and supermassive) evolutionary histories, to the hot accretion flow in dust enshrouded accretion systems (e.g. Sgr A* and similar AGN and star formation systems; see Lee et al. 2009a for discussion), to cosmological implications (e.g. Type Ia SNe light curves are affected by line-of-sight dust), all using X-rays.

X-ray spectra can also determine abundances in different ISM environments (Yao & Wang 2006), thereby opening a window on the study of grain evolution and cycling between diffuse and dense or dark clouds. The current uncertainties for Chandra and XMM abundance measurements usually exceed 20%, due primarily to the low effective area of the spectrometers. As a result, these results do not constrain ISM abundances with more accuracy than using stellar photospheres or UV/optical data. Over 1800 sources (Fig. 4[Right]) have high enough X-ray fluxes ($\gtrsim 5 \times 10^{-12}$ ergs cm^{-2}s^{-1}) for IXO to make high precision (3-10%) O, Mg, Si, and Fe abundance determinations for both diffuse and dense sightlines, including molecular regions where $N_{\rm H} > 5 \times 10^{22}$ cm^{-2} (see Figure 4[Left]). Along the less dense sightlines with X-ray and UV-bright sources, UV/optical gas-phase abundance measurements can be combined with X-ray determinations of the total abundances to extract the ratio of gas-to-dust directly (e.g. Cunningham et al. 2004). X-ray observations will also probe abundances beyond the Milky Way: between 10-100 ultra-luminous X-ray sources (ULXs) have X-ray fluxes that will allow robust abundance measurements beyond our Galaxy. With spectral resolution $R > 1000$, the Galactic and distant contributions can be separated simply using known velocity separations.

With the additional XAFS studies of dust composition possible for over 200 sources along different sightlines, we can also discriminate between different grain models. With these many sight-lines, we will obtain valuable information on the chemical uniformity of the ISM, including mixing and enrichment.

Dust-induced X-ray Scattering

Scattered X-rays also provide information on dust grain sizes, positions, and *composition*, via *imaging* studies of the arcminute-scale halos around X-ray bright sources created by small-angle scattering in interstellar dust grains (Draine 2003). In some cases, we can even use such studies to more accurately determine distances to compact objects or even other galaxies (see Trümper & Schönfelder 1973 for a description of the method; Predehl et al. 2000; Draine & Bond 2004; Xiang et al. 2007 for applications). Measuring the location and size of grains – seen most dramatically in the dust-scattered rings around X-ray bursts (Vaughan et al. 2004) – provides information about the grain environment and their formation processes when combined with composition and abundance studies discussed previously.

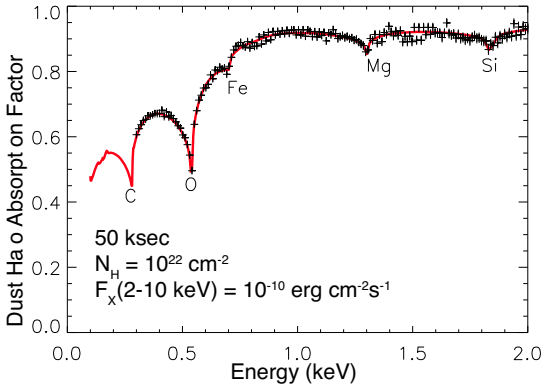

Fig. 5.— *A 50 ksec IXO simulations showing the effects of different elemental composition on scattering halo properties as a function of energy. This will allow the abundances in dust grains as a function of grain size to be measured directly from the scattered halo.*

The intensity of the halo created by small-angle scattering of X-rays by dust is especially sensitive to the large end of the grain size distribution, as these grains dominate the scattering cross section ($\sigma \propto \rho^2 a^4$). In addition, every IXO observation of 20 ksec or longer of a moderately bright source ($>10^{-11}$ erg s^{-1} cm^2) with $N_H \gtrsim 10^{21}$ cm^{-2} will contain a detectable X-ray dust halo. By measuring the total *scattered* halo intensity *as a function of energy* in bright sources – *absorption* features from the elemental grain composition can be measured (Costantini et al. 2005), as shown in Figure 5 for an IXO simulation. **These X-ray halos will directly measure the composition of the large grains.**

Existing interstellar grain size distributions have been developed through information gathered from UV/optical/NIR extinction, polarization, IR emission, and depletion. By combining measurements towards hundreds of sight-lines, modelers have constrained the composition, shape, and grain size distributions from tens of Å up to ∼0.5 μm; above this size, grains act as size-independent "gray" particles in these wavebands. Despite the lack of detailed information, the models agree that even in the diffuse ISM, grains larger than 0.1μm contain most of the dust mass in the ISM. Moreover, most interstellar dust resides in dense molecular clouds, where UV/optical observations are difficult to impossible.

Early interstellar grain models used an approach consisting of a population of bare silicate and graphite grains in a simple power law size distribution, designed to reproduce the "average" Galactic UV extinction curve (Mathis et al. 1977). Since that time, many workers have developed models that were constrained by data from different wavelength regimes, as more information became available (e.g. Dwek et al. 1997; Li & Greenberg 1997; Li & Draine 2001; Weingartner & Draine 2001; Zubko et al. 2004). However, a mismatch of

up to $\sim 30\%$ between the total grain mass and the available metals remains in many models (see Figure 1; Draine 2003b; Zubko et al. 2004). It is not yet clear if the solution will involve changes to the ISM abundances or to the grain models. Halos seen with Chandra and XMM have already shown that adjusting the grain porosity does not solve the problem (Smith et al. 2002; Smith 2008; Valencic & Smith 2008); more accurate abundance data are sorely needed.

Amongst other advantages, X-ray studies will afford us a window into giant molecular clouds, which are opaque to UV and optical light. While grains may coagulate there and/or grow envelopes of ices and organic material (e.g. Clayton & Mathis 1988; Vrba et al. 1993; Whittet et al. 2001), what little we know about these chemical warehouses come from observed molecular transitions in the IR and microwave, which are primarily sensitive to ice and organic compounds. Theoretical work by Cho & Lazarian (2005) offer that far-IR and sub-millimeter polarization studies may shed light on grain sizes in dark clouds ($A_V > 10$), although this remains to be demonstrated. By capitalizing on the well-known sensitivity of X-ray scattering halos on grain sizes, X-rays can be used to provide, again, an orthogonal means by which we can assess dark cloud cores to compare with studies in the IR. The halos of bright objects behind these clouds will let us examine the grain growth processes which heretofore have been shrouded in mystery, while the observed fine structure near photoelectric absorption edges discussed above will provide valuable information on the composition and growth of organic mantles.

REFERENCES

Asplund, M. et al. 2005, ASP Conf Ser, v336, 25
Chlewicki,G& Laureijs,R 1988, A&A, 207, L11
Cho, J., & Lazarian, A. 2005, ApJ, 631, 361
Clayton, D. & Mathis, J. 1998, ApJ, 327, 911
Costantini, E. et al. 2005, A&A, 444, 187
Cunningham, N. J. et al. 2004, ApJ, 611, 353
de Vries, C. & Costantini, E. 2009, A&A, in press
Draine, B. T. & Lee, H. M. 1984, ApJ, 285, 89
Draine, B. T. 2003, ApJ, 598, 1026
Draine, B. T. 2003, ARA&A, 41, 241
Draine, B. & Bond, N. 2004, ApJ, 617, 987
Dwek, E., et al. 1997, ApJ, 475, 565
Grevesse, N. & Sauval, A. J. 1998, SSRv, 85, 161
Juett, A. et al. 2004, ApJ, 612, 308
Juett, A. et al. 2006,ApJ, 648, 1066
Lee, J. C. et al. 2001, ApJ, 554, L13
Lee, J. C. & Ravel, B. 2005, ApJ, 622, 970
Lee, J. C. et al. 2002, ApJ, 567, 1102
Lee, J. C., Xiang, J., Ravel, B., Kortright, J. B., & Flanagan, K. 2009a, ApJ, in press
Lee, J. C., Xiang, J., Hines, D., Ravel, B. & Heinz, S. 2009b, ApJ, in preparation
Li, A., & Greenberg, J. M. 1997, A&A, 323, 566
Li, A., & Draine, B. T. 2001, ApJ, 554, 778
Li, A. 2005, ApJ, 622, 965
Lisse, C. M. et al. 2008, ApJ, 673, 1106
Mathis, J. S., Rumpl, W., & Nordsieck, K. H. 1977, ApJ, 217, 425
Predehl, P. et al. 2000, A&A, 357, L25
Paerels, F., et al. 2001, ApJ, 546, 338
Paerels, F., & Kahn, S.. 2003, ARA&A, 41, 291
Pradhan, A. K. et al. 2003, MNRAS, 341, 1268
Savage, B & Sembach, K. 1996, ARA&A, 34, 279
Schattenburg, M. & Canizares, C. 1986, ApJ, 301, 759
Smith, R. et al. 2002, ApJ, 581, 562
Smith, R. K. 2008, ApJ, 681, 343
Sofia, U.J. & Meyer, D. M. 2001, ApJ, 554, 221
Takei, Y. et al. 2002, ApJ, 581, 307
Trümper J., Schönfelder V., 1973, A&A, 25, 445
Ueda, Y. et al. 2004, ApJ, 609, 325
Valencic, L. & Smith, R. 2008, ApJ, 672, 984
Vaughan, S. 2004, ApJ, 603, L5
Vrba, F. J. et al. 1993, AJ, 105, 1010
Weingartner,J. & Draine,B. 2001, ApJ, 548, 296
Whittet, D. C. B. et al. 2001, ApJ, 550, 793
Whittet, D. C. B.. "Dust in the Galactic Environment" (Philadelphia:IoP Publishing)
Wilms, J. et al. 2000, ApJ, 542, 914
Xiang,J, Lee,J & Nowak,M 2007,ApJ,660,1309
Yao, Y., & Wang, Q. D. 2006, ApJ, 641, 930
Zubko, V. et al. 2004, ApJS, 152, 211

The Missing Baryons in the Milky Way and Local Group

A White Paper submitted to ***The Galactic Neighborhood*** Science Frontiers Panel

Joel N. Bregman
Department of Astronomy
University of Michigan
Ann Arbor, MI 48109-1042
Email: jbregman@umich.edu
Telephone: 734-764-3454

Robert A. Benjamin: University of Wisconsin - Whitewater
Massimiliano Bonamente: University of Alabama in Huntsville
Claude R. Canizares, Massachusettes Institute of Technology
Ann Hornschemeier: NASA Goddard Space Flight Center
Edward Jenkins: Princeton University
Felix J. Lockman: National Radio Astronomy Observatory, Green Bank
Fabrizio Nicastro: Harvard Smithsonian Center for Astrophysics
Takaya Ohashi: Tokyo Metropolitan University
Frtis Paerels: Columbia University
Mary E. Putman: Columbia University
Kenneth Sembach: Space Telescope Science Institute
Norbert Schulz: Massachusettes Institute of Technology
Blair Savage: University of Wisconsin
Randall Smith: Harvard Smithsonian Center for Astrophysics
Steve Snowden: NASA/GSFC
Noriko Yamasaki: ISAS/JAXA
Yangsen Yao: University of Colorado
Bart Wakker: University of Wisconsin

1. The Science Issues

The Milky Way and all other galaxies are missing most of their baryons in that the ratio of the known baryonic mass within R_{virial} to the gravitating mass, Ω_{baryon}/Ω_M is 3-10 times less than the cosmic ratio determined from WMAP (e.g., Hoekstra et al. 2005, McGaugh 2007). This is verified not only in studies of other individual galaxies (e.g., M33 is missing 90% of its baryons; Corbelli 2003) but in large ensembles of galaxies, based on weak lensing studies (e.g., Gavazzi et al. 2007; Parker et al. 2007). Evidently, galaxy formation and evolution leads to a separation between baryons and dark matter. Not only is the energy needed to produce this separation enormous, it must be central to the galaxy formation process.

One possibility is that the baryons fell into the dark matter potential and were subsequently ejected during a galactic wind phase, driven by supernovae or an active galactic nucleus. The other possibility is that most of the gas never collapsed into the dark matter potential because it was heated prior to the collapse. This pre-heating would be spatially distributed and most likely due to supernovae, such as during a Population III phase. In either case, understanding the flow of baryons into and out of galaxies in the evolving universe is essential for ultimately understanding galaxy formation and evolution.

Low redshift galaxies and their environments are the end result of these heating and mass inflow/outflow events over cosmic time. Fortunately, the events producing the low redshift universe leave distinctive observational signatures. For example, the overall heating and ejection (or pre-heating, with little ejection) could be deduced from the extent and temperature of the gas today, along with the mass of metals produced and their elemental ratios. To answer these scientific questions, we must

- ***Discover the missing Galactic and Local Group baryons by measuring the extended distribution of baryons around the Milky Way and in the Local Group.***

- ***Measure the temperature and metallicity properties of the missing baryons to determine the processes responsible for the baryon/dark matter separation***

The characteristic temperature of a potential well like the Milky Way is $1\text{-}3\times10^6$ K, so it is critical to trace this hot gas, which is only detectable in X-rays. Perhaps the best place to discover and study missing galactic baryons is in the vicinity of the Milky Way, where both absorption and emission studies can be brought to bear.

Surrounding the Milky Way is a multiphase halo of gas that is a few kpc in thickness. The hot component was detected with *ROSAT*, where it is found to have a temperature of 1×10^6 K (e.g., Pietz et al 1998; Snowden et al. 2000) and a scale height of about 4 kpc, which is similar to hot halos seen around other spirals. Also, there is considerable OVI gas (Bowen et al. 2008), indicative of gas at $10^{5.5}$ K if it is in ionization equilibrium. Lower ionization absorption line gas is also observed, as is neutral hydrogen. This picture is consistent with material cooling from $\sim10^6$ K, such as in a galactic fountain or galactic accretion.

Another hot component, a larger halo was discovered in the last few years through the detection of X-ray absorption lines (OVII, OVIII; Nicastro et al. 2002; Rasmussen, Kahn, and Paerels 2003). As traced by the OVII absorption line (Figure 1), a 10^6 K gas diagnostic, the extent of this hot material can be estimated, and although poorly known, it is likely to be in the range 20-100 kpc (Bregman and Lloyd-Davies 2007; Yao et al. 2008). This is similar to the size

of the high velocity clouds of HI around the Milky Way and M31, which lie within 50 kpc of their host system. None of these components, hot or cold, account for the missing baryons.

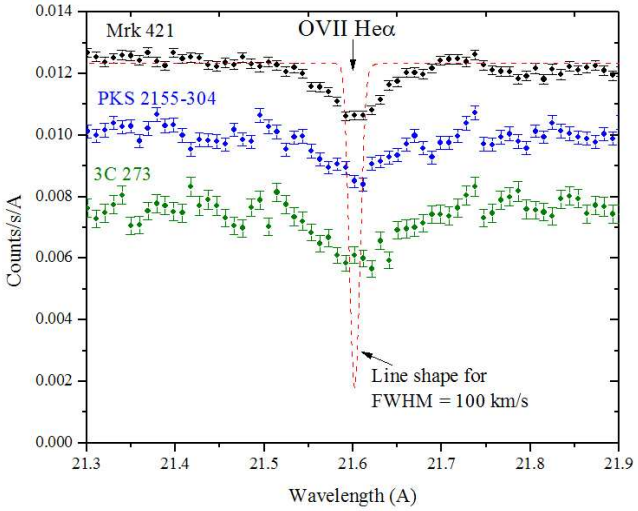

Figure 1. The three brightest AGNs show absorption from OVII Heα at z ≈ 0, indicative of 10^6 K gas around the Milky Way or in the Local Group. The instrumental resolution of these *XMM RGS* spectra is about 360, only slightly worse than that of *Chandra*, but far less than the R = 3000 value that is needed to resolve the expected line shape (in red).

There are clues that a more extensive hot medium is present. The high velocity clouds of HI, at a distance of 5-20 kpc from the disk, must be interacting with a hotter more dilute medium to produce the ubiquitous OVI absorption features (Fox et al. 2004). A hot dilute medium on a scale of a few hundred kpc is inferred from the apparent stripping of HI in Local Group dwarf galaxies (Blitz and Robishaw 2000; Grcevich and Putman 2009). They find that for dwarfs within 270 kpc of the Milky Way or M31, HI is not detected, but it is present in the more distant dwarfs. From this, the mass of the ambient medium responsible for stripping is inferred. This dilute and presumably hot medium represents $\sim 10^{10}$ $M_\odot$, which is impressive, but still not sufficient to account for the missing galactic baryons. However, if this medium was comparable to the size of the Local Group or larger, the gas mass would be of cosmological significance.

The evidence points to a Milky Way halo plus a more extensive Local Group medium, so to characterize the properties of each, they must be separated observationally. There are three ways in which these two components can be distinguished observationally: by temperature; by velocity; and by spatial distribution on the sky. In terms of temperature, the characteristic potential well depth of the Milky Way and Local Group is $1\text{-}3\times10^6$ K, and while they both may have the identical temperature, there are reasons to believe they are different. Galactic X-ray emission studies indicate a temperature of 1.2×10^6 K for the thick halo (Snowden et al. 2000). In contrast, a higher temperature is expected for a Local Group medium, or of a medium that was expelled from the Galaxy ($2\text{-}3\times10^6$ K, if not greater). In this temperature range, differences of only a factor of two lead to a dramatically different set of C, N, and O column densities, as inferred from Figure 2. By combining emission observations in the same direction as absorption line data, we can infer information about the abundance, if the gas is cospatial. The emission measure contains the electron density while the absorption is proportional to the ionic column, so by combining them, abundances can be derived.

A complementary diagnostic for distinguishing between Galactic and Local Group components is the velocity of the gas, which should vary by a few hundred km s^{-1}. For example, the difference between the heliocentric velocity and the Galactocentric velocity can be up to 316 km s^{-1}, depending on the line-of-sight. If there is a hot Galactic halo that is rotating with the Milky Way, it will produce a clear signature of velocity as a function of longitude. Relative to the Galactocentric velocity, M31 differs by -250 km s^{-1} and the barycenter of the Local Group differs by about -100 km s^{-1}. The velocity differences depend on latitude and longitude on the sky, so with good velocity centroids, the different components are separable. With sufficiently high velocity resolution, one could separate components that have similar ionic distributions. The intrinsic Doppler widths of the lines are about 50 km s^{-1} and the sound speed of the gas is 100 km s^{-1} (typical of turbulence, if present), so component identification is possible in principle, but impossible at the resolution of existing instruments (700 km s^{-1}).

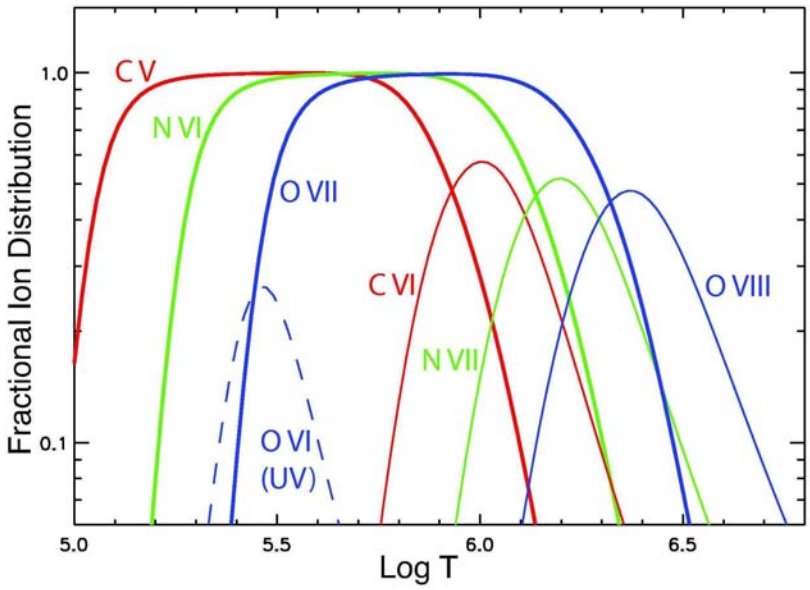

Figure 2. The fractional ionization distribution for the six most easily detectable ions from X-ray absorption line measurements, plus OVI (a UV line). The ions C VI, N VII, and O VIII should trace the ambient gas in the potential well of the Milky Way and Local Group, which has an equivalent temperature of $1\text{-}3\times10^6$ K. The lower temperature ions, such as O VI and C V, trace cooling gas or material in conductive or turbulent interfaces. The presence of multiple elements at similar temperatures allows one to measure abundance ratios.

A third and very powerful approach for separating the various components is the angular distribution, which was used with *ROSAT* emission observations to reveal the flattened hot gas halo around the Milky Way (Pietz et al. 1998; Snowden et al. 2000). Also, it is possible to separate absorption by hot gas from the Milky Way with that of the Local Group. The Local Group is non-spherical so gas will be extended along the long axis of the system (toward M31; l = 121°) while Galactic gas has its highest column density in sight lines across the Galaxy (Figure 3). Furthermore, the size of a Galactic halo can be inferred from the distribution of column densities with Galactic latitude and longitude. An initial effort along these lines was carried out with *XMM* observations of the OVII absorption line (Bregman and Lloyd-Davies 2007). It supports the presence of a hot Galactic halo, but the size and distribution of the hot halo are

poorly known, primarily due to the limited number of sightlines and the poor S/N of the observations. The *XMM* data showed the weaker O VIII resonance line along four sightlines and so was not useful for angular studies.

The gas masses in an extended Galactic halo and in the Local Group are considerable. Current observations give us the ionic column densities, which can be converted to masses when a radius for the absorbing region is adopted. A Galactic halo of radius 100 kpc corresponds to a gas mass of $10^{10.5}$ $M_{\odot}$, while if the OVII absorption line is caused by Local Group gas, the mass is $10^{12.5}$ $M_{\odot}$, exceeding the baryon content of all Local Group galaxies(Rasmussen, Kahn, and Paerels 2003; Nicastro et al. 2002); this could account for the missing baryons.

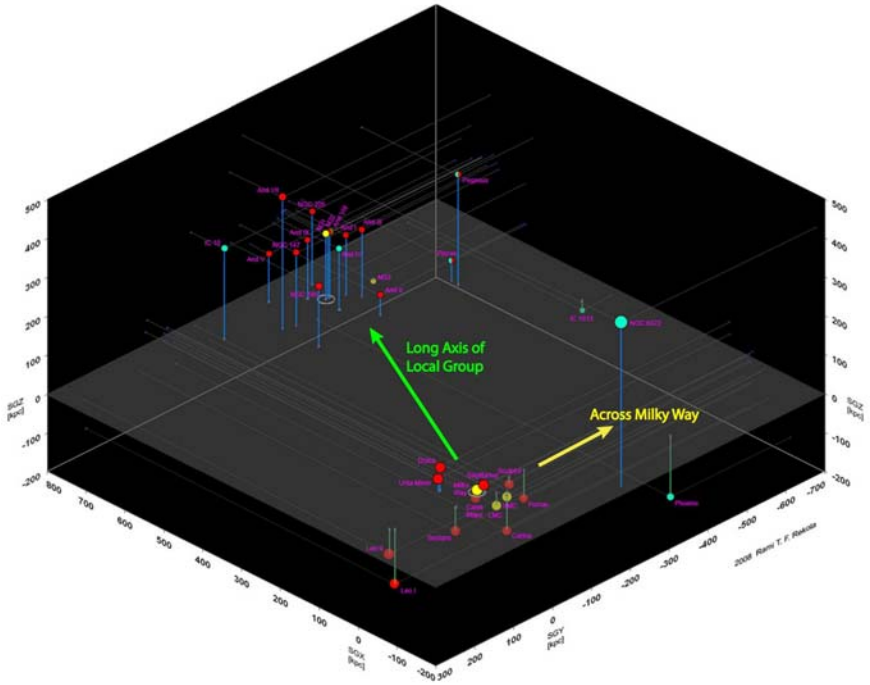

Figure 3. A three-dimensional representation of most of the Local Group, showing the vector directions across the Milky Way and along the long axis of the Local group, which differ by 120°.

2. Observational Considerations

The observed X-ray absorption lines are 5-20 times larger than those expected from the WHIM, which originate in lower density regions. This is why OVII at z = 0 has been detected along 10 lines of sight at S/N = 3-13 with *XMM* and *Chandra*. Many more lines of sight are needed to determine the size of a Galactic halo and a Local Group medium. To achieve the science goals, we need line centroids of 100 km/sec or less, and column density measurements for at least 100 objects.

Both goals are easily achieved with a future X-ray mission such as the *International X-Ray Observatory* (*IXO*), which has a baseline spectral resolution of 100 km s^{-1} (centroids to 10-30 km/sec can be obtained) and it is 15 times faster than *XMM* for spectral line detection, so we can measure absorption lines toward hundreds of AGNs. Many of these observations will be obtained for free because the gratings are always present, so adequate spectra will be obtained for any observation of an AGN brighter than about 1×10^{-11} erg cm^{-2} s^{-1} that is observed for

longer than 30 ksec. More than 100 AGNs will be observed in this parallel mode, based on the usage of previous X-ray telescopes and on other anticipated *IXO* projects. There are many known objects yet brighter, and in the *ROSAT* All Sky Survey, there are 421 objects with fluxes above 1×10^{-11} erg cm^{-2} s^{-1} (most of which are AGN; Figure 4), for which high-quality spectra could be obtained with modest observing times (Figure 5). Investigators might propose targeted programs such as: additional lines of sight across the Milky Way ($-45° < l < 45°$), to better constrain Galactic halo models and measure halo rotation; observations of the hot halos of Local Group galaxies, using AGNs projected within a virial radius; or observations of the Magellanic Stream and high velocity clouds, complementing the UV studies of OVI (Wakker et al. 2003). We expect this to be a vibrant field with IXO that will use several Msec of time, depending on how projects are conducted.

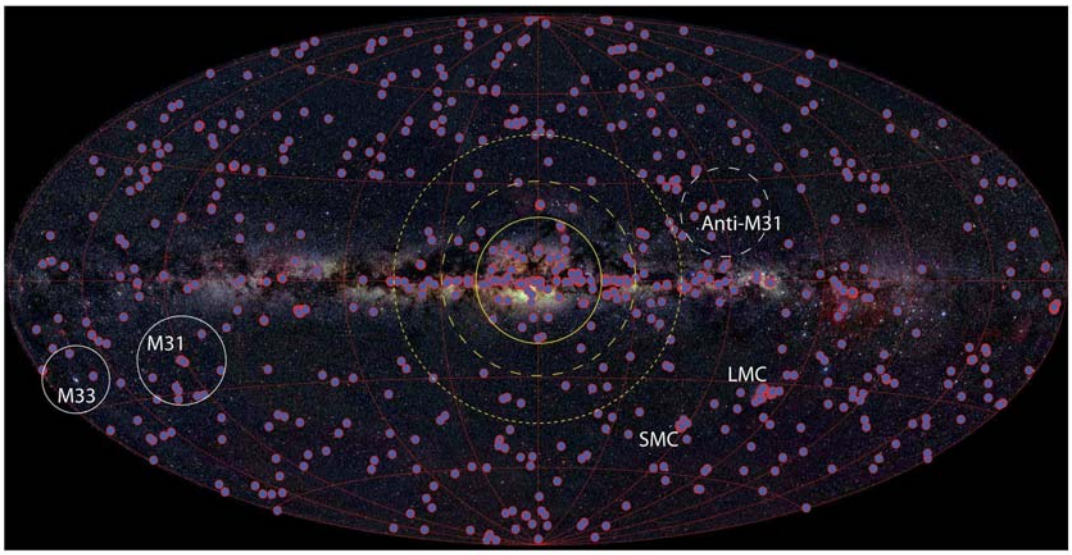

Figure 4. An optical image of the Milky way with the 421 X-ray sources with $F_X > 1\times10^{-11}$ erg cm^{-2} s^{-1} (0.5-2.5 keV), all of which can produce high-quality X-ray absorption line spectra (Fig. 5; nearly all sources away from the plane are AGNs). Regions around the bulge (yellow circles) will have the largest columns in a Galactic model and should show redshifts (1st quadrant) and blueshifts (4th quadrant) caused by rotation. A Local Group component should have relatively low column densities in the anti-M31 direction and the greatest columns along the long axis of the Local Group, toward M31 and M33.

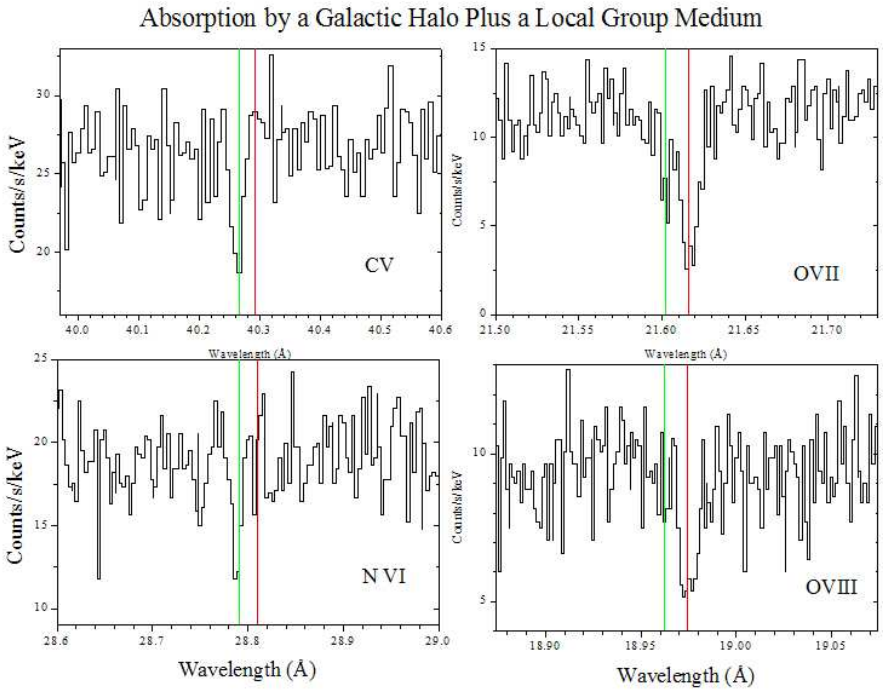

Figure 5. A simulated IXO grating spectrum with the baseline resolution and collecting area (R = 3000, 1000 cm^2) of a background AGN with the product of the flux and exposure time of ($F_x/2\times10^{-11}$ erg/cm^2/s) (t/50 ksec). There are two components in the model, a 0.8×10^6 K Galactic halo component (green line) and a 2×10^6 K Local Group medium, offset by 200 km/s (red line). The cooler Galactic component is detected at the lower temperature ions while the hotter Local Group medium is detected in the higher temperature ions and shifted in velocity.

References

Blitz, L., & Robishaw, T. 2000, ApJ, 541, 675.
Bowen, D.V. et al. 2008, ApJS, 176, 59.
Bregman, J.N., and Lloyd-Davies, E.J. 2007, ApJ, 669, 990.
Fox, A.J., Savage, B.D., Wakker, B.P., Richter, P., Sembach, K.R., & Tripp, T.M. 2004, ApJ, 602, 738.
Grcevich, J., & Putman, M.E 2009, arXiv:0901.4975.
Nicastro, F., Zezas, A., Drake, J., Elvis, M., Fiore, F., Fruscione, A., Marengo, M., Mathur, M., and Bianchi,S. 2002, ApJ, 573, 157.
Pietz, J., Kerp, J., Kalberla, P.M.W., Burton, W.B., Hartmann, D., and Mebold, U. 1998, A&A, 332, 55.
Rasmussen, A., Kahn, S.M., and Paerels, F. 2003, in "The IGM/Galaxy Connection", ed. J.L. Rosenberg and M.E. Putman (Kluwer, Dordrecht), p. 109.
Snowden, S.L., Freyberg, M.J., Kuntz, K.D., & Sanders, W.T. 2000, ApJS, 128, 171.
Wakker, B.P., et al. 2003, ApJS, 146, 1.
Yao, Y., Nowak, M. A., Wang, Q. D., Schulz, N. S., and Canizares, C. R. 2008, ApJ, 672, L21.

The Behavior of Matter Under Extreme Conditions

A White Paper Submitted to the *Astro2010* Decadal Survey of Astronomy and Astrophysics

F. Paerels[1], M. Méndez[2], M. Agueros[1], M. Baring[3], D. Barret[4], S. Bhattacharyya[5], E. Cackett[6], J. Cottam[7], M. Díaz Trigo[8], D. Fox[9], M. Garcia[10], E. Gotthelf [1], W. Hermsen[11], W. Ho[12], K. Hurley[13], P. Jonker[11], A. Juett[7], P. Kaaret[14], O. Kargaltsev[9], J. Lattimer[15], G. Matt[16], F. Özel[17], G. Pavlov[9], R. Rutledge[18], R. Smith[10], L. Stella[19], T. Strohmayer[7], H. Tananbaum[10], P. Uttley[12], M. van Kerkwijk[20], M. Weisskopf[21], S. Zane[22]

[1] Columbia University, [2] University of Groningen, [3] Rice University, [4] CESR Toulouse, [5] Tata Institute of Fundamental Research, Mumbai, [6] University of Michigan, [7] NASA Goddard Space Flight Center, [8] European Space Astronomy Centre, ESA, [9] Penn State University, [10] Harvard-Smithsonian Center for Astrophysics, [11] SRON Netherlands Institute for Space Research, [12]University of Southampton, [13] University of California at Berkeley, [14] University of Iowa, [15] SUNY Stony Brook, [16] Università degli Studi Roma Tre, [17] University of Arizona, [18] McGill University,[19] Osservatorio Astronomico di Roma, [20] University of Toronto, [21] NASA Marshall Space Flight Center, [22] Mullard Space Science Laboratory

The Behavior of Matter Under Extreme Conditions

Abstract

The cores of neutron stars harbor the highest matter densities known to occur in nature, up to several times the densities in atomic nuclei. Similarly, magnetic field strengths can exceed the strongest fields generated in terrestrial laboratories by ten orders of magnitude. Hyperon-dominated matter, deconfined quark matter, superfluidity, even superconductivity are predicted in neutron stars. Similarly, quantum electrodynamics predicts that in strong magnetic fields the vacuum becomes birefringent. The properties of matter under such conditions is governed by Quantum Chromodynamics (QCD) and Quantum Electrodynamics (QED), and the close study of the properties of neutron stars offers the unique opportunity to test and explore the richness of QCD and QED in a regime that is utterly beyond the reach of terrestrial experiments. Experimentally, this is almost virgin territory.

1 Introduction: The Fundamental Properties of Matter at High Densities

Seven decades after the first speculation on the existence of gravitationally bound neutron configurations (Landau 1932, 1938), we still know very little about the fundamental properties of neutron stars. Initial attempts to model their mechanical properties were based on the assumption that the matter can be adequately described as a degenerate gas of free neutrons, but it has become progressively clear that the cores of neutron stars must in fact be the stage for intricate and complex collective behavior of the constituent particles.

Over most of the range of the density/temperature phase plane, Quantum Chromodynamics (QCD) is believed to correctly describe the fundamental behavior of matter, from the subnuclear scale up. The ultimate constituents of matter are quarks, which are ordinarily bound in various combinations by an interaction mediated by gluons to form composite particles. At very high energies, a phase transition to a plasma of free quarks and gluons should occur, and various experiments are currently probing this low-density, high temperature limit of QCD (*e.g.* Tannenbaum 2006). Likewise, the QCD of bound states is beginning to be quantitatively understood; recently, the first correct calculation of the mass of the proton was announced (Dürr et al. 2008).

The opposite limit of high densities and low (near zero, compared to the neutron Fermi energy) temperature QCD has been predicted to exhibit very rich behavior. At densities exceeding a few times the density in atomic nuclei ($\rho \sim 3 \times 10^{14}$ g cm^{-3}), exotic excitations such as hyperons, or Bose condensates of pions or kaons may appear. It has also been suggested that at very high densities a phase transition to strange quark matter may occur. When and how such transitions occur is of course determined by the correlations between the particles, and the ultra-high-density behavior of matter is governed by many-body effects. This makes the direct calculation of the properties of matter under these conditions from QCD extremely difficult.

Figure 1 shows the temperature-chemical potential phase plane, in which the locus of the phase transition from the hadron gas to the quark-gluon plasma has been indicated. The

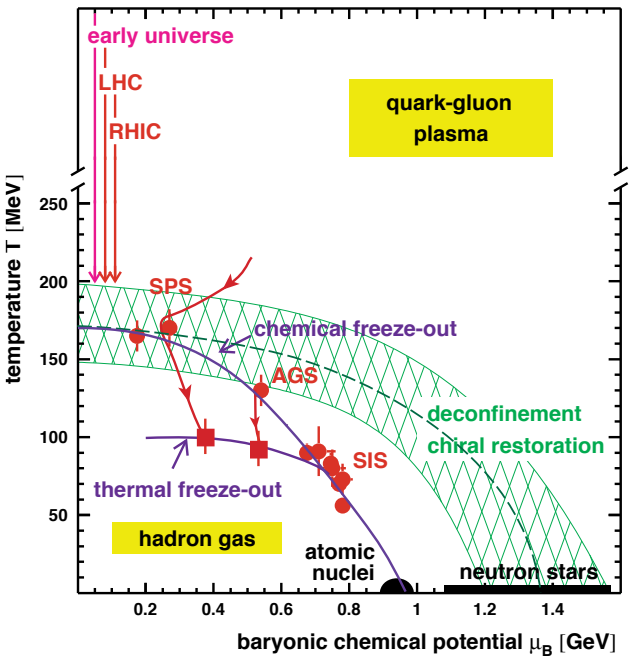

Figure 1: At high energies or high densities, normal hadronic matter is expected to dissolve into a quark-gluon plasma, as shown in the upper right hand corner of the temperature-chemical potential phase plane; the green zone marks the transition region. Terrestrial experiments probe the low-density, high-temperature limit (shown below 'Early Universe'). The high-density, low-temperature limit is expected to be marked by the appearance of exotic matter and phase transitions. This regime, beyond the density in atomic nuclei, can only be probed by astrophysical observations of neutron stars (*Courtesy NA49 Collaboration, SPS, CERN*)

only possible way to probe the high density, low temperature limit of QCD is by observations and measurements of the densest material objects in nature, neutron stars.

2 The Mass-Radius Relation of Neutron Stars

The relation between pressure and density, the equation of state, is the simplest way to parameterize the bulk behavior of matter. It governs the mechanical equilibrium structure of bound stars, and, conversely, measurements of quantities such as the mass and the radius, or the mass and the moment of inertia of a star, probe the equation of state. Figure 2 shows the mass-radius plane for neutron stars, with a number of possible mass-radius relations based on various assumptions concerning the equation of state (Lattimer and Prakash 2007). Two families of solutions have been indicated: the equations of state for stars made up of bound quark states (baryons and mesons), and solutions for stars in which a phase transition has converted most of the stellar matter to strange quark matter. The former stars are gravitationally bound, and for a degenerate fermion gas, the radius generally decreases with increasing mass of the configuration. The quark stars, on the other hand, are self-bound, and exhibit, very roughly, an increase in radius with increasing mass. In the same figure, a number of constraints have been indicated, derived from, for instance, the maximum stable mass of neutron stars, and a number of broad constraints derived from observations (such as the high spin frequencies of two neutron stars). It is obvious that definitive constraints can only be derived from simultaneous measurement of masses and radii of individual neutron stars.

Effective discrimination between different families of hadronic equations of state will require a relative precision of order 10% in mass and radius, and similar requirements apply to the strange equations of state. In order to settle the question as to whether strange stars

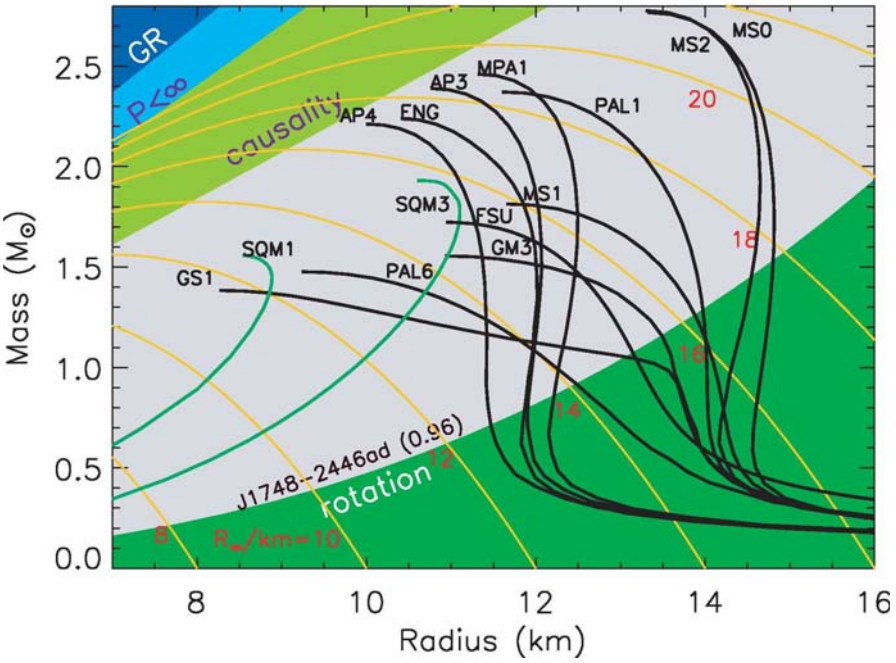

Figure 2: The mass-radius relationship for neutron stars reflects the equation of state for cold superdense matter. Mass-radius trajectories for typical EOSs are shown as black curves. Green curves (SQM1, SQM3) are self-bound quark stars. Orange lines are contours of radiation radius, $R_\infty = R/\sqrt{1-2GM/Rc^2}$. The dark blue region is excluded by the GR constraint $R > 2GM/c^2$, the light blue region is excluded by the finite pressure constraint $R > (9/4)GM/c^2$, and the light green region is excluded by causality, $R > 2.9GM/c^2$. The green region in the right-hand corner shows the region $R > R_{\rm max}$ excluded by the 716 Hz pulsar J1748-2446ad (Hessels et al. 2006). From Lattimer and Prakash (2007).

exist in nature, the requirements depend on stellar mass. Since the hadronic and strange mass-radius relations cross in the region $\sim 1.3 - 1.8 M_\odot$, $12 - 16$ km (ironically, those are the textbook values for the mass and the radius!), we need to be able to probe a range of masses, or else have to rely on very difficult high-precision measurements.

3 Breakthrough Potential: X-ray Observations

3.1 Current Status

Neutron stars have been the subject of intensive radio observations for forty years, and this work has indeed produced a wealth of fundamental advances (see for instance, Blandford et al. 1993); probably the most famous among these is the confirmation of the prediction of the gravitational wave power emitted by a relativistic binary based on Einstein's quadrupole formula, which earned Hulse and Taylor a Nobel prize (for recent data, see for instance Weisberg and Taylor 2005). As far as the fundamental properties of the stars themselves are concerned, precise radio pulse arrival time measurements on double neutron star binaries have produced a series of exquisite mass determinations, with a weighted average stellar mass of $M_{\rm NS} = 1.413 \pm 0.028 M_\odot$ (the error is the weighted average deviation from the mean;

see, for instance, Lattimer and Prakash 2007). But we need the mass and the radius, or two other quantities derived from the internal structure, simultaneously. There is currently no hope of measuring the stellar radii for the neutron stars for which we have a precise mass, from radio or other observations (with one possible exception, see below).

Most of what we know about the fundamental properties of ordinary stars is based on a close study of the emission spectrum emerging from their photospheres. Neutron stars are small and relatively far away; detecting optical or UV radiation from their surfaces is extremely difficult, and in any case, the optical/UV emission will be on the Rayleigh-Jeans tail of the stellar spectrum, which is not particularly sensitive to the stellar properties. Optical radiation has been detected in a few cases (see Kaspi, Roberts, and Harding 2006 for a review), but it is likely that this corresponds to emission from an unknown fraction of the stellar surface, which makes it impossible to use these data for radius measurement. Looking for higher-luminosity objects means looking for hotter objects (assuming the radii of all neutron stars are comparable in size), and the natural wavelength band for photospheric observations is the X-ray band.

X-ray emission originating on the surfaces of neutron stars was first detected in X-ray bursts from accreting neutron stars in Low-Mass X-ray Binaries (LMXBs), and photospheric emission has also been detected from quiescent and isolated objects (*e.g.* Strohmayer and Bildsten 2006; Guillot et al. 2009, and references therein). These data had low spectral resolution and often limited signal-to-noise; they have provided a very rough check on the order of magnitude of neutron star radii, but precise measurement awaits the development of stellar atomic spectroscopy of neutron stars, as well as a series of more exotic techniques that take advantage of general relativistic effects on the surface emission. With observations performed with the diffraction grating spectrometers on the *Chandra* and *XMM-Newton* observatories, this problem has come to the threshold of being resolved—the next step, based on sensitive, time resolved X-ray spectroscopy and energy-resolved fast photometry has the unique potential of finally providing the window into QCD that the 'Cold Equation of State' will open up.

The current observational situation is roughly the following. There is evidence for atomic photospheric absorption in the burst spectrum of at least one accreting neutron star (EXO0748−646; Cottam, Paerels, & Mendez 2002), which has led to a measurement of the gravitational redshift at the stellar surface ($z = 0.35$). Likewise, the distance to a number of hot, intermittently accreting neutron stars is known, because they are located in Globular Clusters. Once accretion ceases, the atmospheres of these stars should simply consist of pure H, and the spectrum can be calculated; this sample of stars with known distance can be extended (Guillot et al. 2009, and references therein). Three apparently isolated neutron stars have a parallax measurement (Walter and Lattimer 2002; Kaplan, van Kerkwijk, and Anderson 2002, 2007; Pavlov et al. 2008).

3.2 Opportunities

Several techniques are available with sensitive X-ray spectroscopy and fast photometry. Spectroscopic observations of X-ray bursts give the atomic absorption spectrum, which, through pressure broadening and GR effects, is sensitive to both the acceleration of gravity at the stellar surface, as well as the redshift. Measuring two different functions of mass and radius

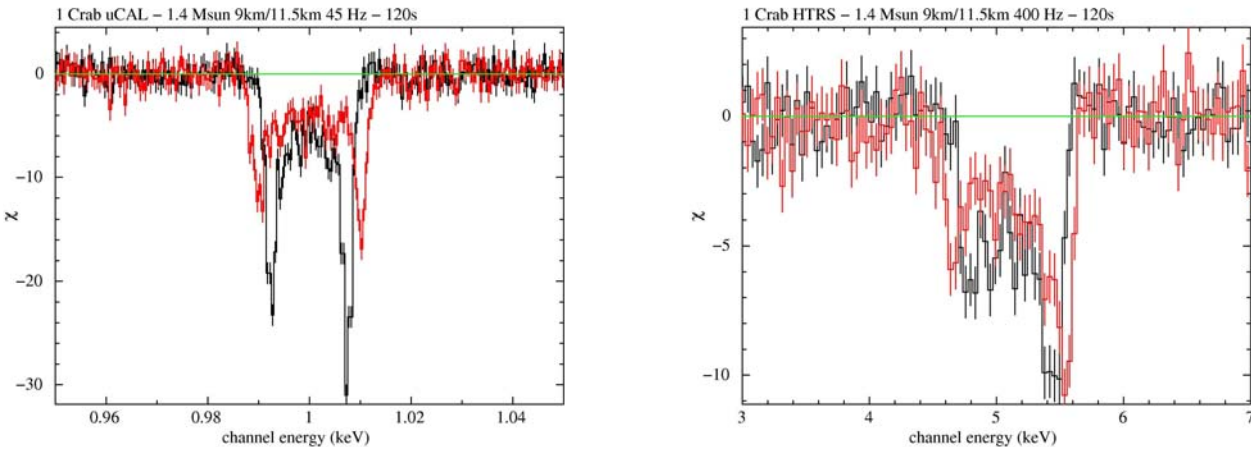

Figure 3: **High resolution X-ray spectroscopy of the photospheric emission of a hot neutron star is sensitive to the fundamental stellar parameters**, through the effects of pressure broadening, relativistic kinematics (rotation, Doppler shift, time dilation, beaming), and general relativity (light bending around the star, gravitational redshift, frame dragging) on atomic absorption lines (Özel and Psaltis 2003; Bhattacharyya, Miller, and Lamb 2006). The absorption line spectrum of a $1.4 M_\odot$ neutron star, spinning at 45 Hz, showing the effects of rotational Doppler-splitting, observed at 2 eV spectral resolution (*left panel*), in 120 sec of exposure of a moderately bright X-ray burst with the microcalorimeter spectrometer as envisioned for the *IXO* mission. Black and red histograms refer to a star with a radius of 9 and 11.5 km, respectively. Emission is concentrated in a hot equatorial belt, seen at 5 degree inclination. The absorption line is Fe XXVI Hα. **High time resolution spectroscopy can phase-resolve the Doppler broadening** of a rapidly spinning star (400 Hz) if the surface emission is azimuthally asymmetric. With $\sim$ 100 eV energy resolution, and sub-msec time resolution (such as for the fast timing instrument on *IXO*), the Doppler profiles *in the right hand panel* will be phase-resolved, allowing unambiguous determination of the line broadening mechanism, and an absolute radius measurement (Fe XXVI Lyα; same stellar parameters as before).

thus gives mass and radius, separately. For neutron stars at known distance, measured fluxes compared to the flux emerging from the stellar photosphere will give the stellar radius. The continuum spectral shape is sensitive to the surface gravity, again allowing a mass and radius measurement.

The ability to time- and energy-resolve emission from bursting or spinning stars provides unique observational leverage. In particular, a capability to perform rapid (tens of microseconds or less) spectroscopy allows resolving (and uniquely identifying) the severe Doppler broadening associated with high stellar spin frequencies known to occur in most LMXBs. For objects with a known spin period, the Doppler broadening provides a direct measurement of the stellar radius. GR light bending effects on the phase modulation (of the absorption lines as well as the total flux) again produce a measurement of the acceleration of gravity at the surface. In cases where an atomic absorption line is detected, a redshift measurement is sufficient (with redundancy in the pressure broadening). Note that the magnetic field strengths in LMXB's are small enough ($< 10^9$ G) that Zeeman splitting is not important.

High-speed, high-time resolution photometry of quasi-periodic intensity fluctuations as-

sociated with the inner accretion disk in accreting neutron stars can yield absolute sizes, if light-travel time effects can be resolved (reverberation). A time-delay spectrum within the frequency range of the variability immediately provides the physical size of the inner rim of the accretion disk, where reprocessed soft photons come from, and hence an upper limit to the neutron-star radius in km, independent of the other stellar parameters (Gilfanov et al. 2003; Vaughan et al. 1997, 1998). Likewise, Fe K line emission reverberation yields the same information (Cackett et al. 2008).

There is multiple redundancy in several techniques, and we will have a choice Fof techniques to cover a range of expected stellar spin periods (spin frequencies up to several hundred Hz have been measured in LMXBs). Most of the necessary theoretical development (full radiative transfer neutron star atmosphere models, effects of light bending on distant observer flux spectrum, etc.) is in place.

The precision required to make definitive measurements of the neutron star mass-radius relation is within reach with currently feasible technology. The energy resolution of cryogenic X-ray spectrometers, such as microcalorimeters, is sufficient to detect photospheric absorption lines and measure their profiles. The count rate capability, time resolution, and CCD-style energy resolution of Si drift detectors meet the requirements of fast energy-resolved timing. The *International X-ray Observatory*'s capabilities, with a high energy resolution microcalorimeter spectrometer[1], and a high time-resolution medium energy-resolution spectrometer[2] are ideal for a definitive solution to the Cold Equation of State problem. With the effective area, energy resolution, and timing capability of *IXO*, the list of potential targets is at least a dozen deep for X-ray burst sources, and several quiescent LMXBs will be observable as well.

Finally, the X-ray techniques will complement possible results from radio pulsar observations. The binary radio pulsar PSR J0737 − 3039 is known to exhibit a pulse arrival time evolution of one of the two members that may signal relativistic spin-orbit coupling of the binary. If that is indeed correct, the moment of inertia of this neutron star may be measurable, in addition to its mass, and these two quantities together constrain the equation of state (Lyne et al. 2004; Kramer and Stairs 2008; see also Lattimer and Prakash 2007). The mass of this neutron star is close to the average mass of observed for radio pulsar neutron stars, and so this measurement may have limited leverage on the problem of distinguishing between hadronic and strange equations of state (see Figure 2). Neutron stars in mass-transferring binaries will give us access to a wider range of neutron star masses (of order a solar mass of material can be transferred over the lifetime of an LMXB), to address this fundamental issue.

4 Additional Science

We now know that neutron stars with surface magnetic field strengths in excess of 10^{14} Gauss exist (Duncan and Thompson 1992). At field strengths exceeding $m_e^2c^3/\hbar e = 4.4 \times 10^{13}$ G, QED predicts novel effects, such as vacuum birefringence; in the presence of matter, resonant polarization mode conversion will occur (Lai and Ho 2003, and references therein). Direct X-

[1]the X-ray Microcalorimeter Spectrometer, or XMS instrument

[2]the High Time Resolution Spectrometer, or HTRS instrument

ray spectroscopy of such objects may reveal proton cyclotron resonance absorption at photon energy $0.6(1+z)^{-1}(B/10^{14}\ \mathrm{G})$ keV (Bezchastnov et al. 1996), in spite of the relatively small transition probability (*e.g.* Ho and Lai 2001). The shape and angular dependence of the photospheric X-ray spectrum will reflect these various effects (*e.g.* van Adelsberg and Lai 2006). Alternatively, the spectrum could show atomic absorption features (*e.g.* Zavlin and Pavlov 2002; Hailey and Mori 2002). Moreover, the surface emission of all strongly magnetized neutron stars should exhibit a strong, energy-dependent polarization (Pavlov and Zavlin 2000). With polarizations of up to tens of percent, and a potentially dramatic phase dependence, X-ray polarimetry can probe this regime of QED for the first time.

Finally, should we find neutron stars with a combination of mass and radius that is in conflict with all physically plausible equations of state (for instance, a $1.4M_{\odot}$, 18 km object; see Figure 2), we would have evidence that we are probing modifications to the equation of hydrostatic equilibrium, and not the equation of state: the neutron star mass-radius relation measurements can reveal deviations from the standard theory of gravity. The measurement technique is equally sensitive to neutron star parameters both inside and outside the region of the mass-radius plane covered by the equation of state margins of uncertainty, and so is also an entirely novel probe of gravity itself (Psaltis 2008).

References

Bezchastnov, V. G., Pavlov, G. G., and Shibanov, Yu. A., 1996, in *Gamma Ray Bursts*, AIP Conf. Proc., **384**, 907

Bhattacharyya, S., Miller, M. C., and Lamb, F. K., 2006, *Astrophys. J.*, **664**, 1085

Blandford, R. D., 1993, in *Pulsars as Physics Laboratories*, Oxford UP, 1993

Cackett, E. M., et al. 2008, *Astrophys. J.*, **674**, 415

Cottam, J., Paerels, F., and Méndez, M., 2002, *Nature*, **420**, 51

Duncan, R. C., and Thompson, C., 1992, *Astrophys. J. (Letters)*, **392**, L9

Dürr, S., et al., 2008, *Science*, **322**, 1224

Gilfanov, M., Revnivtsev, M., and Molkov, S., 2003, *Astron. Astrophys.*, **410**, 217

Guillot, S., Rutledge, R. E., Bildsten, L., Brown, E. F., Pavlov, G. G., and Zavlin, V. E., 2009, *Mon. Not. Royal Astr. Soc.*, **392**, 665

Hessels, J. W. T., et al., 2006, *Science*, **311**, 1901

Hailey, C., and Mori, K., 2002, *Astrophys. J. (Letters)*, **578**, L133

Ho, W. C. G., and Lai, D., 2001, *Mon. Not. Royal Astr. Soc.*, **327**, 1081

Kaaret, P., et al., 2006, *Astrophys. J. (Letters)*, **257**, L97

Kaplan, D. L., van Kerkwijk, M. H., and Anderson, J. 2002, *Astrophys. J.*, **571**, 447

——, 2007, *Astrophys. J.*, **660**, 1428

Kaspi, V. M., Roberts, M. S. E., and Harding, A. K., 2006, in *Compact Stellar X-ray Sources*, W. H. G. Lewin and M. van der Klis (Eds.), Cambridge UP, 2006 (astro-ph/0402136)

Kramer, M., and Stairs, I. H., 2008, *Ann. Rev. Astron. Astrophys.*, **46**, 541

Lai, D., and Ho, W. C. G., 2003, *Phys. Rev. Letters*, **91**, 071101

Landau, L. D., 1932, *Physikalische Zeitschrift der Sowjetunion*, **1**, 285

Landau, L. D., 1938, *Nature*, **141**, 333

Lattimer, J. M., and Prakash, M., 2007, *Physics Reports*, **442**, 109

Lyne, A. G., et al., 2004, *Science*, **303**, 1153

Özel, F., and Psaltis, D., 2003, *Astrophys. J.*, **529**, 1011

Pavlov, G. G., and Zavlin, V. E., 2000, *Astrophys. J. (Letters)*, **582**, L31

Pavlov, G. G., Kargaltsev, O., Wong, J. A., and Garmire, G. P., 2008, astro-ph/0803.0761

Psaltis, D., 2008, *Living Reviews in Relativity*, **11**, no. 9 (cited on 1-21-2009)

Strohmayer, T., and Bildsten, L., 2006, in *Compact Stellar X-ray Sources*, W. H. G. Lewin and M. van der Klis (Eds.), Cambridge UP, 2006 (astro-ph/0301544)

Tannenbaum, M. J., 2006, *Rep. Prog. Phys.*, **69**, 2005

van Adelsberg, M., and Lai, D., 2006, *Mon. Not. Royal Astr. Soc.*, **373**, 1495

Vaughan, B. A., et al., 1997, *Astrophys. J. (Letters)*, **483**, L115; erratum, 1998, *Astrophys. J. (Letters)*, **509**, L145

Walter, F. M., and Lattimer, J. M., 2002, *Astrophys. J. (Letters)*, **576**, L145

Weisberg, J. M., and Taylor, J. H., 2005, in *Binary Radio Pulsars*, ASP Conf. Proc., **328**, 25

Zavlin, V. E., and Pavlov, G. G., 2002, MPE Reports, **278**, 273 (astro-ph/0206025)

X-ray Studies of Planetary Systems: An Astro2010 Decadal Survey White Paper

Eric Feigelson[1], Jeremy Drake[6], Ronald Elsner[2], Alfred Glassgold[3], Manuel Güdel[4], Thierry Montmerle[5], Takaya Ohashi[7], Randall Smith[6], Bradford Wargelin[6], and Scott Wolk[6]

[1]*Pennsylvania State University,* [2]*NASA's Marshall Space Flight Center,* [3]*University of California, Berkeley,* [4]*Swiss Federal Institute of Technology Zürich,* [5]*Laboratoire d'Astrophysique de Grenoble,* [6]*Harvard-Smithsonian Center for Astrophysics* [7]*Tokyo Metropolitan University*

1. Introduction

It may seem counterintuitive that X-ray astronomy should give any insights into planetary systems: planets, and their natal protoplanetary disks (PPDs), have temperatures which are far too cool ($100 - 1500$ K) to emit X-rays. However, planets orbit stars whose magnetized surfaces divert a small fraction of the stellar energy into high energy products: coronal UV and X-rays, flare X-rays and energetic particles, and a high-velocity stellar wind. In our Solar System, these components from the active Sun interact with the cool orbiting bodies to produce X-rays through various processes including charge-exchange between ionized and neutral components. **The resulting X-ray emission gives unique insights into the solar activity, planetary atmospheres, cometary comae, charge exchange physics, and space weather across the Solar System** (review by Bhardwaj et al. 2007).

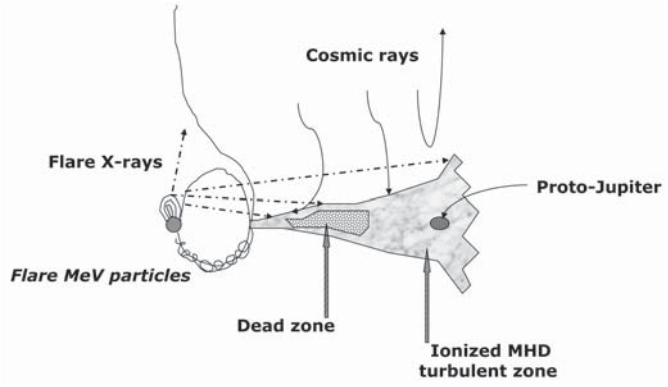

Fig. 1.— *Protoplanetary disk illuminated by flare X-rays and its effects on disk ionization.*

Solar-type stars also universally exhibit enhanced magnetic activity during their youth. X-ray emitting flares in pre-main sequence stars are 100 - 10,000× more powerful and frequent than in older stars like today's Sun, and this emission only gradually declines over the first billion years on the main sequence (reviews by Feigelson et al. 2007; Güdel 2007). The X-rays and energetic particles from flares will irradiate protoplanetary disk gases and solids (review by Glassgold et al. 2000). As a result, it is possible that **the stellar activity of young stars will substantially affect PPDs and planet formation processes** by heating disk outer layers, producing reactive ion-molecular species, inducing disk turbulence via ionization, and explaining conundrums in the meteoritic and cometary record such as isotopic anomalies, chondrule melting, and radial mixing (see Figure 1). Later, X-ray and ultraviolet irradiation will speed evaporation of planetary atmospheres and thereby perhaps affect planet habitability.

Discoveries of X-rays from Solar System bodies were made with the full range of X-ray astronomical satellite observatories over the past three decades, from the discovery of Jupiter's emission with the *Einstein Observatory* and cometary comae with *ROSAT* to the study today of planets and moons with the *Chandra X-ray Observatory* and *XMM-Newton*. X-rays from young stars are now investigated in thousands of pre-main sequence stars in the nearby Galaxy. Today, ~ 40 papers/year are published on the observations and implications of X-ray emission relating to planetary science. But the X-ray emission is faint, time variable and spectrally complex − today's instrumentation can achieve only a small portion of the potential scientific advances in planetary sciences. The planned high-throughput International X-ray Observatory (IXO) will propel this nascent field forward.

We highlight here five studies in planetary science done using X-ray observations. These

studies address in unique ways several of NASA's strategic goals (Science Mission Directorate 2006) concerning the effects of the Sun on its planets, the physics of planetary ionospheres and ion-neutral interactions, the role of stellar activity on planet habitability, and on the formation processes of planetary systems around young stars. These studies will complement NASA's strong program on Solar System exploration, extrasolar planet discovery, and planet formation environments.

2. Probing protoplanetary disks with the iron fluorescent line

The 19^{th} century insights into the origin of our Solar System involving gravitational collapse of cold gas with angular momentum have been validated in recent decades by the profound discoveries of infrared-emitting PPDs disks around nascent stars in nearby star forming regions and discoveries of extrasolar planetary systems around a significant fraction of older stars in the solar neighborhood. However, a number of enigmatic phenomena have been noted which indicate that non-equilibrium high energy processes play some role in planet formation. Laboratory study of meteorites and *Stardust* cometary material, which record processes in the planetesimal stage of our protoplanetary disk 4.567 Gyr ago, reveal flash-melted chondrules, calcium-aluminum-rich inclusions and free-floating grains with daughter products of short-lived spallogenic radionuclides, and composites with annealed or glassy components (reviews by Connolly et al. 2006; Chaussidon & Gounelle 2006). Infrared spectroscopic studies of some distant PPDs with NASA's *Spitzer Space Telescope* reveal heated and ionized gaseous outer layers (reviews by Najita et al. 2007; Bergin et al. 2007). While some of these phenomena can be attributed to the effects of violent events which precede gravitational collapse (such as supernova explosions), others require irradiation of disks by the X-rays and energetic particles from magnetic reconnection flares around the host young star. X-ray ionization should dominate cosmic ray ionization by several orders of magnitude (Glassgold et al. 2000). X-ray astronomers are thus joining the vibrant community of meteoriticists, infrared and millimeter spectroscopists, and theorists seeking **to understand non-equilibrium processes during the protoplanetary disk stage of planet formation.**

A particularly important consequence of X-ray irradiation of PPDs is the predicted induction of MHD turbulence by coupling the slightly-ionized gas to magnetic fields in a sheared Keplerian velocity field via the magneto-rotational instability. Harder X-rays ($>$ 10 keV) from powerful flares can penetrate deeply into protoplanetary disks, and may reach the PPD midplane where planets form. Astrophysicists are enormously interested in the possibility of turbulent PPDs as it appears to solve certain problems (e.g. gas viscosity needed for accretion, inhibition of Type I migration of larger protoplanets) while it raises other problems (e.g. inhibition of grain settling to the disk midplane, promotion of shattering rather than merger of small solid bodies). Stellar X-rays may also be responsible for the ionization needed to propel collimated protostellar bipolar outflows, for the evaporation of icy mantles in PPD grains, and for ion-molecular chemical reactions in the disks. X-rays may play a critical role in the photoevaporation and dissipation of older protoplanetary disks (Ercolano et al. 2008). Figure 1 illustrates various aspects of an X-ray illuminated PPD.

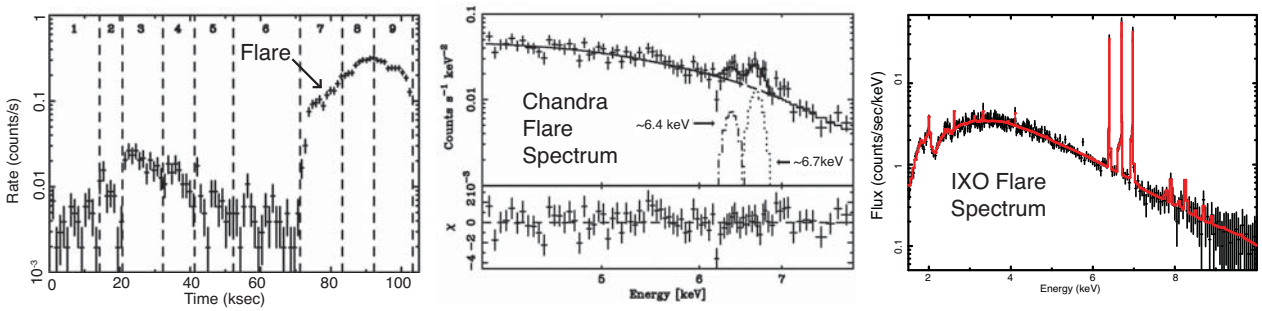

Fig. 2.— *Chandra light curve [Left] and CCD spectrum [Middle] showing the Fe 6.4 keV fluorescent line during a powerful flare from the protostar YLW 16A in the nearby Ophiuchi cloud (Imanishi et al. 2001). The high-ionization emission lines (6.7 keV) arise from the hot plasma confined in the flaring magnetic loop. [Right] Simulation of a 2 ks IXO XMS spectrum at the onset of the YLW 16A flare showing the Fe 6.4 keV fluorescent line. IXO will be able to see flares 100x fainter than currently possible.*

The strongest test of X-ray irradiation of PPDs is the fluorescent iron line at 6.4 keV, which is well-known to appear when a hard X-ray continuum from a central source illuminates cool disk material (e.g., in enshrouded active galactic nuclei and X-ray binary systems). The 6.4 keV emission line has been seen in a few flaring protostellar systems (see Figure 2) but typically lies beyond the sensitivity limit of current instrumentation. With the ~ 200 times improved sensitivity in the fluorescent line compared to *Chandra* and *XMM-Newton*, the IXO X-ray Microcalorimeter Spectrometer (XMS) detector will detect (or place strong constraints on) X-ray irradiation in hundreds of PPDs in the nearby Ophiuchus, Taurus, Perseus and Orion star forming clouds. The IXO Hard X-ray Imager (HXI) will separately establish the intensity of deeply-penetrating X-rays in the $10 - 30$ keV band needed to calculate PPD turbulent and "dead" zones. Prior to IXO's launch, the molecular and dust properties of these disks will be well-characterized by the *Spitzer*, *Herschel* and *James Webb* missions and ALMA telescope. By correlation of X-ray, molecular and solid properties in these systems, IXO should clearly establish the role of X-ray illumination on PPD physics and chemistry. It is not impossible that diversity in X-ray irradiation plays a critical role in the diversity of exoplanetary systems seen around older stars.

3. The complex X-ray emission of Jupiter and Mars

Jupiter is the most luminous X-ray emitter in the Solar System after the Sun. Its emission is complex with several spatially and temporally varying components: charge exchange lines from interaction with solar wind ions, fluorescence and scattering of solar X-rays, and a hard electron brems-strahlung emission (Bhardwaj et al. 2007). Charge exchange is the dominant process where heavy solar energetic ions collide with neutral atoms in the planetary atmosphere, producing a radiative cascade of non-thermal emission lines (e.g. from the $n = 5$ state of hydrogenic O^{7+} at 0.653 keV). In planets like Earth and Jupiter with a strong dipolar

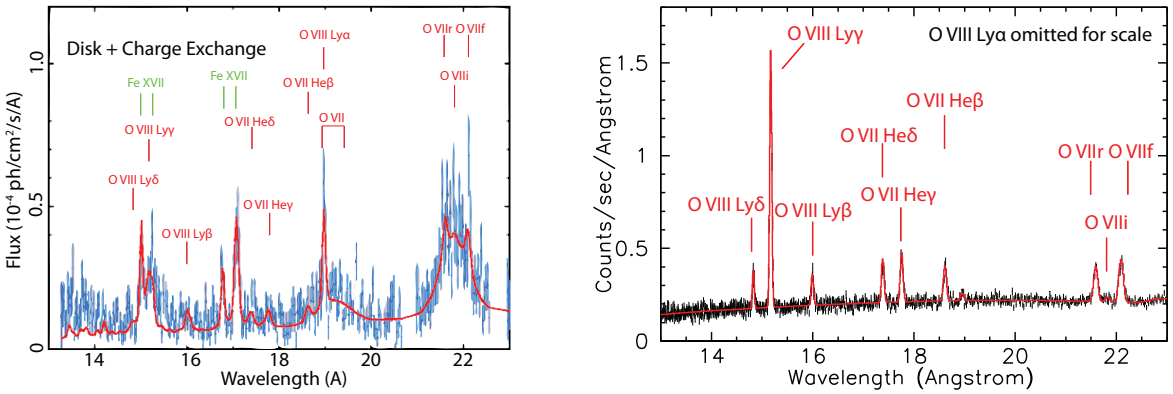

Fig. 4.— [Left] *XMM-Newton spectrum of Jupiter (blue) and a three-component model (red) consisting of auroral charge-exchange lines, solar reflection continuum, hard electron bremsstrahlung continuum(Branduardi-Raymont et al. 2007). [Right] Simulation of a 50 ks IXO spectrum based on the XMM-Newton emission model showing the oxygen charge-exchange emission lines; many more lines are expected.*

magnetic field, these X-ray components are concentrated in auroral regions around the north and south magnetic poles (see Figure 3). K-shell fluorescence from carbon and oxygen is the dominant X-ray emitting process from Venus and Mars where the atmospheres are rich in CO_2 and wind ions are not concentrated toward the poles by strong magnetic fields. High-amplitude variations on timescales of minutes-to-hours can be present in these X-ray components.

Figure 4 shows the best spectra from Jupiter currently available. The IXO spectrum will reveal hundreds of lines with sufficient signal to map the upper atmosphere through the planet's 36 ks rotational period. Repeated visits, particularly at different periods in the solar 11-year activity cycle and several days after powerful solar flares, should show varying ratios of the different emission components elucidating the complex physics of solar-planetary interactions.

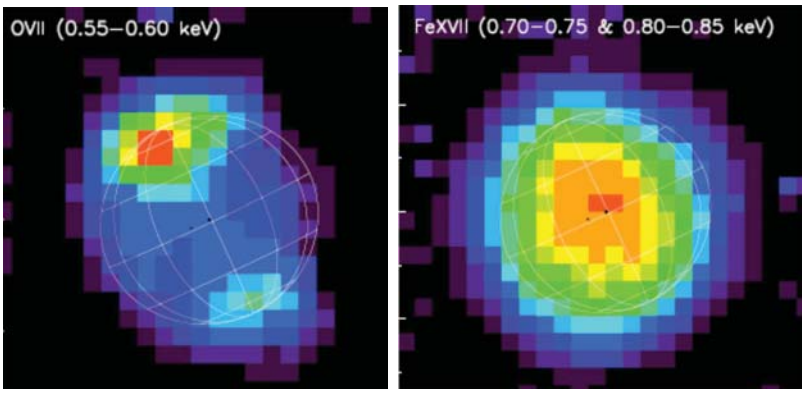

Fig. 3.— *XMM-Newton images of Jupiter in the charge-exchange O VII [left] and fluorescent Fe XVII [right] lines.*

An IXO study of Mars may be particularly important for understanding the evaporative effect of solar X-rays and extreme ultraviolet emission on planetary atmospheres. Martian X-ray emission is dominated by a uniform disk of scattered solar radiation (Mars subtends 18″ at opposition). But remarkably, a faint halo of soft charge exchange lines with unexplained spatial substructure is seen out to $\sim$ 8 planetary radii (Figure 5, Dennerl 2002).

This exceedingly faint X-ray component gives a unique view into planetary exospheres which is inaccessible at other wavelengths. When observed with IXO under a variety of solar wind and flare conditions, the Martian exosphere may provide critical evidence into the complex interactions between stellar X-ray and ultraviolet emission and planetary atmospheres. Indeed, it is possible that Mars' atmosphere is so thin today due to these effect when solar magnetic activity was greatly elevated ~ 4 Gyr ago.

4. Cometary charge exchange

During their perihelion approach to the Sun, cometary ices (mostly water) are evaporated into a large neutral coma which produces strong charge exchange reactions when it interacts with highly-charged solar wind ions (Cravens 1997). X-ray studies provide unique information on this wind-coma interaction region giving insights into charge exchange processes, wind-coma hydrodynamics, and cometary outgassing. Interpretation of cometary X-ray spectra today is complicated as it depends on the solar wind velocity, density and composition, as well as wind ion penetration into the coma, ion-molecular cross-sections, and collisional opacity. These issues can be elucidated by IXO XMS studies (note that grating observations are not feasible due to the spatial extent). X-ray luminosities range from $10^{14} - 10^{16}$ erg/s depending primarily on the comets' encounters with different solar wind states (Bodewits et al. 2007). Several periodic comets and an unknown number of distant comets will enter perihelion during the IXO mission. Spectra will resolve about a dozen charge-exchange emission lines from oxygen above 0.5 keV, and dozens of lines from other elements. Line ratios will change with cometary gas species, solar wind ion composition and wind speed.

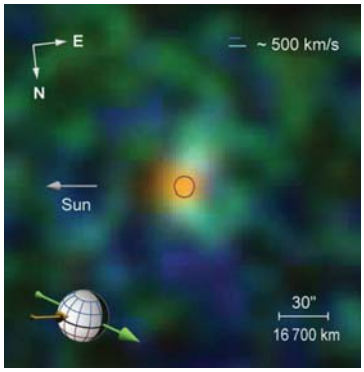

Fig. 5.— *Image of Mars in X-rays derived from XMM-Newton observations: charge exchange $O^{+6}-O^{+7}$ lines in blue, $C^{+4}-C^{+5}$ lines in green, and fluorescent lines in yellow (Dennerl 2006).*

5. Heliospheric charge exchange

X-ray astronomers have increasingly recognized that a significant fraction of the all-sky soft X-ray background arises from time-dependent heliospheric charge-exchange reactions between highly ionized solar wind atoms and interstellar neutrals which penetrate deeply into the heliosphere (Snowden et al. 2004). This has profound implications for our understanding of the Local Hot Bubble and the structure of the Galactic interstellar medium. Earlier X-ray missions also suffer from contamination by charge exchange emission within the terrestrial magnetosphere (Wargelin et al. 2004), but IXO will avoid this component from its location at the Earth-Sun L2 Lagrangian point. From study of the background of dozens of observations with different lines-of-sight through the heliosphere under different solar wind conditions, IXO spectra should provide powerful insights into heliospheric physics and its interactions with its ambient Galactic medium.

6. Atmosphere evaporation in extrasolar planets

Past studies of solar-type stars indicate that X-ray luminosities drop roughly 10-fold between ages of 10^7 and 10^8 yr, another 10-fold between 10^8 and 10^9 yr, and more rapidly between 10^9 and 10^{10} yr (Preibisch & Feigelson 2005). This enhanced X-ray emission during early epochs, and the associated extreme ultraviolet emission which is more difficult to study in young stars, will dissociate and ionize molecules in planetary thermospheres and exospheres so that light atoms escape into the interplanetary medium (Güdel 2007; Penz, Micela & Lammer 2008). Solar wind and flare particles may also erode the *entire* atmosphere if no magnetic field is present. These processes were probably important on Venus, Earth and Mars during the first 10^8 yr and are presently leading to hydrodynamics escape of the atmospheres in extrasolar "hot Jupiters." The atmospheric conditions, and hence the habitability, of planets may thus be regulated in part by the evolution of the ultraviolet and X-ray emission of their host stars. Thousands of extrasolar planets will be known by 2020 through NASA's *Kepler* mission and other planetary search programs. IXO can measure both the quiescent and flare activity of specific stars which will be known to have planets in their habitable zones. Combined with stellar activity evolutionary trends and planetary atmospheric modeling, IXO findings should give unique insights into the atmospheric history of these potentially habitable planets.

7. Summary

X-ray studies of planetary systems are beginning to provide important insights into planetary astrophysics which are inaccessible at other wavelengths. X-ray observations of the host stars reveal the high-energy inputs to protoplanetary disks and planetary atmospheres due to stellar winds and violent magnetic flaring. X-rays from Solar System planets are faint but reveal considerable complexity, a situation well-matched to IXO's high-throughput and high spectral resolution. Charge exchange line emission from interactions between solar wind ions and atmospheric neutrals, along with other processes, are seen in the atmospheres of Jupiter, comets and other Solar System bodies. The X-ray discovery of the Martian exosphere points to evaporation of planetary atmospheres unprotected by magnetic fields, which may play an important role in the habitability of planets. X-ray and infrared spectroscopic studies of protoplanetary disks show that X-ray ionization is present, and theoretical calculations indicate its importance to disk thermodynamics, chemistry and dynamics. It is possible that X-ray illumination is a critical regulator to the formation and early evolution of planets in the disk, but higher sensitivity is needed to study the crucial 6.4 keV fluorescent line. X-ray studies of cometary coma charge exchange, charge exchange distributed throughout the heliosphere, and of stars hosting extrasolar planets are examples of a wealth of IXO studies which will revolutionize this field.

REFERENCES

Bergin, E. A., Aikawa, Y., Blake, G. A., & van Dishoeck, E. F. 2007, in Protostars and Planets V, 751

Bhardwaj, A., Elsner, R. F., Gladstone, R. G., et al. 2007, Planet. Space Sci., 55, 1135

Bodewits, D., Christian, D. J., Torney, M., et al. 2007, A&A, 469, 1183

Branduardi-Raymont, G., Bhardwaj, A., Elsner, R. F., et al. 2007, A&A, 463, 761

Chaussidon, M., & Gounelle, M. 2006, in Meteorites and the Early Solar System II, 323

Connolly, H. C., Jr., Desch, S. J., Ash, R. D., & Jones, R. H. 2006, in Meteorites and the Early Solar System II, 383

Cravens, T. E. 1997, Geophys. Res. Lett., 24, 105

Dennerl, K. 2002, A&A, 394, 1119

Dennerl, K. 2006, Space Sci. Rev. 126, 403

Ercolano, B., Drake, J. J., Raymond, J. C., & Clarke, C. C. 2008, ApJ, 688, 398

Feigelson, E., Townsley, L., Güdel, M., & Stassun, K. 2007, in Protostars and Planets V, 313

Glassgold, A. E., Feigelson, E. D., & Montmerle, T. 2000, in Protostars and Planets IV, 429

Güdel, M. 2007, Living Reviews Solar Phys., 4, 3

Imanishi, K., Tsujimoto, M., & Koyama, K. 2001, ApJ, 563, 361

Najita, J. R., Carr, J. S., Glassgold, A. E., & Valenti, J. A. 2007, in Protostars and Planets V, 507

Penz, T., Micela, G. & Lammer, H. 2008, A&A 477, 309

Preibisch, T., & Feigelson, E. D. 2005, ApJS, 160, 390

Science Plan for NASA's Science Mission Directorate 2007-2016

Snowden, S. L., Collier, M. R., & Kuntz, K. D. 2004, ApJ, 610, 1182

Wargelin, B. J., Markevitch, M., Juda, M., et al. 2004, ApJ, 607, 596

Astro2010 Science White Paper (submitted to both CFP and GCT)

Spin and Relativistic Phenomena Around Black Holes

L. Brenneman, J. Miller, P. Nandra, M. Cappi, G. Matt, S. Kitamoto, F. Paerels, M. Mendez, R. Smith, M. Nowak, M. Garcia, M. Watson, M. Weisskopf

I : Probing the formation and growth of black holes using spin

Ever since the seminal work of Penrose (1969) and Blandford & Znajek (1977), it has been realized that black hole spin may be an important energy source in astrophysics. X-ray observations are uniquely able to answer: **Does black hole spin play a crucial role in powering relativistic jets such as those seen from radio-loud active galactic nuclei (AGN), Galactic microquasars, and Gamma-Ray Bursts?** Indeed, the radio-loud/radio-quiet dichotomy in the AGN population is usually attributed to differences in black hole spin (with correlations between black hole spin and host galaxy morphology being hypothesized in order to explain why radio-loud AGN occur in early-type galaxies; see Figure 1, drawn from Sikora et al. 2007).

The importance of black hole spin goes beyond its role as a possible power source. The spin of a black hole is a fossil record of its formation and subsequent growth history. The details differ somewhat between stellar-mass and supermassive black holes. Given that stellar-mass black holes found in Galactic Black Hole Binaries (GBHBs) are many times more massive than their companion stars, they are unlikely to have changed their spin appreciably since they were formed. To see this, note that a black hole must accrete an appreciable fraction of its original mass in order to significantly change its spin. In the case of GBHBs with low-mass stellar companions, even the accretion of the entire companion star will only change the spin by a small fraction. On the other hand, in GBHBs with high-mass stellar companions, even Eddington-limited accretion will only grow the black hole by a small amount before the high-mass companion explodes. **Thus, the spin of a stellar-mass black hole is a direct relic of the dynamics within the supernova formation event.**

In contrast, **the spin of a supermassive black hole encodes the growth history of the hole and, particularly, the role of mergers versus accretion during the final doubling of the hole's mass** (see Figure 2 drawn from theoretical work by Berti & Volonteri 2008). Successive mergers produce a population of black holes that are spinning at a moderate rate (dimensionless spin parameter $a\sim0.7$, where $a = cJ/GM^2$), whereas powerful (quasar-phase) accretion events will produce very rapidly rotating black holes ($a>0.9$). Yet another possibility is that most black holes have been grown via many short-lived, uncorrelated accretion events, in which case slowly rotating black holes ($a<0.5$) would be expected (King & Pringle 2006).

Despite its importance, we are only now gaining our first tantalizing glimpses of black hole spin in a few objects. Unlike measurements of black hole mass, spin measurements require us to examine observables that originate within a few gravitational radii of the black hole. A powerful probe of this region that can be applied to black hole systems of all masses is obtained through the study of relativistically-broadened spectral features that are produced in the surface layers of the inner accretion disk in response to irradiation by the hard X-ray source (Tanaka et al. 1995). The strongest feature in this reflection spectrum is the iron-Kα line (see Figure 3). For moderate accretion rates (between ~1-30% of the Eddington rate), we expect the iron line emitting part of the disk to extend down to, but be truncated by, the innermost stable circular orbit (ISCO) of the black hole potential (see Reynolds & Fabian 2008 for numerical simulations that support this

assertion). This ISCO-truncation imparts a spin-dependence to the reflection spectrum; black holes with higher (prograde) spin have an ISCO at smaller radius and hence the maximum redshift experienced by the reflection spectrum and the iron line is increased.

High signal-to-noise spectra across a wide band-pass are required to obtain robust spin measurements. The effects of spin on the disk reflection spectrum are not subtle, but the disk spectrum must be decomposed from other complexity in the spectrum such as continuum curvature or the effects of photoionized absorbers. For this reason, current studies (with *XMM-Newton* and *Suzaku*) have been limited to a handful of GBHBs (Miller et al. 2009) and one AGN (MCG-6-30-15; Brenneman & Reynolds 2006).

The International X-ray Observatory (IXO) will make measurements of black hole spin a matter of routine, revolutionizing our knowledge of supermassive black hole spin evolution as well as relativistic jet formation and power. In addition to the superior throughput in the iron-K band, the high spectral resolution in the 0.5-10 keV band coupled with its hard X-ray sensitivity will enable the disk spectrum to be decomposed from other complexities in the spectrum in a completely unambiguous manner. By targeting known AGN (such as those found in the hard X-ray survey obtained from the *Swift/BAT*), IXO will measure the spin of 200-300 supermassive black holes in the local ($z<0.2$) Universe and a handful (5-10) of supermassive black holes out to $z\sim1$. IXO will also easily determine the spin of every accessible GBHB in the Galaxy or the Magellanic Clouds that enters into outburst during the mission lifetime. Since this study is conducted with electromagnetic tracers of black hole spin (rather than gravitational waves), it will be straightforward to study other aspects of these systems. **In short, we will be able to place the role of black hole spin into context, examining the consequences of spin on radio jet power and host galaxy morphology.**

The disk reflection methodology outlined here is powerful since it can be applied uniformly to black holes across the whole range of masses. However, there are other mass-specific techniques that lead to spin constraints. This can be used to provide crucial consistency checks. In GBHBs, detailed examination of the thermal X-ray emission from the accretion disk gives another measurement of the ISCO and hence the spin (Shafee et al. 2006). GBHBs also occasionally display high-frequency quasi-periodic oscillations (HFQPOs) which provide a third (albeit model-dependent) constraint. Finally, a fourth method is provided by polarimetry; the polarization angle of disk emission rotates with energy due to GR effects (Dovciak et al. 2008).

Completely novel consistency checks are possible for the brightest AGN. Rapid iron line variability is expected from orbiting structures within the disk and/or the reverberation of X-ray flares across the disk (see Section 2 below). Both of these phenomena have well defined spin-dependence. Furthermore, the first AGN-QPO has recently been reported (Gierliński et al. 2008) and opens up the possibility of timing-based measurements of supermassive black hole spin.

The IXO census of spins will revolutionize black hole astrophysics. The spins of stellar-mass black holes in GBHBs are natal and hence give a direct window into the birth of these objects. This, in turn, provides a glimpse into the workings of the most powerful explosions in the Universe – at least some stellar mass black holes are believed to be born in long Gamma-Ray Bursts. For AGN, the IXO spin census will allow us to determine the distribution of black hole spins as functions of host galaxy type and redshift. Comparisons with detailed theoretical calculations will determine whether supermassive black hole growth has been dominated by accretion or by mergers. On all mass scales, correlations between black hole spin and the presence of relativistic jets will provide a clean test of the hypothesis that a rapidly rotating black hole is the basic power source for these jets.

II : Strong gravitational physics close to black holes

Black holes provide the ultimate laboratory for studying strong-field gravitational physics. Of course, the most compelling theory of gravity to date is General Relativity (GR). For weak gravitational fields, GR has passed precision tests (within the framework of Parameterized Post Newtonian theory in which all variants of GR are encapsulated), but GR remains essentially untested in the strong-gravity regime. **Given that GR is one of the foundations of modern physics, it is important to explore its predictions in many independent and unbiased ways.**

In luminous black hole systems, the accretion flow is in the form of a thin disk of gas orbiting the black hole. To a very good approximation, each parcel of gas within the disk follows a circular test-particle orbit (e.g. Armitage & Reynolds 2003). **This geometrical and dynamical simplicity makes accretion disks useful for probing the black hole potential and, hence, the predictions of GR.**

Current studies by *XMM-Newton* and *Suzaku* clearly show the broadening and skewing of the disk reflection features in both AGN and GBHBs predicted by GR (due to a combination of the relativistic Doppler shift and gravitational redshift; for a review, see Miller 2007). In a small number of AGN, observations already hint at the power of orbit-by-orbit traces using emission lines (Figure 4). However, most studies must integrate for many orbits of the accretion disk in order to collect enough photons to define the disk reflection spectrum. This time-averaging removes much of the dynamical information and, in particular, makes it impossible to simultaneously measure black hole spin and search for deviations from the predictions of GR.

With its superior throughput, IXO will sweep away this degeneracy. IXO will enable detection of iron line variability on sub-orbital timescales in approximately 20-30 AGN. Any non-axisymmetry in the emission of the iron line (e.g. associated with the expected turbulence in the disk) will lead to a characteristic variability of the iron line, with "arcs" being traced out on the time-energy plane (Figure 5). GR makes specific predictions for the form of these arcs, and the ensemble of arcs can be fitted for the mass and spin of the black hole, as well as the inclination at which the accretion disk is being viewed. Deviations from the predictions of GR can be sought by searching for *apparent* changes of the inferred mass and/or spin with radius in the disk.

A second kind of emission line variability will occur due to the reverberation (or "light echo") of X-ray flares across the accretion disk. Observing this behavior is critical, as it enables an absolute determination of the size scale (GR shifts giving this only in terms of the gravitational radius). Reverberation observations offer unambiguous proof of the origin of the X-ray lines as reflection features, allowing us to map the geometry of the X-ray source and inner accretion flow. The path and travel time of photons close to the black hole is also strongly affected by space-time curvature and frame-dragging. In systems with very rapidly rotating black holes, the region of the accretion disk capable of producing line emission can extend down almost to the event horizon, so we can probe time-delays along photon paths that pass close to the horizon. These photon paths create a low-energy, time-delayed "tail" in the GR reverberation transfer function. The nature of this tail is insensitive to the location of the X-ray source but is highly sensitive to the spacetime metric, so characterizing this will provide another potential test of GR, this time based on photon orbits rather than matter orbits.

The reverberation of individual flares will be accessible to IXO in the brightest few AGN. However, reverberation will be statistically detected in many more AGN and GBHBs via the use of Fourier techniques aimed at detecting the lag between the driving continuum emission and the strongest fluorescent emission lines.

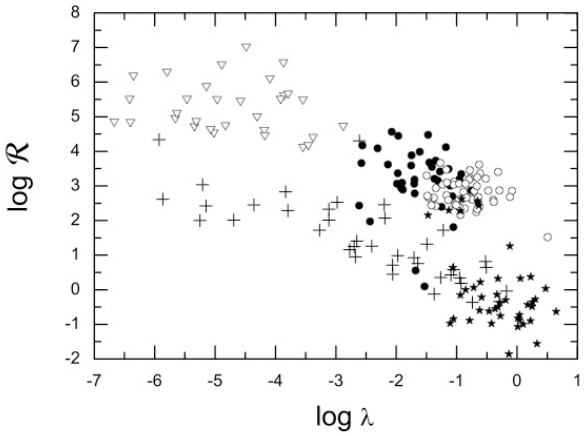

Figure 1 : **The spin-paradigm in AGN** : Radio/optical (5GHz/440nm) flux ratio ℛ against Eddington ratio λ for a sample of AGN (broad-line radio galaxies are filled circles, radio-loud quasars are open circles, Seyfert galaxies and LINERs are crosses, FRI radio galaxies are open triangles, PG quasars are filled stars). The radio-loud/radio-quiet dichotomy is revealed via the existence of two distinct tracks on this plot. The spin-paradigm holds that the upper branch (exclusively early type galaxies) corresponds to rapidly spinning SMBHs whereas the lower branch (all galaxy types) corresponds to slowly spinning SMBHs. **IXO observations of these sources can directly test this paradigm.** (Figure taken from Sikora, Stawarz & Lasota 2007).

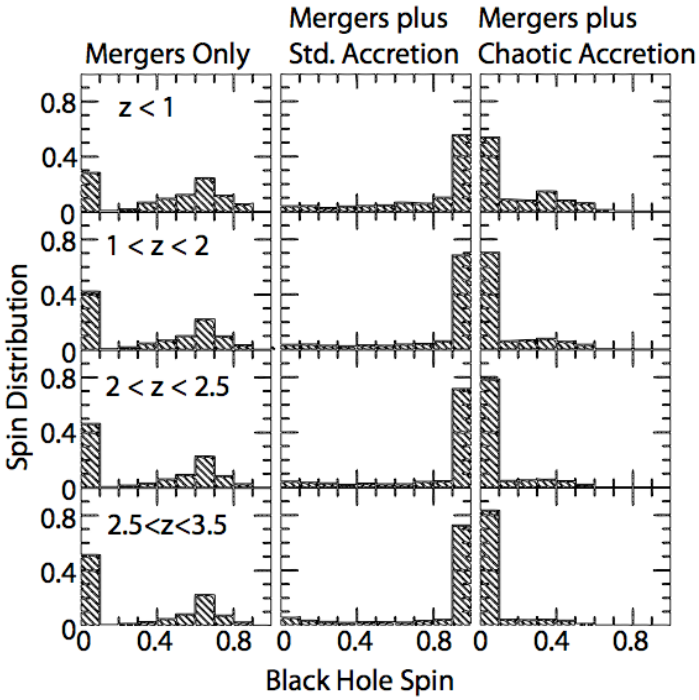

Figure 2 : **Spin as a probe of SMBH growth history**. Left panels show a predicted distribution of SMBH spin in a scenario where seed black holes are formed at high redshift after which the SMBH population evolves purely via SMBH-SMBH mergers. The middle panels show a predicted spin distribution resulting from mergers plus standard (disk) accretion. The right panels show the distribution when appreciable SMBH disk-accretion accompanies merger events. **The spin-distribution is a powerful discriminant between growth histories that may form identical mass-functions**. (Figure adapted from Berti & Volonteri 2008).

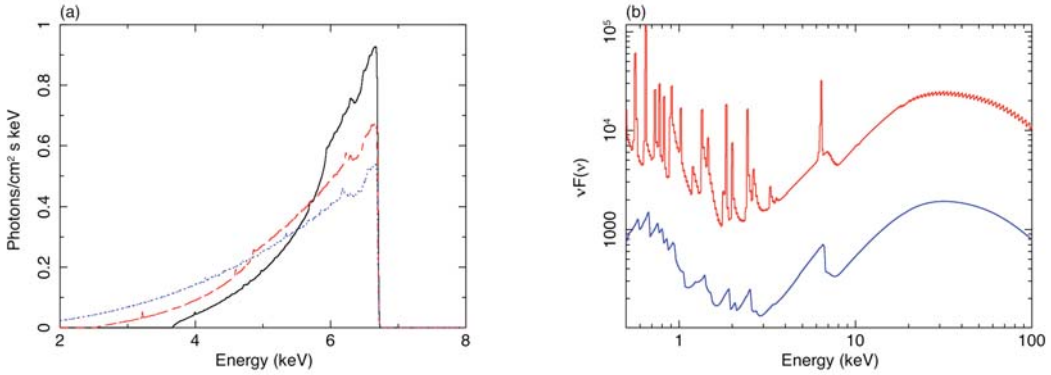

Figure 3: **Relativistically-broadened disk reflection features**. (a) ISCO-truncated iron line profiles for spins of a=0 (black), a=0.7 (red) and a=0.998 (blue). (b) An ionized reflection spectrum from before (top) and after (bottom) the relativistic smearing effects (for a=0.7) are incorporated. **The iron line is a powerful probe of black hole spin**.

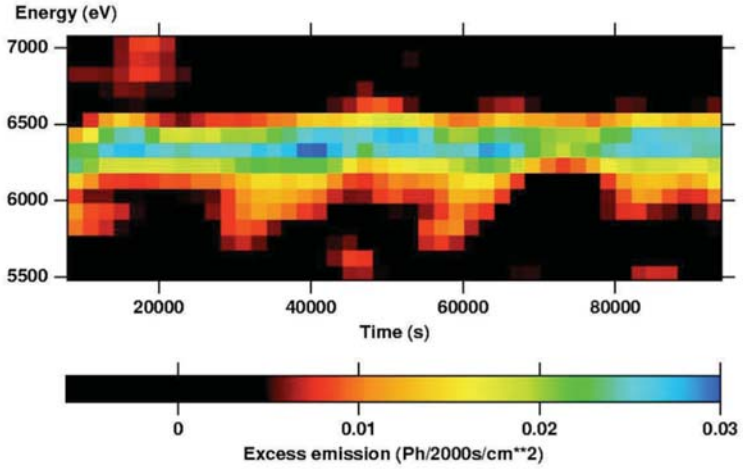

Figure 4: Current observations of AGN are just able to search for emission line variations on the orbital timescale at the ISCO. The plot above depicts Doppler shifts in an iron emission line consistent with Keplerian orbits at the ISCO in the Seyfert AGN NGC 3516. The saw-tooth pattern is exactly that expected for orbital motion in the innermost relativistic regime around black holes. The sensitivity of IXO will make it possible to explore these timescales in fine detail, revealing the nature of the strong-field gravitational potential. (Figure taken from Iwasawa, Miniutti, & Fabian 2004.)

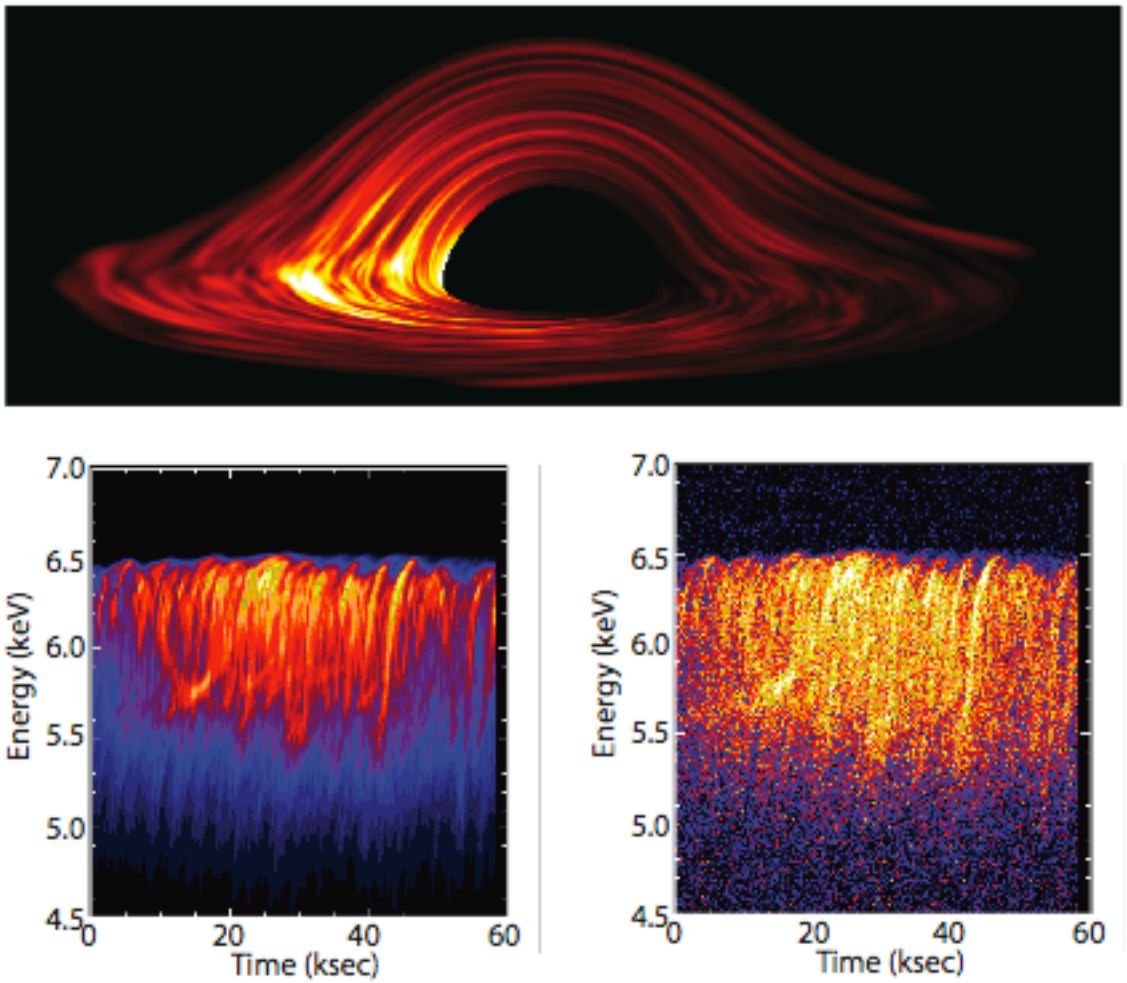

Figure 5: **How does matter behave close to a black hole?** Top panel: Simulated image of a highly-inclined MHD turbulent accretion disk around a Schwarzschild black hole. Bottom left panel : The iron line in the time-energy plane from a turbulent disk viewed at an inclination of 20 degrees. **Note the arcs in the trailed-profile that can be directly mapped to test-particle like orbital motion of hot-spots in the disk.** Bottom right panel : Result of a simulated IXO observation, assuming a 3×10^7 M_{sun} black hole and a 2-10keV flux characteristic of a bright AGN. (Figure adapted from Armitage & Reynolds 2004).
A video of an MHD simulation of a turbulent disk at 30 degrees inclination, and the time-resolved iron lines that it would produce, can be seen at:
http://ixo.gsfc.nasa.gov/documents/resources/posters/aas2009/brenneman_plunge_30i.avi

References

Armitage, P., & Reynolds, C. S., 2003, MNRAS, 341, 1041
Berti, E., & Volonteri, M., 2008, ApJ, 684, 822
Blandford R. D., Znajek R. L., 1977, MNRAS, 179, 433
Brenneman, L.W., Reynolds C. S., 2006, ApJ, 652, 1028
Dovciak, M., et al., 2008, MNRAS, 391, 32
Gierlinski, M., et al., 2008, Nature, 455, 369
Iwasawa, K., Miniutti, G., & Fabian, A. C., 2004, MNRAS, 355, 1073
King A. R., Pringle J. E., 2006, MNRAS, 373, L90
Miller, J. M., 2007, ARA&A, 45, 441
Miller J. M., et al. 2009, ApJ, in press
Penrose R., 1969, Riv. Del. Nuo. Cim, 1, 252
Reynolds C. S., Fabian A. C., 2008, ApJ, 675, 1048
Shafee R., et al. 2006, ApJ, 636, L113
Sikora, M., Stawarz L., Lasota J. P., 2007, ApJ, 658, 815
Tanaka, Y., et al., 1995, Nature, 375, 659
Volonteri, M. et al., 2007, ApJ, 667, 704

MASS-LOSS AND MAGNETIC FIELDS AS REVEALED THROUGH STELLAR X-RAY SPECTROSCOPY

A Science White Paper
for the Astro2010
Stars and Stellar Evolution
Science Frontier Panel

Authors: Rachel A. Osten[†] (STScI), Marc Audard (University of Geneva), Tom Ayres (University of Colorado), Alex Brown (University of Colorado), Jeremy Drake (CfA), Steve Drake (NASA/GSFC+USRA), Marc Gagné (West Chester University), Dave Huenemoerder (MIT), Vinay Kashyap (CfA), Maurice Leutenegger (NASA/GSFC), Jeff Linsky (University of Colorado), Lidia Oskinova (University of Potsdam), Norbert Schulz (MIT), Jurgen Schmitt (Hamburger Sternwarte), Salvatore Sciortino (INAF/Oss. Astr. Palermo), Beate Stelzer (INAF/Oss. Astr. Palermo), Ralph Tuellmann (CfA), Wayne Waldron (Eureka Scientific), Scott Wolk (CfA)

[†] Contact Author: Rachel Osten, Space Telescope Science Institute, 3700 San Martin Drive, Baltimore, MD 21218 USA
e-mail: osten@stsci.edu

Stellar X-ray Astrophysics

Although the typical radiative output of most stars at X-ray wavelengths is a tiny fraction of their total luminosity, X-ray emissions provide important constraints on processes which affect the entire stellar atmosphere and even allow insight into dynamo magnetic field generation occurring deep in the stellar interior. X-ray spectroscopy is required for an assessment of the plasma parameters controlling the X-ray flux. Moderate spectral resolution (R=500-1000) of the plasma parameters of stars with Chandra and XMM-Newton have given us a taste of the science that can be done, but constraints on effective area and spectral resolution have limited the number of stars accessible as well as the science which can be extracted. The applicability of the results are limited to the X-ray brightest stars, which tend to be the most anomalous in their other properties. This white paper addresses two key questions of major importance to stellar astrophysics:

- **How do magnetic fields shape stellar exteriors and the surrounding environment, and how does this vary in stars of differing types?**
- **How rapidly do stars lose mass and angular momentum, and how do rotation and magnetic fields affect stellar winds?**

1 Magnetic Fields and Stellar Exteriors

On our nearest star, the Sun, magnetic fields control non-radiative heating mechanisms that heat plasma to temperatures of 10^4—10^6K (characteristic of chromospheres and coronae, respectively), contained in loop-like structures capable of producing spectacular flaring emissions when magnetic reconnection occurs (e.g. Aschwanden 2002). These magnetic fields are produced as the result of dynamo processes at work in the stars' interiors; the dynamo mechanism will differ with the internal structure of the star, i.e. thin outer convection zone or fully convective star, and this affects the geometry of the large-scale fields produced. The magnetic fields in late-type stars are dynamic, producing changes in observed coronal structures and their effects over a wide range of timescales: minutes during large magnetic reconnection flares; fractions of the rotational or orbital period; years or decades of activity cycles; and evolutionary timescales, as non-uniform magnetic flux distributions affect the rate at which angular momentum loss occurs.

X-ray observations of late-type stars probe the tenuous hot coronal plasma produced by non-radiative heating processes. As the hot coronal plasma is confined in magnetic loops, understanding the characteristics of those loops provides knowledge about the dynamo process by providing constraints on the types of magnetic loops generated in stars with varying parameters (T_{eff}, rotation, internal structure, field strength and covering factor). High-sensitivity and high spectral resolution X-ray observations are needed to probe the detailed plasma physics of structuring and dynamics. The X-ray bright stars currently accessible to moderate resolution (R=500-1000) X-ray spectral studies are extremely magnetically active and thus the conclusions drawn from their study may not be widely applicable. Observations to explore a much wider range of parameter space, such as age, magnetic field strengths, rotation, metallicity, and evolutionary status are needed; these will nicely complement and

extend the solar studies, enabling a more detailed examination of the physics involved in how magnetic fields shape stellar exteriors and the surrounding environment.

Stellar Flares The similar temporal and spectral behavior of X-ray emission during magnetic reconnection flares in a variety of stellar environments provides important clues to the structuring and dynamics of these objects. Recently large X-ray flares have been observed on stars as disparate as active evolved stars (Testa et al. 2007), sub-stellar objects (Stelzer et al. 2006), and young stellar objects with disks (Favata et al. 2005), and the observed temporal behavior of temperature and emission measure appear to follow similar trends as those seen in well-studied solar flares. The interpretation using one-dimensional hydrodynamical loop models developed from studies of solar flares reveals compact loops reminiscent of solar coronal behavior (lengths ~ 0.1 $R_\star$) on evolved stars, yet larger loops (lengths $\sim R_\star$) on fully convective stars, despite the large differences in pressure scale heights. Magnetic reconnection events can be highly dynamic and involve rapid changes in X-ray-emitting composition, temperature, bulk velocities. To make progress in understanding the effects of magnetic reconnection a more complete assessment of the flaring plasma in a variety of flaring stars is needed. This requires constraints on density, elemental abundance, length scale, and velocity, as well as advances in loop modelling. Diagnostics such as the Fe Kα 6.4 keV fluorescence line probe length scales in stellar flares complementary to hydrodynamic modelling; this has been newly used in the study of large stellar flares on stars without disks (Testa et al. 2007, Osten et al. 2007), but requires sensitive X-ray spectrometers with sufficient spectral resolution around 6 keV (R$\geq$ 2000) to extend the diagnostic power of emission from cold iron into the domain of stellar flares. Due to the variety of different effects which operate during a flare (such as particle acceleration, shocks, plasma heating), stellar flares are inherently multiwavelength emitters and coordinated observations across the electromagnetic spectrum are needed to fully understand the flare process. Crucial missing parameters from stellar flare studies are an estimate of the kinetic energy involved in large coronal flares (which can be estimated from bulk coronal motions), necessary to constrain aspects of energy transport and release, and determinations of the nonthermal energy input into the flare process, which can be constrained via nonthermal emission with sensitive ($A_{\rm eff} > 150$ cm^2) hard X-ray detectors at > 20 keV.

The Many Faces of a Star The systematic behavior of X-ray line shifts over the course of several stellar rotations/orbits in short-period active stars (Hussain et al. 2005, Huenemoerder et al. 2006) reveals that stable, large-scale coronal structures exist and can be studied spectroscopically. Current observations are limited to the study of only the brightest objects, integrated over large fractions of a rotation period or orbit, and using only the brightest X-ray emission lines, and thus are highly restricted in the extent to which they can reveal the characteristics of these structures. Better observational constraints are needed to determine the characteristic properties of such stable structures, e.g. temperature, density, and abundance distributions as a function of time during the rotation/orbit, and high spectral resolution observations (R$\geq$ 3000) are needed to spectrally disentangle the X-ray emission from the components of binary systems. Such observations done in conjunction with infrared/optical spectral imaging techniques to determine the starspot distribution and

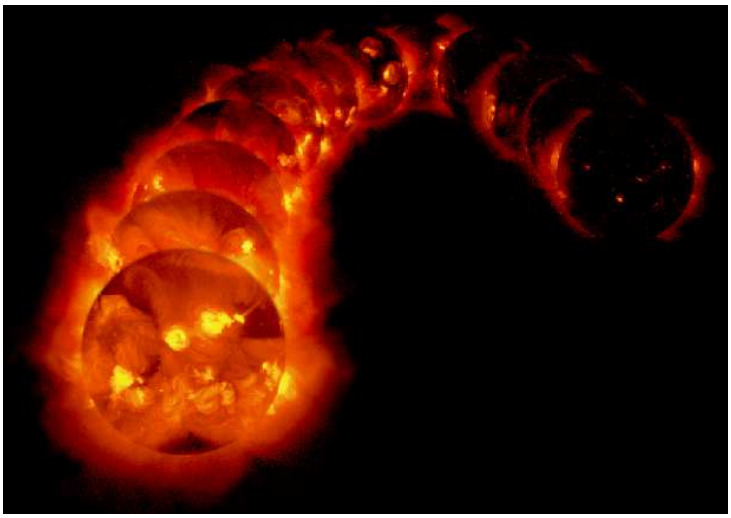

Figure 1: *Yohkoh images of the Sun taken over the course of a solar cycle, illustrating the difference in solar coronal structures from maximum to minimum. Because of the correlation between X-ray emission and magnetic fields, our current capability to study "stars as suns" is limited to those stars with large magnetic filling factors. Large collecting area coupled with adequate spectral resolution is needed to determine the important plasma properties of density and abundance, necessary to infer coronal structures on stars which may be representative of the Sun at its activity cycle minimum.*

photospheric magnetic field distribution, connect the properties of footpoints lower in the stellar atmosphere with the properties of the expanding coronal loops, and allow more inferences to be made about the structuring in stellar exteriors.

"Normal" Stars X-ray bright active stars are known to have high filling factors of magnetic fields on their surfaces, so the observed trends of coronal plasma parameters (temperature, abundance, density) reveal aspects of the nonradiative heating process taking place in regions where magnetic fields are maximally packed with plasma. It is already known that coronal abundance anomalies are a function of X-ray activity, as is the dominant coronal temperature seen in X-ray spectra. However, less active stars have smaller filling factors of magnetic fields and so it is not clear that the same trends will be obtained in objects with lower magnetic activity. Therefore, in order to make progress in understanding the physics of coronal structuring, a range of X-ray luminosities and magnetic field strengths and distributions is needed. The relevant quantities to be determined are the electron densities of the multiple-temperature components, in addition to coronal abundance trends as a function of X-ray luminosity and constraints on coronal loop sizes. These necessitate the use of high spectral-resolution X-ray observations with large collecting area (A_{eff} >1m^2) to "connect the dots" between the well-studied Sun and the magnetically hyperactive X-ray brightest stars, by accessing true solar analogs.

Magnetic Fields in Massive Stars The importance of magnetic fields in massive stars has been revealed in the last few years by direct measurements of surface fields up to kG strength (e.g. Donati et al. 2001, Bouret et al. 2008), by the advances in the theory of dynamo in massive stars (Spruit 2002), by the success of stellar evolution models incorporating magnetic fields (e.g. Maeder et al. 2008), and importantly by X-ray observations of some OB stars (Gagné et al. 2005) which require magnetic channeling of wind shocks to reproduce X-ray line profile and temporal behavior. Along with magnetic fields, stellar rotation is required to understand stellar evolution, mass loss, and shaping of the circumstellar medium. The connection between magnetism, rotation, angular momentum, and mass loss is important but largely unexplored partly due to inadequate effective area to observe variability of X-ray line profiles over magnetic cycle and other time scales.

2 Mass Loss

Stellar mass loss is a key parameter which drives stellar evolution in the upper HR diagram and the chemical evolution of the Universe. The history of mass loss plays an important role in determining massive stellar life as it nears the final supernova explosion or gamma-ray burst (GRB). The delicate interplay between stellar magnetism, rotation, and UV field determines angular momentum and mass loss and defines the properties of the supernova or GRB progenitor. Stellar outflows shape the circumstellar medium and thus are pivotal in interpretation and modelling of the interstellar medium (ISM) in OB associations, and the physics of some supernova remnants and GRB afterglows.

Our current ability to constrain mass loss in the upper half of the HR diagram is limited: because of systematic biases, different observational diagnostics in the radio through UV often yield values which disagree with each other by up to an order of magnitude. This produces significantly different outcomes over evolutionary timescales. Observations of X-ray wind line profiles offer the opportunity to help resolve the uncertainties in current determinations of mass loss. Chandra and XMM-Newton have helped break ground by observing a selection of the brightest O, B, and WR stars, but are limited to a small number of the brightest objects. These observations have shown that magnetism in massive stars plays a role in shaping the stellar wind and X-ray emission, that stellar rotation plays an important role in wind dynamics, and that the winds are inhomogeneous (clumped). These key insights in the physics of stellar winds urge new studies which can extend the sample of stars from which such effects can be seen.

X-ray emission lines of hot stars offer a good diagnostic of the characteristics of their stellar winds (Oskinova et al. 2006, Cassinelli et al. 2008). In single stars the f/i ratios of He-like ions measure the location of the X-ray emitting plasma (Kahn et al. 2001), while the line profiles measure the effective optical depth of the wind (Ignace 2001, Owocki & Cohen 2001). Chandra and XMM-Newton spectra of massive stars show that mass-loss rates derived from Hα and radio free-free emission may be overestimated by a factor of two or more because of clumped plasma in the few bright systems that have been studied (e.g. Kramer et al. 2003, Cohen et al. 2006). This overestimate is enough to significantly change the evolution of these stars. Unfortunately the generality of these results cannot be substantiated since very few stars can be observed with the grating spectrometers of Chandra or XMM-Newton. Fully exploiting these important new X-ray diagnostics requires an increase of resolving power and sensitivity beyond that currently available with Chandra or XMM-Newton. Detailed modeling of high signal-to-noise of X-ray emission lines will yield the distribution of hot plasma in the wind, the mass-loss rates, the degree of wind inhomogeneity, and even the geometrical shape of wind clumps. This wealth of information, when obtained for all types of hot stars, will allow us to infer wind properties for the ensemble of OB stars and thus to provide input for stellar evolution codes and allow us to compute the mechanical energy feedback in starburst regions.

3 Measurements Needed

The previous two sections described major questions in stellar astrophysics. X-ray spectroscopic observations are needed to make headway in these areas.

A Complete Assessment of Flare Energetics The bulk and turbulent velocities which are expected to be present during different phases of stellar flares are currently unconstrained; these potentially represent as much energy as in thermal heating and radiation. Another important parameter, the length scales of the flaring coronal loops, is highly model dependent. In order to detect bulk velocity shifts during a stellar flare, sufficient sensitivity and spectral resolution ($A_{eff} \sim 7000$ cm^2 at 6 keV, 3000 cm^2 at 1–2 keV, R=2000-3000) are needed to see the effect of a spectral line shift during the short time in which it occurs; averaging in time will smear out the signal and produce ambiguous results. The shortest timescales of interest in the soft X-ray emission of various classes of stellar flares may be as short as <10-1000 seconds, particularly in the impulsive phase. The velocities associated with blue-shifts, red-shifts and turbulence associated with chromospheric evaporation in the early flare phases are sometimes of the order of 100 - 400 km/s. The Fe Kα diagnostic at 6.4 keV will also be used to determine loop lengths from X-ray flaring loops illuminating the cold stellar surface, placing another constraint on flare dynamics. In order to make constraints on the energy in accelerated particles during stellar flares, sensitive hard X-ray detectors (A_{eff} >150 cm^2) at >20 keV are needed to investigate the spectral shapes of nonthermal emission.

Velocity Information to Infer Coronal Structures Tidally-locked late-type stars in close binary systems are the ideal systems to probe the orbital/rotational dependence of different coronal structures. They can be studied in a relatively complete manner over the course of several adjacent periods to study coherent coronal structures, but with enough sensitivity to probe how those structures change on the relevant timescales. The most revealing information comes from being able to spectrally resolve the two components, and to study the spectra of the two stars and their changes on timescales that are a small fraction, e.g. $\sim$0.03 of a stellar rotation/orbit, in order to determine changes in the X-ray emission as a function of the period. A grating spectrometer having A_{eff}=3000 cm^2 and R=3000 can determine the orbital dynamics and X-ray source location (Figure 2 left), as well as infer rotational broadening, and turbulent broadening.

The Study of Stars as Suns An X-ray telescope with large throughput ($A_{eff} \geq 1$m^2) will enable a complete and systematic survey of "normal" stars and their X-ray emission, avoiding the bright 'active-star' bias present in existing X-ray surveys. One result of this survey would effectively be a study of the Sun as a star in X-rays, since solar mass stars spanning a range of ages from formation until the end of the main sequence and activity levels will be accessible. One of the parameters determined from spectral analysis which reveals important information about coronal structuring is the inferred plasma density as a function of temperature. A sensitive ($A_{eff} \sim 1.5\times10^4$ cm^2) calorimeter with ΔE =2.5 eV can easily determine the departure from the zero density assumption for helium-like O VII lines to better than 90% on a wide range of cool stars with modest exposure times. Figure 2 right illustrates the range of nearby stars accessible to such a survey, which will enable us to place

the Sun in context of other solar-like stars and test the degree and similarity of solar coronal structures to these coronae.

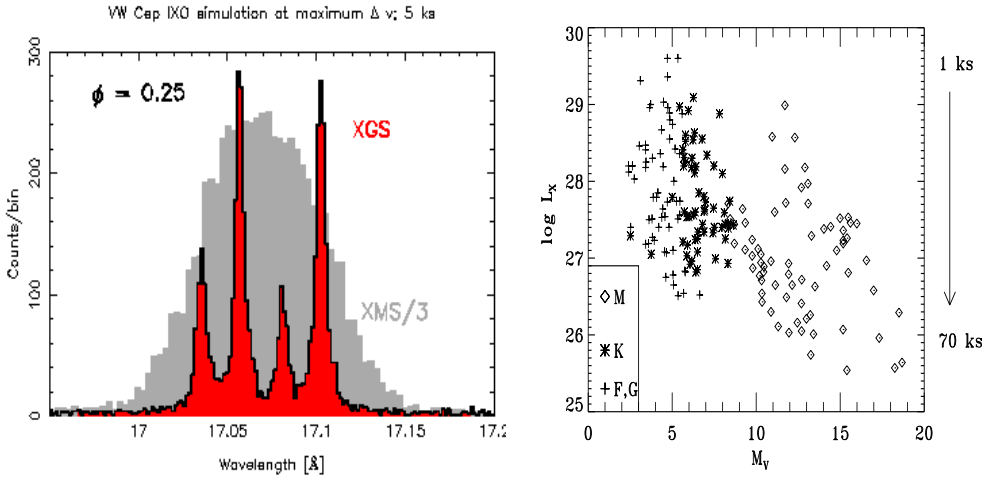

Figure 2: **(left)** *Simulations of the strong Fe XVII lines at 17.05 Å, based on a Chandra/HETGS-derived model (Huenemoerder et al. 2006) for VW Cep, a 0.28 day period contact binary. XGS (red) refers to a grating with R= 3000, $A_{\rm eff}$=3000 cm^2, XMS (grey) refers to a calorimeter with 2.5 eV resolution and $A_{\rm eff}$ >1m^2. The emission measure has been divided between the two stars in a ratio of 2:1, and placed at maximum radial velocity separation of 350 km/s. Both lines of the two stellar components are clearly visible.* **(right)** *Distribution of X-ray luminosities for nearby dwarf stars of spectral type F, G, K, and M, from the NEXXUS database (Schmitt & Liefke 2004), along with the range of calorimeter exposure times needed to establish the density of the cool X-ray emitting plasma. Such observations will expand the sample of stars for which constraints on coronal structure are possible, extending to true solar analogs.*

X-raying the Winds of Hot Stars Line profiles are the most powerful diagnostic in the X-ray emission from massive stars. Significant information from line profiles may be extracted with R∼300 if the signal-to-noise ratio of the data is very high. Thus, the principle requirement is for a very high collecting area ($A_{\rm eff} > 1m^2$). This will allow both the expansion of the sample of observable stars and the observation of the brightest stars at very high signal to noise. Figure 3 illustrates the importance of sensitive observations of massive stars as a main key to unlocking the puzzle of mass loss.

Probing Magnetic Fields, Stellar Rotation, and Winds In a magnetically channeled wind shock, plasma which is driven off the star by radiation is channeled along magnetic field lines, leading to 30-50 MK shocks near the magnetic equator. The f/i ratios of helium-like ionic transitions can be used to determine the location of X-ray emission. With large effective area ($A_{\rm eff}$ >1 m^2) time variability studies can be used to explore changes in the strength and shape of these X-ray lines and determine connections between magnetism, rotation, and plasma from the shocked wind. Magnetic fields need to be invoked to explain X-ray properties of Herbig Ae/Be stars (Stelzer et al. 2009) which require high spectral resolution (R=3000) and large effective area ($A_{\rm eff}$ > 1m^2) to study. Mass loss is also a key feedback parameter behind magnetic activity evolution in cool stars; high spectral resolution (R=3000) observations to deduce coronal structures will allow constraints on this process.

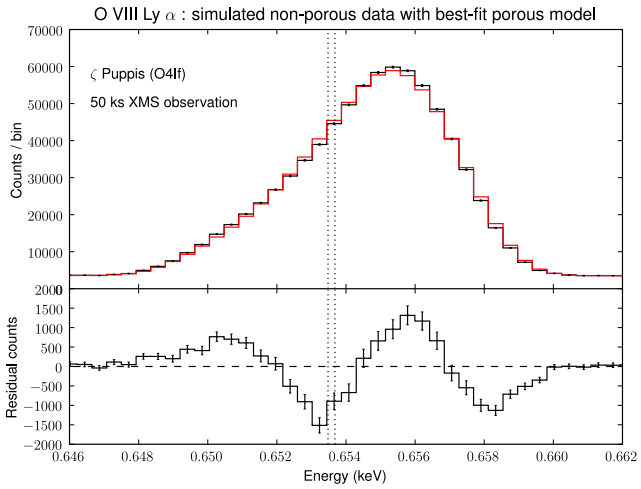

Figure 3: *This figure illustrates the necessity of large effective area ($A_{\rm eff} \sim 1m^2$) in using line profile studies of hot stars to probe mass loss and clumping in the winds. The simulated data (plus signs in the top plot) have been generated under the assumption of a homogeneous wind with a moderate mass-loss rate for a 50 ks exposure time using a calorimeter with $\Delta E = 2.5$ eV, while the model (red histogram) corresponds to a clumpy wind with a mass-loss rate twice the data. Both the spectral resolution and sensitivity are needed to see the disagreement in the residuals between data and model in the lower panel.*

The Multi-wavelength Perspective: Complementarity X-ray spectra are a necessary complement to a full understanding of stellar plasmas provided by astronomical observatories spanning the electromagnetic spectrum. Radio observations (such as made with ALMA, EVLA, SKA) constrain the thermal and nonthermal emission from massive stars/colliding wind shock systems as well as nonthermal emission from magnetically active stars. Infrared and optical polarimetric spectra determine via Doppler and Zeeman Doppler imaging techniques the starspot distribution and photospheric magnetic field distribution on rapidly rotating stars, respectively. Flares are a multi-wavelength phenomenon, producing (on the Sun) emissions from gamma-ray energies to kilometer-wavelengths. X-ray observations detailing the plasma heating process and nonthermal energy deposition require simultaneous measures of nonthermal particles at centimeter wavelengths (ALMA, EVLA, SKA), meter wavelength coherent radiation (LOFAR, MWA, LWA), and the optical white-light photospheric response, to make sense of the multiple physical processes and timescales involved in flares. High spectral resolution with high throughput in X-rays will allow great advances in determining the 3D and dynamic nature of MHD phenomena in stars, which are fundamental in understanding their evolution and interaction with their environment. Thus advances in these other wavelength regions must be complemented by advances in X-ray spectroscopy to exploit fully the information content about stellar mass loss and magnetic fields.

4 References

Aschwanden, M. 2002, SSRv 101, 1
Bouret, J.-C et al. 2008 MNRAS 389, 75
Cassinelli, J. P. et al. 2008 ApJ 683, 1052
Cohen, D. H. et al. 2006 MNRAS 368, 1905
Donati, J.-F. et al. 2001 MNRAS 326, 1265
Favata, F. et al. 2005 ApJS 160, 469
Gagné, M. et al 2005 ApJ 628, 986
Huenemoerder, D. et al. 2006 ApJ 650, 1119
Hussain, G. et al. 2005 ApJ 621, 999
Ignace, R. 2001 ApJ 549, L119
Kahn, S. M. et al. 2001 A&A 365, 312
Kramer, R. H. et al. 2003 ApJ 592, 532
Maeder, A. et al. 2008 A&A 479, L37
Oskinova, L., et al. 2006 MNRAS 372, 313
Osten, R. et al. 2007 ApJ 654, 1052
Owocki, S. P. & Cohen, D. H. 2001 ApJ 559, 1108
Schmitt, J. & Liefke, C. 2004 A&A 417, 651
Spruit, H. C. 2002 A&A 381, 923
Stelzer, B. et al. 2006 A&A 460, L35
Stelzer, B. et al. 2009 A&A 493, 1109
Testa, P. et al. 2007 ApJ 663, 1232

The Cosmic Web of Baryons

A White Paper submitted to ***Galaxies across Cosmic Time (GCT)*** and ***The Cosmology and Fundamental Physics (CFP)*** Science Frontiers Panels

Joel N. Bregman
Department of Astronomy
University of Michigan
Ann Arbor, MI 48109-1042
Email: jbregman@umich.edu
Telephone: 734-764-3454

Claude R. Canizares, Massachusettes Institute of Technology
Reynue Cen: Princeton University
Jan-Willem den Herder: SRON Netherlands Institute for Space Research
Massimiliano Bonamente: University of Alabama in Huntsville
Taotao Fang: University of California, Irvine
Massimiliano Galeazzi: University of Miami
Edward Jenkins: Princeton University
Jelle S. Kaastra: SRON Netherlands Institute for Space Research
Fabrizio Nicastro: Harvard Smithsonian Center for Astrophysics
Smita Mathur: Ohio State University
Takaya Ohashi: Tokyo Metropolitan University
Frtis Paerels: Columbia University
Kenneth Sembach: Space Telescope Science Institute
Norbert Schulz: Massachusettes Institute of Technology
Blair Savage: University of Wisconsin
Randall Smith: Harvard Smithsonian Center for Astrophysics
Noriko Yamasaki: ISAS/JAXA
Bart Wakker: University of Wisconsin

1. The Science Goals

Ordinary matter (baryons) represents ≈4.6% of the total mass/energy density of the Universe but less than 10% of this matter appears in collapsed objects (stars, galaxies, groups; Fukugita & Peebles 2004). Theory predicts that most of the baryons reside in vast unvirialized filaments that connect galaxy groups and clusters (the "Cosmic Web"; Fig 1b). After reionization, the dominant heating mechanism is through the shocks that develop when large-scale density waves collapse in the dark matter. As large-scale structure becomes more pronounced with cosmological time, the gas is increasingly shock-heated, reaching temperatures of $10^{5.5}$-10^{7} K for $z < 1$ (Fig. 1a). Additional heating occurs through star-formation driven galactic winds and AGN, processes that pollute the surroundings with metals.

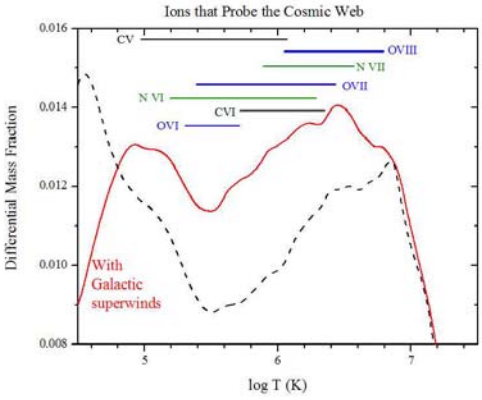

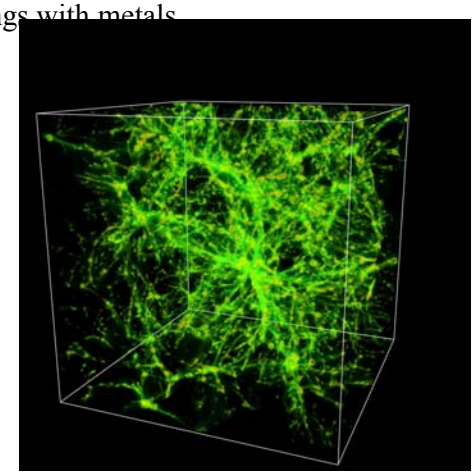

Figure 1. (left panel) The differential gas mass fraction at as a function of temperature at low redshift for the ΛCDM cosmological simulation of Cen & Ostriker (2006). This distribution is sensitive to the presence of galactic superwinds (solid red line; dashed line is without superwinds). The ions with the strongest resonance lines in the 10^{5}-10^{7} K range are shown, and except for OVI (UV line; 1035 Å), the other lines lie in the X-ray band. (right panel) The density distribution of baryons at low redshift from the same simulations. Most of the mass of the WHIM lies within the filaments that connect the higher density regions.

Ly α studies and OVI absorption line studies detect warm baryons, but ~50% of the baryons remain unaccounted for (Danforth & Shull 2008). These "missing baryons" can only be observed through X-ray studies. Therefore, a basic goal is to

• ***Determine if the missing baryons exist in the predicted hot phase***.

In the standard cosmology, chemical enrichment of the IGM occurs through galactic superwinds, a powerful feedback mechanism that also heats the gas. The shocks and superwinds leave distinctive features on absorption lines, such as double-lines (for a line of sight passing through a galactic superwind shell) and turbulent broadening. This feedback mechanism not only extends the cross section of the metal-enhanced regions, its effects are ion-dependent. An example of this is shown below (Figure 2; from Cen and Fang 2005), where there are significant differences between the three oxygen ions.

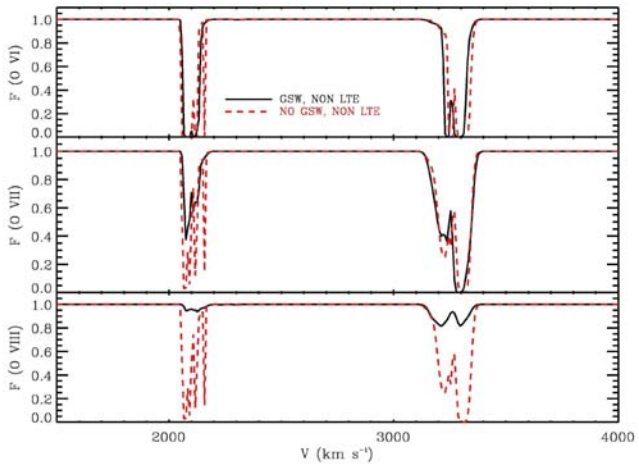

Figure 2. The absorption resulting from a line of sight through the simulation of Cen and Fang (2005; above), with galactic superiwnds (black) and without (red). The superwind region creates a double line absorption profile in this case and the OVIII lines are greatly enhanced.

These observational diagnostics allow us to pursue our second science goal:

- ***Test the large-scale structure and galactic superwind heating of the Cosmic Web***

The extent of the superwinds and the elemental mixing can be determined by studying the spatial relationship between hot gas seen through X-ray absorption and the location of galaxies (Stocke et al. 2006). By studying the same sight lines with X-rays and UV-optical bands, we will discover the relationship of all temperature components to the galactic environment. Therefore, X-ray studies will

- ***Measure the extent of galactic superwinds and the chemical mixing process.***

Finally, the baryons lie in Cosmic Web filaments extending between groups and clusters at 1-2 R_{virial}, as seen in Figure 1. Current surface brightness measurements rarely extend beyond $0.7R_{virial}$, yet they already suggest examples of the expected phenomenon (e.g., Werner et al. 2008). Studies of these structures become feasible when the limiting X-ray surface brightness can be lowered by an order of magnitude. This improvement is now possible, so our last goal is achievable:

- ***Measure the connections of Cosmic Web filaments to galaxy groups and clusters.***

2. Observations Needed to Achieve these Goals

The first three goals are achievable by measuring the He-like and H-like X-ray resonance lines of carbon (C V, C VI), nitrogen (N VI, N VII) and oxygen (O VII, OV III) toward background AGNs (other ions may be detected in a few cases, such as Ne IX, Ne X, Fe XVII, and Fe XVIII). Existing measurements of intergalactic OVII and OVIII are near current instrumental detection thresholds and therefore need confirmation (Nicastro et al. 2005; Kaastra et al. 2006; Bregman 2007; Buote et al.

2009) but the adjacent ion, intergalactic OVI, is detected in the UV along many sightlines and there are clear detections of OVII and OVIII within the Local Group. A conservative estimate of the equivalent width distribution, dN/dz, is obtained from models normalized to the OVI measurements (Cen and Fang 2006, Figure 3; the quality of the OVI normalization will improve significantly with upcoming COS observations). These show that we need an order of magnitude improvement over current sensitivities to conduct an X-ray survey of intergalactic absorption lines from the above elements. In addition, to study the velocity structures of lines, we need resolution that approaches the Doppler width of a line, typically 50-100 km/s, since superwinds from galaxies occur near the escape velocity, 200-1000 km/s.

There is great value to measuring multiple ionic states for understanding the temperature and relative abundance of the gas. With two ionic states, one can infer a temperature, provided that the line structures are the same. With three ions, one can begin to constrain a multi-temperature medium, should one exist (and differences in line structures will be an asset such determinations). From the column densities of three oxygen ions, OVI, OVII, and OVIII, we can test the predicted baryon temperature distributions (Figure 1) in a relative sense, without the need for absolute abundances. Finally, from relative abundance ratios of the elements, we can identify the types of supernovae that has heated and polluted the gas.

Absolute abundance determinations are challenging but possible in some cases. Some OVI abundances have been estimated from UV observations, and for OVII and OVIII measurements along the same lines of sight, their abundances can be estimated as well. Another approach is to obtain absorption line measurements through regions that have emission line detections, around clusters or groups (0.7-2 R_{virial}). The emission measure contains the electron density while the absorption is proportional to the ionic column, so by combining them, one can determine abundances.

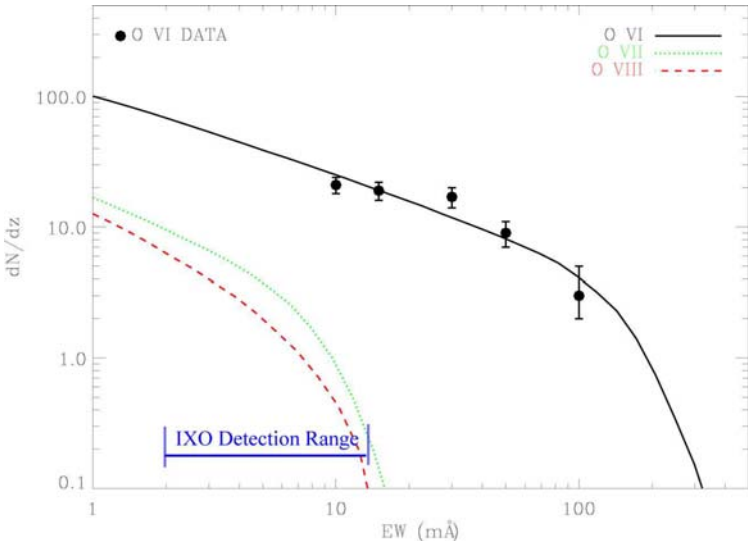

Figure 3. The differential number of absorbers as a function of equivalent width for OVI (λ1035), OVII (Kα), and OVIII (Kα), based on the model of Cen & Fang (2006); the OVI data are from Danforth and Shull (2005). Current claims of OVII and OVIII absorption are well above predictions and would indicate a temperature distribution significantly different than these models. The OVII and OVIII absorption lines predicted from the models, such as those in the range 2-15 mÅ, are not accessible to *Chandra* or *XMM*, but can be measured with *IXO*.

The primary observational program will obtain spectra for 30 known background AGNs, with a median flux of 5×10^{-11} erg cm^{-2} s^{-1} and median redshift of

0.3. Against these AGNs, high-throughput spectroscopy in the 0.3–1.0 keV band will measure the abundant ion stages of heavy elements in the hot IGM (Figure 4). This program will address the hot baryons primarily in the low-redshift universe ($z < 0.5$), which is where the hot gas is predicted to be most common. Also, at low redshift, one can identify and study the galaxies at every detection site.

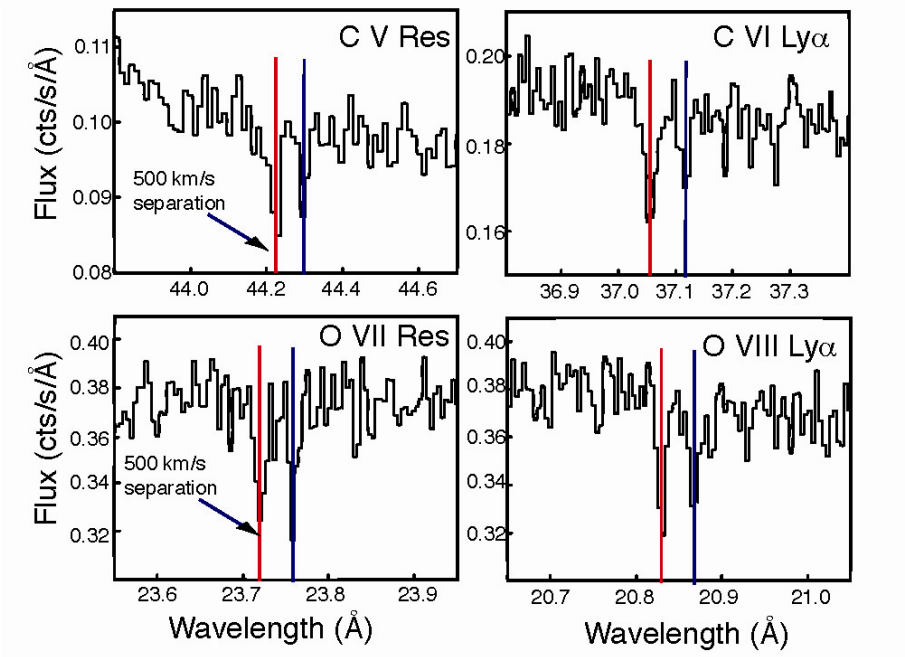

Figure 4. Simulations for *IXO*, with the baseline configuration, of the absorption by the Cosmic Web seen against a background AGN with a 0.5-2 keV flux of 5×10^{-11} erg cm^{-2} s^{-1} and an exposure time of 600 ksec ($z_{abs} = 0.1$); this is the 16th brightest AGN in a sample of 30. There is a multi-temperature gas (as given by Figure 1) with a superwind, producing a double-lined configuration with a separation of 500 km/s. For an AGN at an emission redshift of 0.3, calculations predict one absorption system with the strength shown. The lines shown here would be the signature of a multi-temperature medium with a temperature range of nearly an order of magnitude; additional lines are also detected (NVI, NVII).

The *International X-ray Observatory* (*IXO*) will have a sensitivity to the OVII resonance line that is 15 times better than with XMM or Chandra. The grating spectrometer has a baseline design resolution of 3000 (100 km/s) and a collecting area of 1000 cm^2. With *IXO*, the brightest quartile of sources can be studied in 2 Msec and the entire sample will require 18 Msec, a multi-year project (if the project achieves its goal of 3000 cm^2 in collecting area for the gratings, these times are reduced by a factor of three). The data products from this work will be absorption line measurements for the He-like and H-like species of O, C, and N, which exist in the temperature range 10^5-10^7 K. Simulations show that the OVII line will be the strongest, but that multiple lines will be detected in about 80% of the targets. For each line, we obtain the column density (most lines are optically thin), velocity, and velocity width. We project that we will measure at least 100 OVII lines down to a limit of $10^{14.5}$ cm^{-2}; this will be sufficient to achieve our scientific goals. Potentially, this project can be extended to lower flux levels (especially with a collecting area of 3000 cm^2) since there are 146 sources in the *ROSAT* Bright Source Catalog with $|b| > 15°$ and $F_x > 2\times10^{-11}$ erg cm^{-2} s^{-1}, most of which are AGNs. With 100 or more absorption line systems at low redshifts, it will be possible to construct correlation

functions to compare to cosmological models. This has been carried out with optical-UV quasar absorption line systems and this study would be complementary in that it samples a hotter medium with a greater predicted overdensity.

In addition to the grating spectrometer, there is a quantum microcalorimeter planned for *IXO*, with much more collecting area but far lower spectral resolution (30,000 cm^2, resolution of 250 for the typical absorption line system). Our simulations show that it will be difficult to detect most weak lines with the microcalorimeter (Figure 5). The lines would be unresolved with the microcalorimeter and small gain variations in the instrument could masquerade as lines. However, the microcalorimeter is essential for detecting faint emission, as described below.

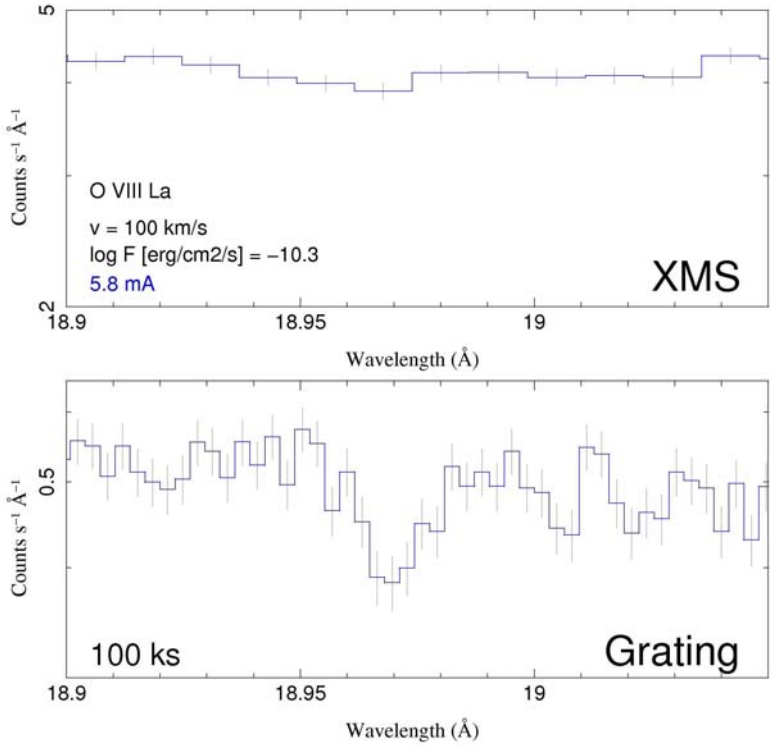

Figure 5. A simulation comparing the grating instrument to the microcalorimeter (XMS) shows the line clearly detected with the grating. Although the same line is formally detected in the XMS, it might be confused with small gain variations in the instrument.

The last goal requires imaging of Cosmic Web filaments as they extend away from galaxy groups and clusters. Such emission has been detected in a few unusual cases, such as the filament connecting Abell 222 and Abell 223 (Werner et al. 2008). However, in these cases, the overdensity (150-300) is somewhat higher than the typical predicted Cosmic Web filaments (10-200 for the hot gas).

From models, the temperature of gaseous filaments extending from clusters is typically $0.2\text{-}1\times10^7$ K, depending on the location in the filament (and on the model), so the bandpass used will be 0.3-1.5 keV. These observations are background-limited, and at an energy of about 0.5 keV, much of the background is due to line emission within the Milky Way. An enormous improvement in sensitivity can be realized by observing between the strong Milky Way lines. Such spectral imaging observations are possible with the quantum microcalorimeter, where the strong Milky Way emission lines are resolved and can be excluded. Also, *IXO* has sufficient angular resolution to remove most point sources (which do not

dominate the background at 0.5 keV) and it has greater collecting area than previous instruments (by a factor of 15 at the relevant energies). The target clusters and groups must have a redshift great enough that the emission lines from the filament are shifted away from the strong Galactic emission lines (e.g., OVII). The optimum redshift ranges are 0.04-0.12 and 0.18-0.28. At these redshifts, target clusters will require mosaic observations to cover the outer regions where the filaments emerge. Even with these advantages, we are unlikely to reach overdensities down to 30, which will be the province of *Gen-X*. *IXO* should be able to measure emission from gas with overdensities near or below 100, which is beyond the classical virial radius. In practice, filaments extending from the clusters will have densities higher than the mean overdensity at that radius (closer to 100), which will aid in detection. *IXO* can be used to search for such filaments in the regions from 0.7-2 R_{virial} with an observing time of about 1 Msec per cluster. A sensible program would begin by observing three clusters and enlarge the program as warranted by the results.

References

Bregman, J.N. 2007, ARA&A, 45, 221.
Buote, David A., Zappacosta, Luca, Fang, Taotao, Humphrey, Philip J., Gastaldello, Fabio, Tagliaferri, Gianpier 2009, arXiv0901.3802.
Cen, R., & Fang, T. 2006, ApJ, 650, 573.
Cen, R., & Ostriker, J.P. 2006, ApJ, 650, 560.
Croft, R.A.C., Di Matteo, T., Dave, R., Hernquist, L., Katz, N., Fardal, M.A., & Weinberg, D.H. 2001, ApJ, 557, 67.
Danforth, C.W., and Shull, J.M. 2008, ApJ, 679, 194.
Fukugita, M., & Peebles, P.J.E. 2004, ApJ, 616, 643.
Kaastra, J.S., Werner, N., Herder, J.W.A.d., Paerels, F.B.S., de Plaa, J., Rasmussen, A.P., & de Vries, C.P. 2006, ApJ, 652, 189.
Nicastro, F., et al. 2005, ApJ, 629, 700.
Stocke et al., 2006, ApJ, 641, 217.
Werner, N., et al. 2008, A&A, 482, L29.

Cosmological Studies With A Large-Area X-ray Telescope

A. Vikhlinin[1], S. W. Allen[2],
M. Arnaud[3], M. Bautz[4], H. Böhringer[5], M. Bonamente[6], J. Burns[7],
A. Evrard[8], J. P. Henry[9], C. Jones[1], B. R. McNamara[10], D. Nagai[11],
D. Rapetti[2], T. Reiprich[12]

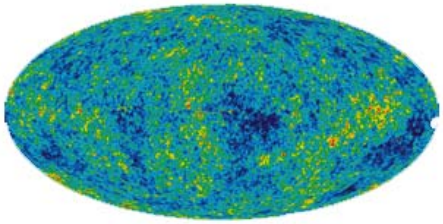

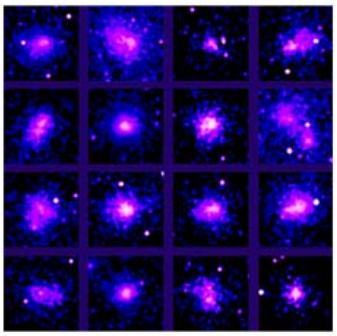

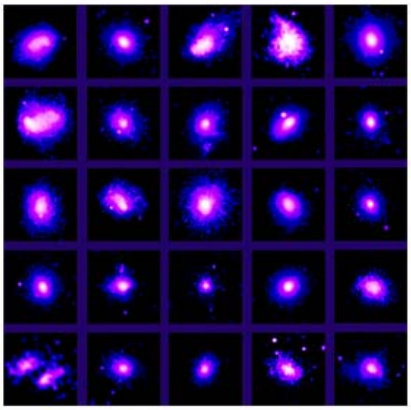

[1] Harvard-Smithsonian Center for Astrophysics [2] Stanford University [3] CEA/DSM/DAPNIA/SAP, CEA-Saclay [4] MIT [5] MPE [6] University of Alabama [7] University of Colorado [8] University of Michigan [9] University of Hawaii [10] University of Waterloo [11] Yale University [12] University of Bonn

1 X-ray cluster cosmology

Clusters of galaxies are a very promising cosmological tools, in particular because X-ray, SZ and optical and near-infrared data can be combined to minimize systematic errors in identifying and characterizing the cluster population. Mass selection systematics are smallest for X-ray or SZ selection, and there is concrete hope for further reduction in these uncertainties in the near future. X-ray astronomy in particular has played an important role in establishing the current cosmological paradigm. In the early 1990s, X-ray measurements of the baryonic mass fraction in nearby galaxy clusters, coupled with improved measurements of the Universal mean baryon density, provided some of the first compelling evidence that we live in a low density Universe [1]. Starting with early 1990's, X-ray measurements of the local number density of clusters and its evolution have also consistently pointed out towards a low-density Universe and a relatively low value of amplitude of matter fluctuations, σ_8, [2–7], a result since confirmed by cosmic microwave background (CMB) studies, cosmic shear, and other experiments [8–12].

Robust and precise understanding of dark matter and dark energy and how they shape the structure and evolution of our Universe can be obtained only through multiple, independent tests. The next generation of X-ray observatories will, among many other things, provide powerful, new tools to probe the structure and mass-energy content of the Universe. These tools will be highly complementary to the best other planned cosmological experiments (Planck, JDEM, LSST). In particular, the unique capabilities of the International X-ray Observatory (IXO) will allow the fullest possible exploitation of forthcoming cluster surveys made at X-ray and other wavelengths, and enable the tightest possible control of systematic uncertainties. Together, a powerful X-ray observatory and these other experiments should enable a quantum leap in our understanding of the Universe.

Cosmological studies in X-rays use observations of galaxy clusters. X-ray data for clusters are crucial since ~ 85% of the baryons within them are in the form of hot X-ray emitting gas. Precise measurements of the X-ray brightness and temperature of this gas permit two powerful and independent types of cosmological tests.

Firstly, observations with a powerful X-ray observatory such as IXO will constrain the growth of cosmic structure, primarily by providing accurate measurements for high-redshift galaxy clusters detected in new, large X-ray and SZ surveys. The eROSITA or proposed WFXT X-ray missions, for example, will discover ~ a few $\times 10^5$ clusters within $z \lesssim 2$, but provide only limited information on the individual properties of high-z objects. Utilizing its much greater collecting area and improved spatial and spectral resolution, IXO will provide precise X-ray mass proxies for a complete subset of these clusters, enabling a much tighter coupling between the survey fluxes and theoretically predicted mass function [13, 14]. This will dramatically enhance the power of these surveys to constrain cosmological parameters [15, 16]. A large catalog of serendipitously discovered clusters will further extend our knowledge of clusters to fainter X-ray fluxes and higher redshifts, beyond $z = 2$.

The second type of cosmological test possible at X-rays is primarily geometric and, like type Ia supernovae (SNIa), constrains the expansion history of the Universe, measuring distance-redshift relation, $d(z)$. Here, the constraints will primarily come from measurements of the X-ray emitting gas mass fraction, $f_{\rm gas}$, in the largest, most dynamically relaxed galaxy clusters: $f_{\rm gas}$ is a theoretically-predicted and observationally-verified 'standard quantity' associated with large clusters (see [17] and references therein). Additional, independent constraining power will also be obtained from the combination of X-ray observations with measurements of the SZ effect in the same clusters.

The ability of IXO to measure the primary X-ray observables (X-ray brightness, temperature,

metallicity and, for the first time, velocity structure in high-z objects) to exquisite precision in a large subset of high-redshift clusters will, when coupled with external information from state-of-the-art hydrodynamical simulations, gravitational lensing studies and follow-up SZ observations, enable the tightest possible control of systematic uncertainties in all cosmological measurements using galaxy clusters.

2 Measuring the growth of cosmic structure

The main techniques proposed to study growth of cosmic structure in future cosmological experiments are 1) measuring the evolution of the mass function of galaxy clusters; 2) wide-area cosmic shear surveys; and 3) using redshift-space distortions in the galaxy-galaxy correlation function. The cosmic shear method is currently the only growth of structure component of the proposed JDEM mission. At present, the constraints on dark energy from cosmic shear and redshift-space distortions are weak. In contrast, the constraints from X-ray studies of the cluster mass function are relatively strong and developing rapidly. The dominant systematic effects in the X-ray method are clear and ways to address them have been identified and are being vigorously pursued using e.g. follow-up gravitational lensing studies, SZ observations, and hydrodynamical simulations.

Recent X-ray studies of the evolution of the cluster mass function using the *Chandra* X-ray Observatory to follow up ROSAT X-ray selected clusters, have convincingly demonstrated that the growth of cosmic structure has slowed down at $z < 1$, due to the effects of dark energy. These measurements have been used to improve the determination of the equation state parameter [16] and to place first constraints on possible departures from General Relativity [18]. With IXO, working in concert with other mutli-wavelength facilities to exploit new cluster surveys, it will be possible to make similar measurements out to redshifts $z \sim 2$, providing a unique and critical insight into cosmic structure growth.

2.1 The basics of cluster mass function measurements The mass function of galaxy clusters, $n(M)$, is an exponentially sensitive indicator of the linear density perturbation amplitude at the $\sim 10\,h^{-1}$ Mpc scale. Given precise cluster masses, the perturbation growth factor in a given redshift bin can be recovered to 1% accuracy from a sample of only 100 clusters in the $10^{14} - 10^{15}$ solar mass range (for fixed values of all other cosmological parameters). This high sensitivity is the main reason why 'counting clusters' provides such an attractive technique for studying the growth of structure.

At present, cluster surveys provide a degenerate combination of constraints on the growth of mass perturbations and the overall geometric properties of the Universe. [This is simply because the volume elements and masses derived from observations are both a function of $d(z)$]. However, looking ahead a decade from now, we can expect techniques such as SNIa, BAO and the X-ray $f_{\rm gas}(z)$ method to have measured $d(z)$ with sufficient precision that the evolution of the cluster mass function will become an essentially 'pure' growth of structure test. At this point, precise mass function measurements will bring unique degeneracy-breaking power, powerfully and straightforwardly enabling significant improvements in constraining the evolution of the dark energy equation of state and in helping to distinguish the origin of cosmic acceleration.

One of the most interesting applications for growth of structure data is in testing theories that attempt to explain cosmic acceleration by modifying the standard rules of gravity (General Relativity) on large scales. In general, modifications to GR will affect theoretical predictions for the cluster mass function by changing both the growth rate of linear perturbations and modifying the process of non-linear collapse. The process of non-linear collapse is already well calibrated for GR-based dark energy models [14]. As the field of research matures, we can expect that the calibration will also become similarly robust for other interesting non-GR models. The com-

bination of precise X-ray and lensing, as well as SZ and optical-dynamical, measurements of the baryonic and dark matter distributions in individual clusters will also aid in probing modified gravity theories on Megaparsec scales because in non-GR theories, dynamic and weak lensing mass estimated in general are not expected to yield the same value.

2.2 Strategy for mass function measurements Systematic, not statistical, uncertainties provide the limiting factor in cosmological measurements based on the cluster mass function. The cluster catalog provided by future X-ray survey missions will be very large and, due to the strengths of X-ray techniques, should have excellent purity and completeness. The primary need will be the accurate calibration of cluster masses. Mass uncertainties are generally of two kinds: 1) systematic *average* biases in the derived masses; and 2) *scatter* in the mass measurements for individual clusters. Both sources of uncertainty are damaging. For example, systematic uncertainties of ±10% in the mean cluster mass at a given redshift automatically lead to ±3% uncertainties in the growth factor.

No single cluster mass measurement technique can address both uncertainties. However, the *combination* of X-ray and lensing methods provides an approach that is both bias-free and has minimal intrinsic scatter, and is also insensitive to detailed physics of cluster formation.

X-ray hydrostatic analyses can provide low-scatter, and even relatively low-bias, mass estimates for the most dynamically relaxed clusters. However, for most systems, systematic scatter and biases in hydrostatic mass estimates are expected at the 20 – 30% level. Although IXO will be able to measure and/or eliminate some such sources of uncertainty (e.g., by measuring bulk motions and turbulence in the intracluster medium via high-resolution X-ray spectroscopy), controlling them at the few percent level from X-ray data alone would appear to be impossible. However, *one does not require hydrostatic X-ray mass estimates for cluster mass function work*. High-resolution cosmological simulations have shown that the parameter $Y_X = T \times M_{\rm gas}$, where T is the average temperature derived from the X-ray spectrum and $M_{\rm gas}$ the gas mass derived from the X-ray surface brightness profile, provides a high-quality proxy for the total mass. The simulations, using different codes, with or without including non-gravitational heating and cooling of the cluster gas, and with different numerical techniques for treating these effects, all show that $M_{\rm tot} \propto Y_X^{\alpha}$, with $\lesssim 10\%$ scatter and a slope very close to the prediction of self-similar theory, $\alpha = 3/5$ (see [15] and later works). The low scatter in the $M_{\rm tot} - Y_X$ relation is therefore a very *robust* theoretical prediction, and the only prediction we need to implement the test outlined below. The minimal scatter in the $M_{\rm tot} - Y_X$ (and also $M_{\rm tot} - M_{\rm gas}$) relations is confirmed by Chandra observations (e.g., [17, 19]).

Weak lensing techniques have a lower limit on the accuracy of mass measurements for individual clusters of 20 – 30%, due to projection effects. This scatter is too large for "precision cosmology" with the cluster mass function. However, *on average*, weak lensing masses are free of bias [20]. By combining the X-ray and lensing approaches, and drawing on their individual strengths, one can obtain mass measurements for samples of clusters that are both low in intrinsic scatter and are bias free.

Once the systematic scatter in the X-ray mass proxy has been reduced to $\lesssim 10\%$, it will have only a small effect on cosmological measurements from the cluster mass function. The dominant uncertainties are then associated with the weak lensing data and establishing the *normalization* of the $M_{\rm tot} - Y_X$ relation in each redshift bin.

Observational calibration of the $M_{\rm tot} - Y_X$ relation is essential. These cannot (currently) be predicted by theory with percent level accuracy. The necessary weak lensing measurements will come from survey data collected by ground

and space-based projects like Pan-STARRS, DES, LSST, JDEM and JWST, but also from targeted ground- and space-based observations. The capabilities of 6m-class telescopes such as Magellan or Subaru are adequate for average weak lensing measurements out to $z \sim 1$; beyond that, some kind of space-based data will be required. It could be either JWST pointings or survey data from JDEM or EUCLID. Assuming that the weak lensing data will provide $M_{\rm tot}$ with 30% scatter and minimal average bias, then by observing ~ 100 clusters in each redshift bin we will normalize the $Y_X - M$ relation at that redshift to $\sim 3\%$. Given 3% accuracy in the normalization of the $Y_X - M$ relation, one can derive the linear perturbation amplitude at this redshift to 1% accuracy. If one were to conservatively assume a factor of two degradation in these measurements (representing a 'pessimistic' scenario), then the same data will still constrain the linear perturbation amplitude to 2% accuracy at each redshift.

Both the weak lensing and X-ray components are essential to this work. If one has only weak lensing masses for the clusters, one cannot accurately reconstruct the mass functions because of the large and unavoidable $\sim$ 30% scatter in the individual mass measurements. Conversely, if one has only precise, X-ray measured Y_X or $M_{\rm gas}$ parameters, it would be hard to control systematic biases in the mass at the level sufficient for the 1–2% growth measurements. Only the combination of the two techniques circumvents these problems.

2.3 The cluster samples Future, scheduled X-ray and SZ surveys will easily provide the samples of clusters required for this work. For example, eROSITA will carry out a sensitive all-sky X-ray survey that will detect $\sim 200,000$ clusters, and this sample will have > 100 clusters per $\Delta z = 0.1$ bin out to $z = 1.5$. The serendipitous cluster catalog constructed by IXO will probe two orders of magnitude lower in X-ray flux over a smaller area and, together with SZ experiments, extend the target list to $z = 2$ and beyond. Proposed next-generation X-ray survey missions like WFXT would extend these surveys yet further.

Selecting 100 massive, X-ray bright clusters in each $\Delta z = 0.1$ redshift bin spanning the range $0 < z < 2$ gives a sample of 2000 clusters requiring weak lensing and X-ray followup. Precise spectroscopic redshifts will automatically be provided for each cluster by the X-ray observations, but can also be obtained in a dedicated optical followup program.

The effective area of the survey-optimized X-ray telescopes telescopes will be insufficient to measure Y_X, even with deep pointed observations, for clusters at $z \geq 0.8$. At higher redshifts, the required Y_X measurements will only be possible with a powerful observatory such as IXO. Detailed exposure time estimates show that $\approx$ 10 Msec of IXO observing time will be required to carry out this program. This is moderate, but by no means prohibitive, investment of observing time over the lifetime of the mission, and will provide a cosmological measurement of fundamental importance. The expected, reconstructed structure growth history is illustrated in Fig. 1. The redshift range of $0 < z < 2$ spans the entire epoch of accelerated expansion. At the highest z, these studies will dovetail into planned Ly-α forest observations.

2.4 Expected results from the $G(z)$ measurement Growth of structure, $G(z)$, data are highly complementary to cosmological expansion history measurements in constraining, for example, the dark energy equation of state. For illustration, we have computed the combined constraints from a SNAP-like SNIa experiment (adopted from [21]) together with the $G(z)$ data from the combined X-ray+weak lensing studies discussed above. The results are shown in Fig.2. Because the distance- and growth-based constraints are nearly orthogonal, their combination improves the equation of state uncertainties by a factor of 2.5. Cluster growth of structure data will provide a vital complement to the JDEM mission, especially if that mission emphasizes $d(z)$ measurements.

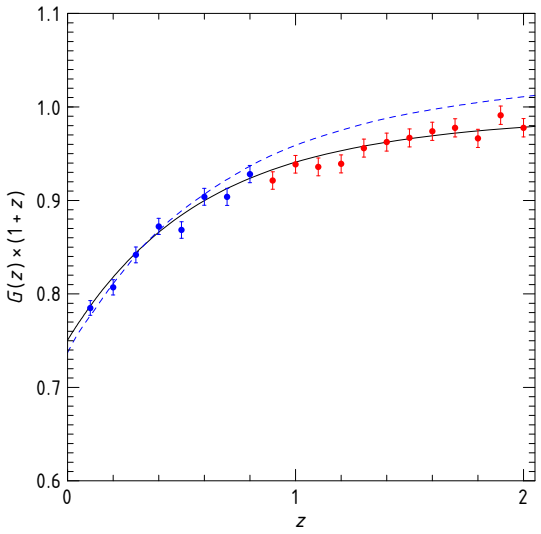

Fig. 1— The normalized growth factor of density perturbations, $G(z)$, constructed from follow-up X-ray and weak lensing observations of 2000 clusters detected in sensitive X-ray surveys. The extension of $G(z)$ measurements to $z = 2.0$ will be possible only with the high sensitivity of IXO. The high-z ($z > 0.8$) data points are crucial for testing non-GR models of cosmic acceleration. For example, the dashed line shows the $G(z)$ function predicted for a DGP model with the same expansion history as the quintessence model depicted by the solid curve.

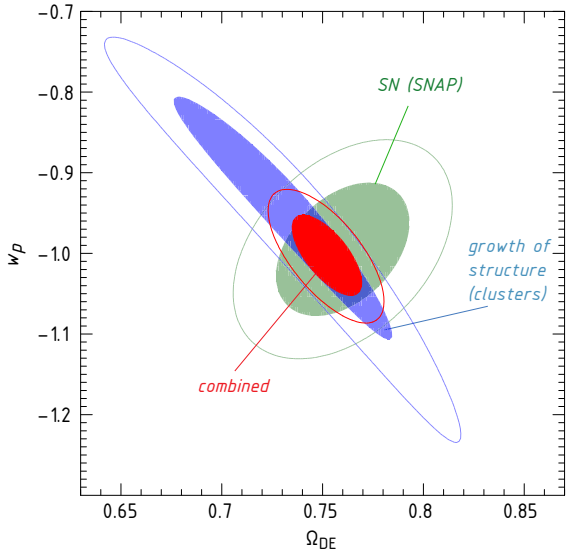

Fig. 2— The improvement in the dark energy equation of state constraints obtained from the combination of distance-based techniques (projected results are shown for the SNAP SNIa experiment), and X-ray growth of structure measurements. Contours show the two-parameter 68% and 95% confidence regions, assuming Planck priors. The combination of SNIa and X-ray growth of structure data improves the equation of state uncertainties by a factor of ~ 2.5. w_p is the value of equation of state at "pivot" redshift, where it is best constrained by the given experiment.

Regardless of the accuracy in the equation of state measurements achieved by JDEM, the next big question will be whether the cosmic acceleration is caused by a physical scalar field or modifications of General Relativity on large scales. The X-ray cluster data will be crucial for testing such models because they, in general, significantly modify the growth factor with respect to GR dark energy models with similar distance-redshift relations. For example, the $d(z)$ relation for a DGP modified gravity model (REF) can be almost indistinguishable from the $d(z)$ of a quintessence model with $w \simeq -0.8$. The growth factor, however, is substantially different, as illustrated by the solid and dashed lines in Fig.1. A DGP-type modification of the growth history will be easily detectable with the proposed IXO measurements at $z > 1$.

A more quantitative demonstration of IXO capabilities in constraining non-GR theories can be based on the so called "growth index", γ [22]. For GR and a very wide range of "physical" dark energy models, such as quintessence, γ is close to 0.55. Therefore, departures from General Relativity can be searched for by detecting deviations in γ from 0.55. For example, $\gamma = 0.68$ is predicted for the DGP model. The projected $G(z)$ measurements in Fig.1 will constrain γ to ± 0.022 (0.045) using cluster data only, and to ± 0.018 (0.034) from combination of the cluster and Planck data, assuming that the masses of light neutrinos are known). The values in parentheses are for the "pessimistic" calibration scenario in which projected uncertainties for mass calibration are degraded by a factor of 2, as discussed above. Huterer & Linder predict [22] that γ will be constrained to ± 0.044 from combination of the supernovae and weak lensing measurements from a SNAP-type mission combined with Planck CMB priors.

3 Probing the expansion history with $f_{\rm gas}(z)$

The ratio of baryonic-to-total mass in clusters should closely match the ratio of the cosmological parameters Ω_b/Ω_m because the matter content of the largest clusters of galaxies is expected to provide a fair sample of the matter content of the Universe [1]. The baryonic mass in clusters is dominated by X-ray emitting gas, the mass of which exceeds the mass in stars by a factor of ~ 6, with other sources of baryonic matter being negligible. The combination of X-ray measurements of $f_{\rm gas}$ with optical/near-IR estimates of the stellar mass, and determinations of Ω_b and H_0 from e.g. CMB data, can therefore be used to measure Ω_m.

Measurements of $f_{\rm gas}$ as a function of redshift also probe the acceleration of the Universe. This constraint originates both from the fact that for the largest clusters $f_{\rm gas}$ is predicted to be a near-invariant quantity with minimal intrinsic scatter [23, 24] and from the dependence of the $f_{\rm gas}$ measurements (which are derived from the observed X-ray temperature and density profiles, assuming hydrostatic equilibrium) on the assumed distance to the clusters: $f_{\rm gas} \propto d^{3/2}$. The latest results from this experiment [17] using Chandra data for 42 hot, relaxed clusters, give marginalized constraints of $\Omega_M = 0.28 \pm 0.05$ and $\Omega_\Lambda = 0.86 \pm 0.22$ (Fig.3). The Chandra data confirm that the Universe is accelerating at 99.99% confidence, comparable in significance to the best current SNIa data combined. We emphasize that systematic scatter remains *undetected* in current Chandra $f_{\rm gas}$ data for hot, relaxed clusters, despite a weighted-mean statistical distance error of only 5% [17]. This compares favorably with SNIa, where systematic scatter is detected at the 7% level in the individual distance estimates [25].

The prospects for $f_{\rm gas}$ studies with IXO have been studied in detail in [26]. An investment of $\sim$ 10 Ms of IXO time to measure $f_{\rm gas}$ to 5% (corresponding to 3.3% accuracy in distance) in each of the 500 hottest, most X-ray luminous, dynamically relaxed clusters detected in future cluster surveys, will be sufficient to constrain cosmological parameters with a DETF [21] figure of merit (FoM) of 20–40. This range in FoM spans pessimistic to optimistic assumptions regarding systematic uncertainties [26]. Similar cosmological constraints would also be achievable by observing the best 250 clusters for 40 ks each, on average; such a strategy may prove useful at higher z if the fraction of relaxed clusters is found to drop faster than expected. Gravitational lensing data will again be used to pin-down the mean hydrostatic mass bias in each redshift bin. (These biases are not expected to exceed 10% for the largest, relaxed clusters.)

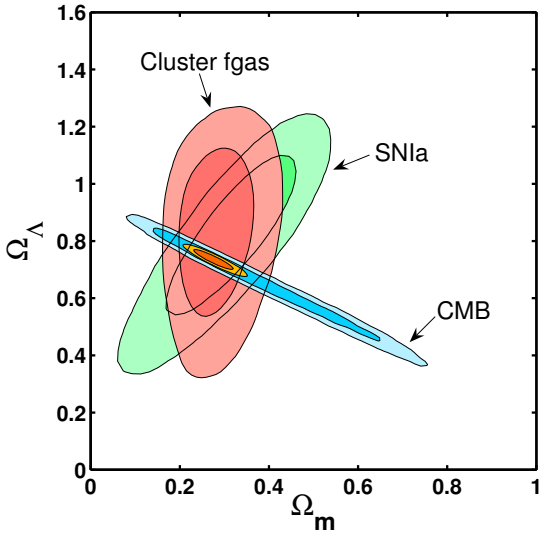

Fig. 3— Constraints on $\Omega_M - \Omega_\Lambda$ from the current *Chandra* $f_{\rm gas}$ measurements.

The constraints on the expansion history (see Fig. 4) from the IXO $f_{\rm gas}$ experiment are comparable to, or exceed, those expected for future 'Stage IV' ground and space-based SNIa and BAO experiments [21]. In particular, the $f_{\rm gas}$ data are expected to provide a very precise measurement of the mean matter density, $\Omega_{\rm m}$. Most importantly, the very different natures of the astrophysics and systematics affecting the $f_{\rm gas}$, SNIa and BAO experiments will ensure maximum robustness when the results are combined. The addition of follow-up SZ observations will boost the IXO FoM still further, providing independent

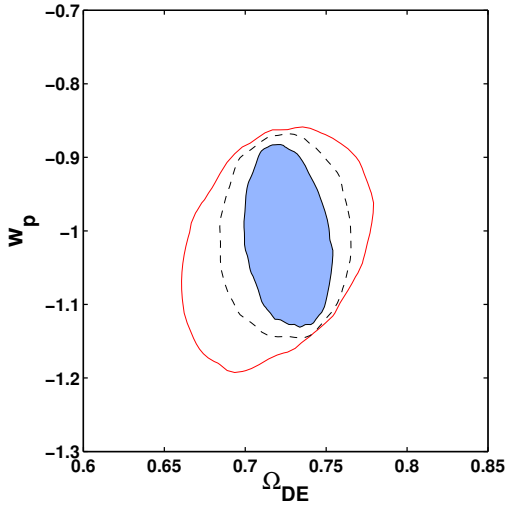

Fig. 4— The projected 95% confidence contours for the IXO $f_{\rm gas}$ experiment in the $\Omega_{\rm DE} - w_p$ plane for the default dark energy model and optimistic (2%; blue, solid contour), standard (5%; dashed contour) and pessimistic (10%; red contour) allowances for systematics. The figure presented in an identical style to the DETF report [21] to allow direct comparison with those results.

constraining power via the classic 'XSZ' experiment that combines X-ray and SZ measurements of the Compton y-parameter [26, 27]. Although less intrinsically powerful, than the $f_{\rm gas}$ test, the XSZ experiment rests on different assumptions and has different systematic uncertainties. The optimal IXO observing strategies for both the $f_{\rm gas}$ and XSZ experiments are identical and will use the same X-ray observations of the largest, dynamically relaxed clusters [26].

4 Summary

A moderate investment of observing time with the International X-ray Observatory to study high-redshift galaxy clusters detected in future large-scale surveys, will provide cosmological measurements of fundamental importance. IXO observations, combined with lensing follow-up, will measure the perturbation growth factor from $z = 0 - 2$ with an accuracy comparable to, or possibly better than, that expected from observations of cosmic shear with JDEM, and redshift-space distortions with EUCLID. The growth of structure data derived from clusters will significantly improve our knowledge of the dark energy equation of state and will aid in constraining non-GR models for cosmic acceleration. IXO observations of the largest, dynamically relaxed clusters will provide a powerful, independent measurement of the cosmological expansion history using the apparent $f_{\rm gas}(z)$ trend. Systematic and statistical errors from this technique are competitive with SNIa and BAO studies, making the test extremely useful for improving the accuracy and reliability of the geometric cosmological measurements planned for LSST and JDEM. Only by employing a range of powerful, independent approaches, including those discussed here, can robust answers to puzzles as profound as the origin of cosmic acceleration be expected.

References

[1] White, S. D. M. et al., 1993, Nature, 366, 429
[2] Henry, J. P. & Arnaud, K. A., 1991, ApJ, 372, 410
[3] Reiprich, T. H. & Böhringer, H., 2002, ApJ, 567, 716
[4] Eke, V. R. et al., 1998, MNRAS, 298, 1145
[5] Borgani, S. et al., 2001, ApJ, 561, 13
[6] Allen, S. W. et al., 2003, MNRAS, 342, 287
[7] Schuecker, P. et al., 2003, A&A, 398, 867
[8] Spergel, D. N. et al., 2007, ApJS, 170, 377
[9] Komatsu, E. et al., 2008, arXiv:0803.0547
[10] Dunkley, J. et al., 2008, arXiv:0811.4280
[11] Benjamin, J. et al., 2007, MNRAS, 381, 702
[12] Fu, L. et al., 2008, A&A, 479, 9
[13] Jenkins, A. et al., 2001, MNRAS, 321, 372
[14] Tinker, J. et al., 2008, ApJ, 688, 709
[15] Kravtsov, A. V., Vikhlinin, A. & Nagai, D., 2006, ApJ, 650, 128
[16] Vikhlinin, A. et al., 2008, arXiv:0812.2720
[17] Allen, S. W. et al., 2008, MNRAS, 383, 879
[18] Rapetti, D. et al., 2008, arXiv:0812.2259
[19] Vikhlinin, A. et al., 2008, arXiv:0805.2207
[20] Corless, V. L. & King, L. J., 2009, arXiv:0901.3434
[21] Albrecht, A. et al., 2006, astro-ph/0609591
[22] Huterer, D. & Linder, E. V., 2007, Phys. Rev. D, 75, no. 2, 023519
[23] Nagai, D., Vikhlinin, A. & Kravtsov, A. V., 2007, ApJ, 655, 98
[24] Fang, T., Humphrey, P. J. & Buote, D. A., 2008, arXiv:0808.1106
[25] Jha, S., Riess, A. G. & Kirshner, R. P., 2007, ApJ, 659, 122
[26] Rapetti, D., Allen, S. W. & Mantz, A., 2008, MNRAS, 388, 1265
[27] Bonamente, M. et al., 2006, ApJ, 647, 25

The Evolution of Galaxy Clusters Across Cosmic Time

A Science Working Paper for the 2010 Decadal Survey

M. Arnaud[1], H. Bohringer (MPE), C. Jones (CfA), B. McNamara (University of Waterloo), T. Ohashi (Tokyo Metropolitan University), D. Patnaude (CfA), K. Arnaud (NASA/GSFC), M. Bautz (MIT), A. Blanchard (Laboratorie d'Astrophysique de Toulouse-Tarbes), J. Bregman (University of Michigan), G. Chartas (Penn State University), J. Croston (University of Hertfordshire), L. David (CfA), M. Donahue (Michigan State University), A. Fabian (IfA, Cambridge), A. Finoguenov (MPE), A.Furuzawa (Nagoya University), S. Gallagher (University of Western Ontario), Y. Haba (Nagoya University), A. Hornschemeier (NASA/GSFC), S. Heinz (University of Wisconsin), J. Kaastra (SRON), W. Kapferer (University of Innsbruck), G. Lamer (Astrophysikalisches Institut Potsdam), A. Mahdavi (San Francisco State University), K. Makishima (The University of Tokyo), K. Matsushita (Tokyo University of Science), K. Nakazawa (The University of Tokyo), P. Nulsen (CfA), P. Ogle (Spitzer Science Center), E. Perlman (University of Maryland, Baltimore County), T. Ponman (University of Birmingham), D. Proga (University of Nevada, Las Vegas), G. Pratt (MPE), S. Randall (CfA), T. Reiprich (Argelander-Institut für Astronomie), G. Richards (Drexel University), K. Romer (University of Sussex), M. Ruszkowski (University of Michigan), R. Schmidt (Astronomisches Rechen-Institut), R. Smith (CfA), H. Tananbaum (CfA), A. Vikhlinin (CfA), J. Vrtilek (CfA), D. Worrall (University of Bristol)

[1]CEA-IRFU
Service d'Astrophysique
Ormes des Merisiers
91191 Gif sur Yvette Cedex
France
email: Monique.Arnaud@cea.fr

The large scale structure of the present Universe is determined by the growth of dark matter density fluctuations and by the dynamical action of dark energy and dark matter. While much progress has been made in recent years in constraining the cosmological parameters, and in reconstructing the evolution in the large–scale structure of the dark matter distribution, **we still lack an understanding of the evolution of the baryonic component of the Universe.** How normal, baryonic matter collects in dark matter gravitational wells and forms galaxies and clusters is not understood well enough to make precise predictions about what we see, from first principles.

Present observations, as well as theoretical work, indicate that baryonic structure formation on various scales is deeply interconnected: galaxy formation depends on the large scale environment in which galaxies are found, and on the physical and chemical properties of the intergalactic gas from which they form, which in turn is affected by galaxy feedback. Due to the complex behavior of the baryonic matter, progress has been driven largely by observations and requires us to study simultaneously the evolution of the hot and cold components of the Universe.

Located at nodes of the cosmic web, clusters of galaxies are the largest collapsed structures in the Universe with total masses up to 10^{15} $M_{\odot}$. Over 80% of their mass resides in the form of dark matter. The remaining mass is composed of baryons, most of which (about 85%) is a diffuse, hot T $> 10^7$ K plasma (the intracluster medium, ICM) that radiates primarily in the X-ray band. Thus in galaxy clusters, through the radiation from the hot gas and the galaxies, we can observe and study the interplay between the hot and cold components of the baryonic matter and the dark matter. X-ray observations of the evolving cluster population provide a unique opportunity to address such open and fundamental questions as:

- How do hot diffuse baryons dynamically evolve in dark matter potentials?
- How and when was the excess energy which we observe in the intergalactic medium generated?
- What is the cosmic history of heavy-element production and circulation?

Our current knowledge comes primarily from detailed studies of clusters in the relatively nearby Universe (z<0.5). **Major advances will come from high throughput, high spectral and spatial resolution X-ray observations that measure the thermodynamic properties and metal content of the first low mass clusters emerging at z $\sim$ 2 and directly trace their evolution into today's massive clusters.** X-ray observations at high spectral resolution also will open completely new vistas in discovery space by directly probing the dynamics of the hot gas by mapping the velocity field and turbulence.

How do hot baryons dynamically evolve in dark matter potentials?

Clusters grow via accretion of dark and luminous matter along filaments and the merger of smaller clusters and groups. X-ray observations show that many present epoch clusters are indeed not relaxed systems, but are scarred by shock fronts and contact discontinuities, and that the fraction of unrelaxed clusters likely increases with redshift. Although the gas evolves in concert with the dark matter potential, this gravitational assembly process is complex, as illustrated by the temporary separations of dark and X-ray luminous matter in massive merging clusters such as the "Bullet

Figure 1: **Left:** As shown here for the "Bullet Cluster" (1E 0657-56), following the subcluster – cluster collision, the X-ray gas (in pink) and the dark matter as traced by the lensing (in blue) can become separated. **Right:** Contours of radio synchrotron emission due to relativistic particles, possibly (re)accelerated by shocks and gas turbulence, overlaid on the Bullet cluster X-ray image.

Cluster" (see Figure 1, left). In addition to the X-ray emitting hot gas, the relativistic plasma seen through synchrotron emission in merging clusters (Figure 1, right) is an important ICM component with at present few observational constraints.

Major mergers are among the most energetic events in the Universe since the Big Bang, releasing up to 10^{64} ergs of gravitational potential energy through the merger of two large subclusters. There are important questions to be answered, both to understand the complete story of galaxy and cluster formation from first principles and, through a better understanding of cluster physics, to increase the reliability of the constraints on cosmological models derived from cluster observations (see white paper by Vikhlinin et al.). These include: (1) How is the gravitational energy that is released during cluster hierarchical formation dissipated in the intracluster gas, thus heating the ICM, generating gas turbulence, and producing significant bulk motions? (2) What is the origin and acceleration mechanism of the relativistic particles observed in the ICM? (3) What is the total level of nonthermal pressure support, which should be accounted for in the cluster mass measurements, and how does it evolve with time? To answer these questions, more than an order of magnitude improvement in spectral resolution is required, while keeping good imaging capabilities, to map velocities and turbulence.

High-resolution X-ray spectral imaging can determine the subcluster velocities and directions of motions by combining redshifts measured from X-ray spectra (which give relative line-of-sight velocities) and total subcluster velocities deduced from temperature and density jumps across merger shocks or cold fronts [1]. These measurements combined with high quality lensing observations from instruments such as the LSST will probe how the hot gas reacts in the evolving dark matter potential.

X-ray line width measurements will allow the level of gas turbulence to be mapped in detail for the first time. As an example, Figure 2 shows that the 2.5 eV resolution of the *IXO* calorimeter can distinguish line widths of 100, 300, and 500 km s^{-1} in a small (1 arcmin^2) region of the very

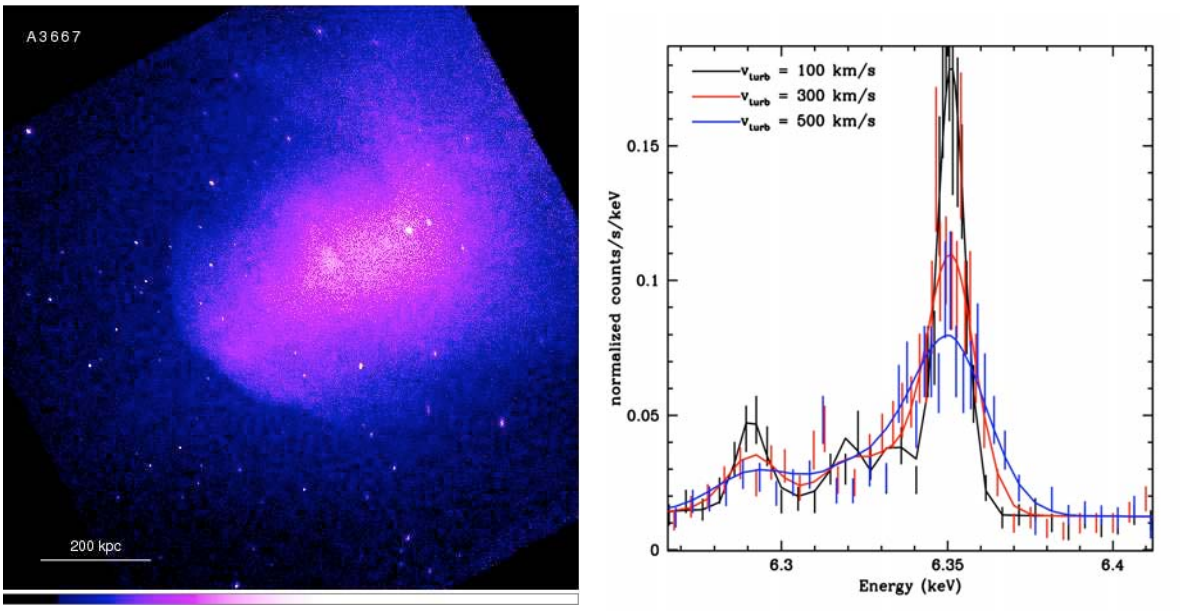

Figure 2: **Left:** 500 ksec *Chandra* image of the z=0.055 merging cluster A3667. **Right:** The 6 keV Fe line region of three simulated (*IXO*) calorimeter spectra for a 1 arcmin^2 region in the very faint shock southwest of the A3667 merging subcluster. The exposure time of the simulations is 200 ksec. The three spectra correspond to different levels of turbulence, with line widths of 100, 300, and 500 km s^{-1}. Since this cluster is undergoing a merger, we also expect to see line shifts due to gas bulk motions.

faint shock of the merging cluster A3667. For a high redshift cluster (with a luminosity of $\sim 10^{44}$ erg s^{-1} at z = 1), the line width could still be measured to an accuracy of 70 km s^{-1} in a 100 ksec exposure, and more precisely if more time is invested.

Sensitive hard X-ray (10–40 keV) imaging can reveal inverse Compton emission from the ICM. Although this emission has so far not even clearly been detected, it promises unique information on the energy density of the relativistic particles, and when combined with next generation radio observatories like SKA, would probe the history of magnetic fields in clusters. Capabilities like those of *IXO* are needed to understand these observationally elusive, but important components of the ICM.

Further crucial insight into cluster assembly can be gleaned from measurements of the *dark matter* distribution in the most relaxed systems. Cosmological numerical simulations of large-scale structure collapse robustly predict that the dark matter distribution should be cuspy, vary with system mass, and evolve with time. Current X-ray observations of bright, local systems confirm the cuspy nature of the distribution, and show some indication for a variation with mass [2,3]. With *IXO*, we can dramatically increase the mass range available for these tests, and, for the first time, tackle the question of evolution by determining the mass profiles up to high redshift ($z \sim 2$), even for low mass systems .

How and when was the excess energy in the intergalactic medium generated?

One of the most important revelations from X-ray observations, supported by recent optical and IR studies, is that non-gravitational processes, particularly galaxy feedback from outflows created by supernovae and supermassive black holes (SMBH), must play a fundamental role, both in the history of all massive galaxies and in the evolution of groups and clusters as a whole. Galaxy feedback is likely to provide the extra energy required to keep the gas in cluster cores from cooling all the way down to molecular clouds, to account for the energy (i.e. entropy) excess observed in the gas of groups and clusters, to cure the over-cooling problem, to regulate star formation, and to produce the red sequence (Note the additional discussion in the "Cosmic Feedback" white paper by Fabian et al.).

It is now well established from *XMM-Newton* and *Chandra* observations of local clusters and groups that their hot atmospheres have much more entropy than expected from gravitational heating alone [4,5,6]. Determining when and how this non-gravitational excess energy was acquired will be an essential goal of the next generation X-ray observatory. Galaxy feedback is a suspected source, but understanding whether the energy was introduced early in the formation of the first halos (with further consequence on galaxy formation history), or gradually over time by AGN feedback, SN driven galactic winds, or an as-yet unknown physical process, is crucial to our understanding of how the Universe evolved.

The various feedback processes, as well as cooling, affect the intergalactic gas in different ways, both in terms of the level of energy modification and the time-scale over which this occurs. Measuring the evolution of the gas entropy and metallicity from the epoch of cluster formation is the key information required to disentangle and understand the respective role for each process. Since non-gravitational effects are most noticeable in groups and poor clusters, which are the building blocks of today's massive clusters, these systems are of particular interest.

A major challenging goal of a future next generation X-ray observatory is thus to study the properties of the first small clusters emerging at $z\sim2$ and directly trace their thermodynamic and energetic evolution to the present epoch.

Future wide-field Sunyaev-Zel'dovich, X-ray (e.g. SRG/eRosita) and optical-IR surveys will discover many thousands of clusters with $z<2$, but will provide only limited information on their individual properties. These surveys will provide excellent samples of clusters for follow-up IXO studies. In addition, ~ 4 low mass clusters per deg^2, with $M > 10^{13}$ $M_\odot$, will be detected serendipitously within the $18' \times 18'$ field of the *IXO* Wide Field Imager. Deep *IXO* observations will determine the X-ray properties of even these low mass systems.

The power of a high throughput, high resolution X-ray mission to study in detail high z clusters is illustrated in Figure 3 which shows simulated, deep spectra for high redshift systems as would be obtained with the *IXO* calorimeter. These will provide gas density and temperature profiles, and thus entropy and mass profiles to $z \sim 1$ for low mass clusters (kT ~ 2 keV, Fig. 3, middle) and for rarer more massive clusters, such as JKCS 041 (Fig. 3, right) up to $z \sim 2$, with a precision currently achieved only for local systems. Measurements of the global thermal properties of the first poor clusters in the essentially unexplored range z = 1.5–2 also will become possible (Fig. 3, left).

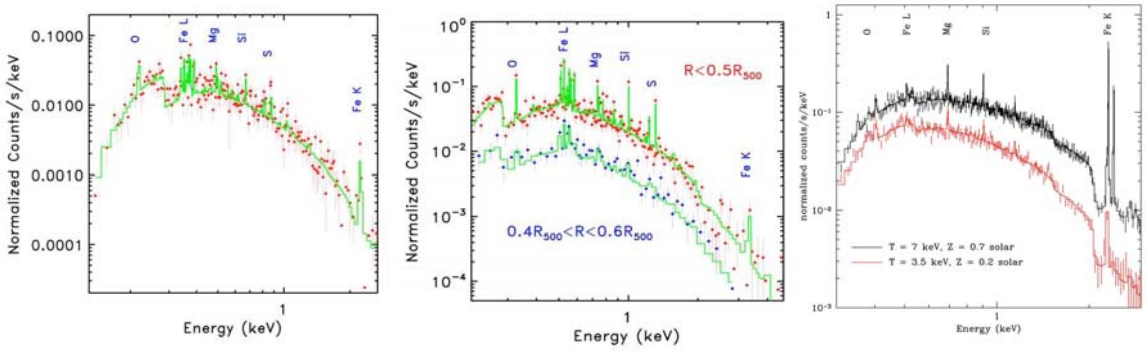

Figure 3: X-ray spectra of high redshift clusters and groups will yield gas temperatures and metallicity profiles. **Left:** *IXO* 250 ksec observation of a low mass (kT=2 keV) z=2 cluster with a bolometric luminosity of 7.7×10^{43} erg s^{-1}. Overall temperature and abundances can be measured accurately: $\pm$3% for kT, $\pm$3.5% for O and Mg, $\pm$25% for Si and S, and $\pm$15% for Fe. **Middle:** The same cluster, but at z=1, observed for 150 ks and for two spectral extraction regions. In the $0.4R_{500}$–$0.6R_{500}$ annulus (R_{500} is a fiducial outer radius of the cluster where the mean cluster mass density is a factor of 500 above the cosmic critical density), the temperature and iron abundances are measured with an accuracy of $\pm$5% and $\pm$20% respectively, illustrating the capability of *IXO* to measure temperature and abundance profiles at z=1, even for low mass systems. **Right:** Simulated *IXO* spectra for the z=1.9 cluster JKCS 041 based on Chandra observations [7]. In an *IXO* exposure of 200 ks, the gas temperature of the core (assumed to be 7 keV) is determined to 3% uncertainty and the overall metallicity to 3%. In the outer region, the gas temperature (assumed to be 3.5 keV) is equally well constrained, while the metallicity is measured to 5%.

What is the cosmic history of heavy element production and circulation?

A fundamental astrophysical question is the cosmic history of heavy-element production and circulation. This is strongly related to the history of star formation, the time and environmental dependence of the stellar initial mass function (and thus the cosmic history of Type I and II SNe) and the circulation of matter and energy between various phases of the Universe. As large 'closed' boxes of the Universe, clusters of galaxies are excellent laboratories to study nucleosynthesis. While the next generation of optical/IR/sub-mm observatories such as JWST, TMT/GMT and ALMA will provide essential information on the star formation history, only sensitive X-ray measurements of lines emitted by the hot ICM, where most of the metals reside, will directly determine the metal abundances in the ICM to high redshifts.

The first open question concerns the production of heavy elements over cosmic time. Chandra and XMM-Newton observations of clusters hint at Fe abundance evolution from z=1 to the present [8,9]. To give a definitive answer on when the metals are produced, we need to extend abundance studies to higher redshifts and for all astrophysically abundant elements. In local systems, the abundance pattern of elements from O to the Fe group, that are produced by supernovae, indicate that both type I and type II SN contribute to the enrichment [10]. However, these measurements only provide a fossilized integral record of the past SN enrichment and thus the evolution of supernovae remains largely unconstrained. Furthermore, the main source of C and N, which can originate from a wide variety of sources (including stellar mass loss from intermediate mass stars,

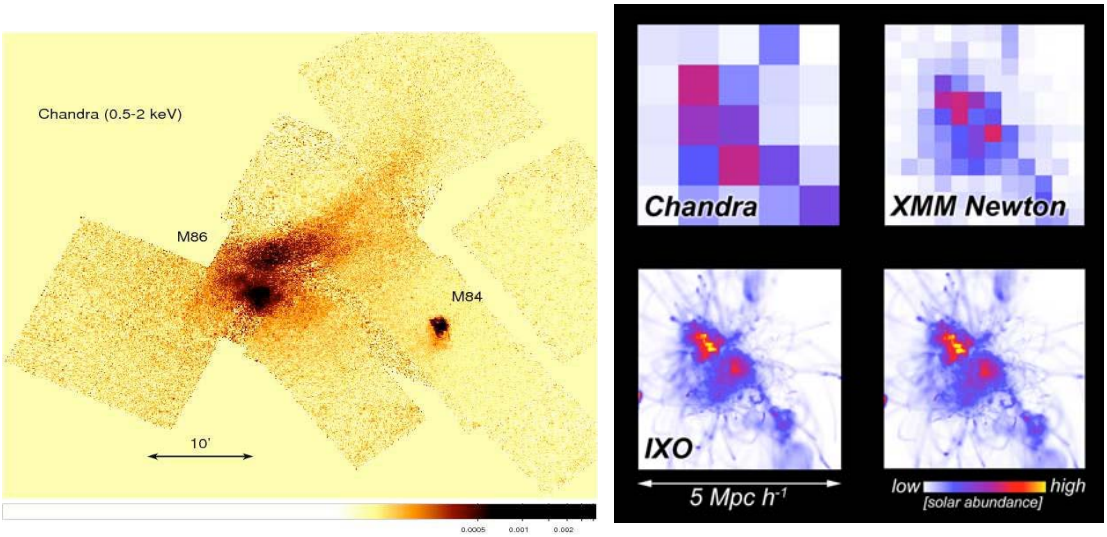

Figure 4: **Left:** X-ray emission from the Virgo elliptical galaxy M86 and its 380 kpc ram pressure stripped tail dominates this mosaic of Chandra images. Sensitive, high resolution X-ray spectroscopy will measure the metallicity along the tail and in the surrounding cluster gas. **Right:** Chandra, XMM, and *IXO* simulations show the metal abundance and distribution in a merging cluster. In this example, a merging 7 keV cluster of $L_X = 2 \times 10^{44}$ erg s^{-1} at z = 0.05 is observed for 30 ksec by each observatory compared to the actual assumed metal distribution (lower right panel). In this example, the calorimeter will image a 0.3×0.3 Mpc region. A similar cluster at z=0.1 would produce a comparable map in $\sim$ 100 ksec and the *IXO* field of view would be 0.54×0.54 Mpc. Several exposures would be required to map the whole region.

whose cosmic history is poorly known) is still under debate.

The second fundamental – and even more complex – open question is how the metals produced in the galaxies are ejected and redistributed in the ICM. Although AGN outflows as well as galaxy–galaxy interactions can add metals to the ICM, studies of local cluster abundance profiles suggest that the metal enrichment of the ICM is due primarily to galactic winds and ram pressure stripping of enriched gas from galaxies by the ICM [10], an example being the ram-pressure stripped tail of the Virgo cluster galaxy M86, shown in Figure 4 (left). These processes would result in different distributions for the metallicity within the cluster and over time. For example, at high redshifts, galactic winds are expected to be effective at enriching the ICM, while at lower redshifts, when massive clusters have formed, the dense ICM, especially in the cluster cores, can ram-pressure strip the enriched gas from galaxies and can even suppress galactic winds and quench star formation. The enriched material is not expected to be immediately mixed with the ICM, and in fact in the brightest, best studied nearby clusters, current X-ray observations show that the metallicity distribution in the ICM is inhomogeneous [11]. Thus by mapping the metallicity in samples of clusters over cosmic time, one can untangle the various transport processes that contribute to the enrichment. In addition, if the mass in metals is calculated assuming that the metallicity is uniform, this will miss estimate the true metal mass in the clusters.

Measurements of the metallicity distribution in clusters, for a wide range of masses, dynamical states, and redshifts, are required in order to understand the ejection and redistribution process within clusters. These studies would also have far reaching consequences for our understanding of

the excess energy that is present in the ICM, as some of the transport processes (SNe winds and AGN outflows) also inject energy into the ICM, as well as for our understanding of environmental effects on the galaxy star formation history, when combined with optical and IR observations.

A high-throughput, high-resolution X-ray observatory, such as *IXO*, is required to provide answers to the questions concerning the production, circulation, and evolution of heavy elements in the ICM. The energy resolution of the calorimeter, much smaller than the equivalent width of the strongest emission lines, combined with good spatial resolution will allow a dramatic improvement in the abundance measurements. This is illustrated in Figures 3 and 4. Metal content and abundance patterns could be traced up to z $\sim$ 2 even in low mass clusters (Fig. 3, left). Element profiles will be measured up to z $\sim$ 1 for poor clusters and up to z $\sim$ 2 for more massive objects (Fig. 3, center and right). In addition, in more nearby clusters, we will be able to resolve the 2D metal distribution down to the relevant physical mixing scales (Fig. 4, right), and study in detail the process of metal injection by measuring the metallicity in the core and along the stripped tails of infalling galaxies (e.g. M86, Fig. 4, left). We will also be able to measure for the first time, the abundance of trace elements like Mn to Cr in a significant number of clusters. The production of these elements by SNe Ia is very sensitive to the metallicity of the progenitor star and thus X-ray spectroscopy will provide additional strong constraints on the cosmic history of SNe enrichment.

Concluding Remarks

Numerical simulations have reached a stage where modeling, including all hydrodynamical and galaxy formation feedback processes, is becoming feasible, although AGN feedback modeling is still in its infancy. The appropriate physics of these processes is not always clear, and advances are largely driven by observation. Thus, constant confrontation between numerical simulations of galaxy cluster formation and observations is essential for making progress in the field. *IXO* observations of the hot baryons, the most significant baryonic mass component of clusters, combined with observations of the cold baryons (from Herschel, JWST, ALMA, and ground based optical telescopes) as well as radio observations (e.g. SKA) will provide, for the first time, the details for a sufficiently critical comparison. We expect that the major breakthrough of a detailed understanding of structure formation and evolution on cluster scales, as well as understanding the cosmic history of nucleosynthesis, will come from simulation–assisted interpretation and modeling of these new generation observational data.

References

1: Vikhlinin, A. et al. 2001, ApJ, 551, 160; **2:** Pointecouteau, E., et al. 2005, A&A, 435, 1; **3:** Voigt, L., & Fabian, A. C., 2006, MNRAS, 368, 618; **4:** Buote, D., et al. 2007, ApJ, 664, 123; **5:** Pratt, G., et al. 2006, A&A, 446, 429; **6:** Sun, M. et al. 2008, arXiv0805.2320; **7:** Andreon S., et al. 2008 arXiv0812.1699; **8:** Maughan, B., et al. 2008, ApJ. Suppl., 2008, 174, 117; **9:** Balestra, I., et al. 2007,A&A, 462, 429; **10:** Kapferer, W., et al. 2007, A&A, 466, 813; **11:** Sauvageot, J.-L., 2005, A&A, 444, 673

Starburst Galaxies: Outflows of Metals and Energy into the IGM

A White Paper for the Astro2010 Decadal Survey

David K. Strickland (Johns Hopkins University)
Ann Hornschemeier (NASA/GSFC)
Andrew Ptak (Johns Hopkins University)
Eric Schlegel (University of Texas – San Antonio)
Christy Tremonti (MPIA & U. Wisconsin)
Takeshi Tsuru (Kyoto University)
Ralph Tüllmann (Harvard)
Andreas Zezas (Harvard)

Starburst Galaxies: Outflows of Metals and Energy into the IGM

Key Question: What is the contribution of mass, metals and energy from starburst galaxies to the Intergalactic Medium?

Summary of Present Knowledge: Starburst galaxies drive galactic-scale outflows or "superwinds" that may be responsible for removing metals from galaxies and polluting the Intergalactic Medium (IGM). Superwinds are powered by massive star winds and by core collapse supernovae which collectively create $T \lesssim 10^8$ K bubbles of metal-enriched plasma within star forming regions. These over-pressured bubbles expand, sweep up cooler ambient gas, and eventually blow out of the disk into the halo. In the last decade tremendous progress was made in mapping *cool* entrained gas in outflows through UV/optical imaging and absorption line spectroscopy. These studies demonstrated that superwinds are ubiquitous in galaxies forming stars at high surface densities and that the most powerful starbursts can drive outflows near escape velocity. Theoretical models of galaxy evolution have begun to incorporate superwinds, using various ad-hoc prescriptions based on our knowledge of the cool gas. However, these efforts are fundamentally impeded by our lack of information about the *hot* phase of these outflows. *The hot phase X-ray emitting phase of a superwind contains the majority of its energy and newly-synthesized metals, and given its high specific energy and inefficient cooling it is also the component most likely escape from the galaxy's gravitational potential well. Knowledge of the chemical composition and velocity of the hot gas are crucial to assess the energy and chemical feedback from a starburst.* A high priority for the next decade is to enable direct measurements to be made of the rates at which starburst galaxies of all masses eject gas, metals, and energy into the IGM.

Experimental Requirement Necessary to Answer Key Question: A high sensitivity X-ray imaging spectrometer capable of measuring velocities in faint diffuse X-ray emission from plasmas in the temperature range $10^6 \lesssim T(K) \lesssim 10^8$, with a velocity accuracy of $\lesssim 100$ km/s. Such spectral resolution automatically allows detailed line-based plasma diagnostics, and thus composition, energetics and flow rates can be derived.

1 Feedback between Stars, Galaxies and the IGM

We now know that galaxies and the IGM are intimately connected by flows of matter and energy. Both accretion onto galaxies and outflows from galaxies or their central black holes link galaxies to the IGM in what has been termed "Cosmic Feedback." To obtain a deeper physical understanding of either galaxy formation and evolution or the IGM requires that we better understand the physical processes that link them.

In many respects Cosmic Feedback is analogous to Stellar Feedback within galaxies. Stars return both energy and matter back into the interstellar medium (ISM) from which they formed: either mechanically via metal-enriched stellar winds (primarily from massive stars) and supernovae (SNe), or via ionizing photons from hot massive stars. This combination of energetic and chemical "feedback" also plays an important, but currently poorly understood, role in galaxy formation and evolution (see e.g. Kauffmann et al. 1999; Cen et al. 2005; Scannapieco et al. 2008).

Mechanical feedback (stellar winds and SNe) is the primary physical mechanism creating the hot phases of the ISM in star-forming galaxies (spiral, irregular and merging galaxies). The plasmas making up the hot phases of the ISM have temperatures in the range $T = 10^6$

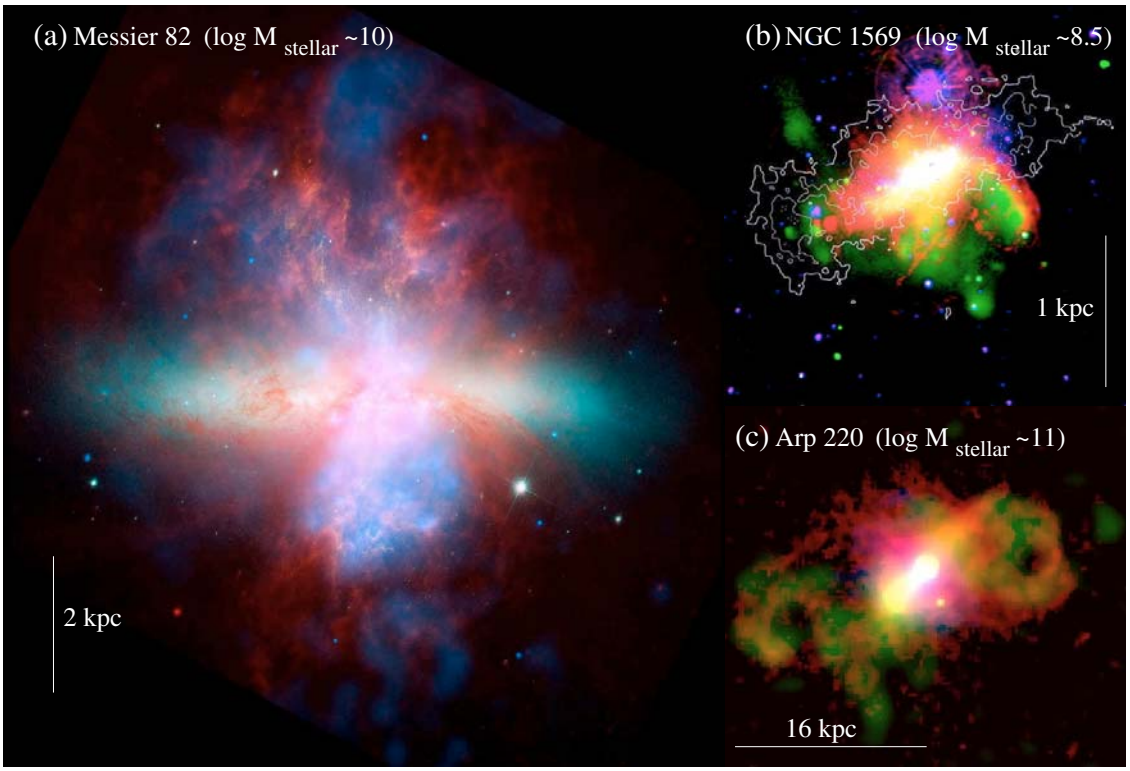

Fig. 1: Superwinds in nearby starburst galaxies of different mass. (a) Messier 82: The archetype of a starburst-driven superwind, as seen by the three NASA Great Observatories. Diffuse thermal X-ray emission as seen by *Chandra* is shown in blue. Hydrocarbon emission at 8μm from *Spitzer* is shown in red. Optical starlight (cyan) and Hα+[NII] emission (yellow) are from *HST ACS* observations. (b) The dwarf starburst NGC 1569. X-ray emission is shown in green, Hα emission in red, optical starlight in blue, and HI column density as white contours (Martin et al. 2002). (c) The Ultra-luminous IR galaxy and merger-driven starburst Arp 220. X-ray emission is shown in green, Hα emission in red, and J-band starlight in blue.

– 10^8 K and predominantly emit and absorb photons in the X-ray energy band from $E \sim 0.1$ – 10 keV. Line emission (from highly-ionized ions of the astrophysically important elements O, Ne, Mg, Si, S, and Fe) dominates the total emissivity of plasmas with temperatures $T \lesssim 10^7$ K, and at higher temperatures Ar, Ca and in particular Fe also produce strong lines. Although the hot phases probably do not dominate the total mass of the ISM in normal spiral galaxies (observationally the properties of the hot phases are uncertain and remain a subject of vigorous ongoing research) they dominate the energetics of the ISM and strongly influence its phase structure (Efstathiou 2000). X-ray observations are a natural and powerful probe of the composition and thermodynamic state of hot phases of the ISM in and around galaxies, and thus are also a powerful tool for exploring the physics of feedback.

This White Paper focuses on the intersection of Cosmic and Stellar Feedback. The intense star formation occurring in starburst galaxies leads to the creation of energetic metal-enriched outflows or superwinds that may pollute the IGM with metals and energy. A high priority for the next decade is to enable direct measurements to be made of the rates at which starburst galaxies of all masses eject gas, metals, and energy into the IGM.

2 Starburst-Driven Superwinds

Superwinds are large-angle (opening angles $\gtrsim 30°$), multi-phase, galactic-scale ($R \gtrsim 5$ – 20 kpc) outflows that have been observed in starbursting galaxies of all masses and environments. Indeed, starburst galaxies with superwinds account for $\sim 20\%$ of the high mass star formation in the local Universe, having been observed in all galaxies where the average star formation rate per unit area exceeds $\Sigma_{\rm SF} \gtrsim 10^{-1}\, M_\odot\, {\rm yr}^{-1}\ {\rm kpc}^{-2}$ (Heckman et al. 1990; Lehnert & Heckman 1996; Veilleux et al. 2005, see Fig. 1). The UV-selected star-forming galaxies at $z \sim 2 - 4$ that may dominate the total star formation density at these redshifts are known to drive powerful winds that appear to be physically identical to local superwinds (see e.g. Pettini et al. 2001; Shapley et al. 2003). Thus superwinds are a fundamental aspect of the Universe as we know it.

Superwinds are the strongest candidate for the cause of a number of current astrophysical puzzles: the origin of the galaxy mass-metallicity relationship ($M-Z$), and more specifically the galaxy mass versus effective yield relationship, $M - y_{\rm eff}$, which suggest that lower mass galaxies have lost significant fractions of all the heavy elements ever created by their stars (Tremonti et al. 2004); the source of the metal enrichment of the IGM (e.g. Songaila 1997; Simcoe et al. 2006); and the creation of $\sim$ 100-kpc-scale holes in the IGM at redshift $z \sim 3$ (Adelberger et al. 2003).

Although we have good reasons to suspect that superwinds are solely or partly responsible for these phenomena we have yet to robustly quantify their role. We do not know the rates at which even local starbursts eject gas, metals and energy, in particular because these are dominated by the hottest and most tenuous gaseous phases. Even if winds are significant contributors to IGM enrichment we do not know what type of galaxy dominates ejection (Which masses? What level of star formation? Is galaxy environment important?), and over what range of epochs this process is significant. There is still much we don't know about the IGM baryon and metal budget. The galaxy $M - y_{\rm eff}$ relationship is not a measure of the instantaneous metal ejection efficiency for starbursts of a given mass, and is potentially misleading because $y_{\rm eff}$ is only a sensitive barometer of metal loss in gas rich systems with little star formation subsequent to the burst (Dalcanton 2007). For example, some authors argue that only winds from the lowest mass galaxies can reach the IGM (Ferrara & Tolstoy 2000; Keeney et al. 2006), while others argue that winds can indeed escape from powerful starbursts in more massive galaxies (Strickland et al. 2004b).

Solving these problems requires the capability to directly measure the pollution rate of the IGM with gas, metals, energy and momentum by superwinds in galaxies covering a broad range of galaxy mass and star formation activity.

2.1 What We Currently Know About Superwinds

Superwinds are driven by merged core-collapse SN ejecta and stellar winds, which initially create a $T \sim 10^8$ K metal-enriched plasma within the starburst region. This over-pressured gas expands and breaks out of the disk of the host galaxy, converting thermal energy into kinetic energy in a bi-polar outflow, which can potentially reach a velocity of $3000\,{\rm km\,s^{-1}}$. This tenuous wind-fluid sweeps up and accelerates cooler denser ambient disk and halo gas. Radiation pressure may also play a role in accelerating the dense entrained gas.

Theoretical models predict that the entrained cool gas is accelerated to lower velocities than the hot, metal-enriched, gas (e.g. Chevalier & Clegg 1985; Strickland & Stevens 2000,

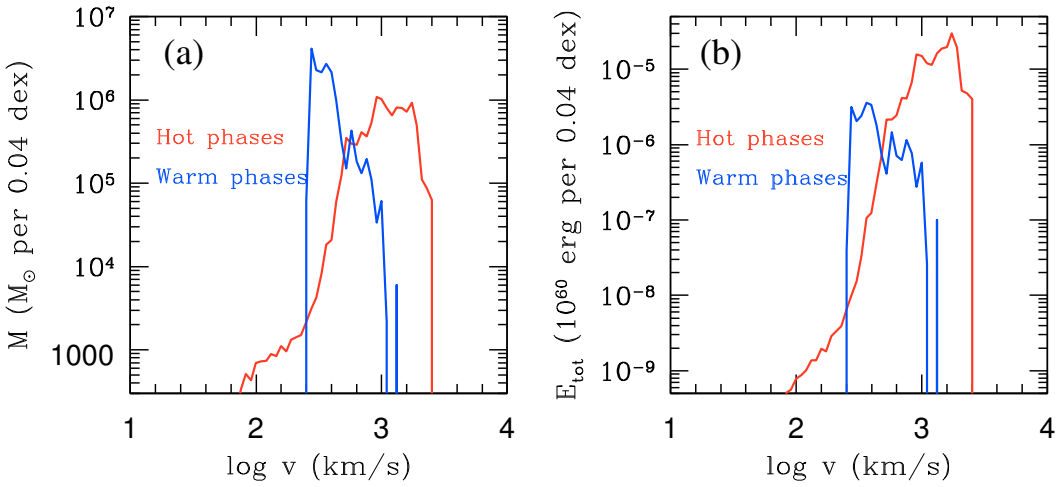

Fig. 2: Gas mass and total energy (thermal plus kinetic) as a function of velocity in a hydrodynamical simulation of a starburst-driven superwind. Current theoretical models for superwinds predict that the hot phases ($6.3 \leq \log T \leq 8.3$, shown in red) have systemically higher outflow velocities than the warm neutral and ionized phases ($3.8 \leq \log T \leq 4.2$, shown in blue) that are currently used to measure velocities in superwinds. From Strickland & Dinge (in preparation).

see Figs. 2 & 3). All existing observational velocity measurements of superwinds are of the entrained cooler material, e.g. warm neutral and ionized gas with outflow velocities in the range 200 – 1000 km s^{-1} measured using UV/optical emission and/or absorption lines (see Shapley et al. 2003; Rupke et al. 2005; Martin 2005). Although this material has velocities that are near galactic escape velocity, we expect that the hot phases are indeed escaping.

The theoretical models predict that the majority of the energy (90%) and metal content in superwinds exists in the hot ($T \geq 10^6$ K) phases, with the kinetic energy of such gas being several times the thermal energy. Thus the metal-enriched phases are most likely to escape into the IGM. This material has long been observationally elusive, although we know believe we have firmly detected it in X-ray emission (Strickland & Heckman 2007; Tsuru et al. 2007).

The current generation of X-ray telescopes offer spectral-imaging with a spectral resolution of order $\Delta E \gtrsim 100$ eV over the 0.3 – 10 keV energy band (Chandra ACIS, XMM-Newton EPIC and Suzaku XIS). At this resolution the emission lines are strongly blended, preventing the use of line-ratio-based spectral diagnostics. *This spectral resolution is too low to allow line shifts or broadening to be measured, preventing any direct measurement of the velocity of the hot gasses.* Nor can existing X-ray gratings be used to obtain higher spectral resolution, because the X-ray emission is both spatially extended and faint.

Nevertheless spectral imaging observations with *Chandra* and *XMM-Newton* detect thermal X-ray emission from hot gas in superwinds extending out to 5 – 30 kpc from the plane of edge-on starburst galaxies (Strickland et al. 2004a; Tüllmann et al. 2006). Forward-fitting techniques do allow certain spectral parameters such as temperature, emission integral ($n_e^2 V$), and relative elemental abundances (suggestive of enrichment by core-collapse SN) to be crudely estimated under the assumption of collisional ionization equilibrium. Obtaining accurate plasma diagnostics, in particular of ionization state and elemental abundances, will require higher spectral than existing X-ray observatories can provide.

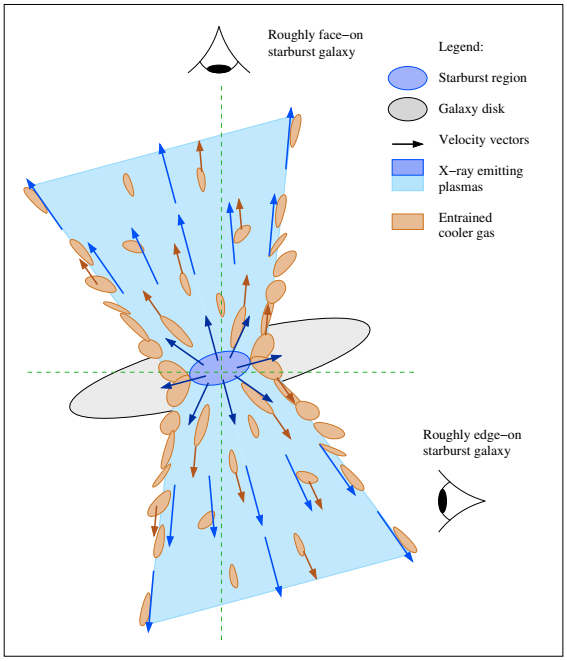

Fig. 3: Schematic diagram of a superwind viewed from different angles, with phase-dependent velocity vectors added to illustrate the line of sight velocity components expected. The combination of galaxy inclination and geometrical divergence within the wind leads to velocity shifts in the line centroids and line broadening or splitting. The resulting velocity components along the line of sight are significant fractions of the intrinsic velocity even in roughly edge-on starbursts. This diagram is simplified in that no acceleration or deceleration or change of geometry of the flow with position is shown. In practice we would look for such changes (in particular in roughly edge-on systems) using spatially-resolved X-ray spectroscopy. [Figure best viewed in color.]

Although the average galaxy with a superwind at $z \sim 3$ has a higher net star formation rate than the average local starburst, local starbursts with superwinds cover the same range of fundamental wind parameters such as warm gas outflow velocity and mass flow rate, and star formation rate per unit area, as high redshift starbursts. There are no significant obstacles that prevent us from applying the physics of local superwinds to superwinds at the epoch of galaxy formation.

3 Creating A Future for Superwind Studies

Without direct measurements of the velocity of the hot gas in a superwind, which can only be obtained with a high resolution X-ray imaging spectrometer, we can not know whether the hot metals created in the starburst have sufficient energy to escape the galactic gravitational potential well and reach the IGM.

High spectral resolution would automatically allow the use of line-ratio-based temperature and ionization state diagnostics, and thus lead to more accurate elemental abundance determinations. Combined with velocity measurements we would obtain the mass, metal and energy flow rates that we require to assess the impact and influence of superwinds.

High sensitivity will allow robust spectroscopy of the very faint soft X-ray emission from the halos of starburst galaxies and the accumulation of moderately-sized samples of local galaxies covering meaningful ranges in parameter space. We require measurements of gas velocity and ejection rates in superwinds covering a range of different galaxy mass and star formation rate to assess which class of galaxies dominates the metal enrichment of IGM in the present-day Universe, and in order to relate the results to higher redshift galaxies and local galaxy properties such as the galaxy $M - y_{\rm eff}$ relationship.

This is not to suggest that advances in theoretical or other observational capabilities are neither welcome nor necessary. For example, UV/optical spectroscopy of the warm neutral and warm ionized phases (entrained gas) in superwinds provides the vital link that allows us to relate the properties of $z \ll 1$ superwinds to the starburst-driven outflows at redshifts

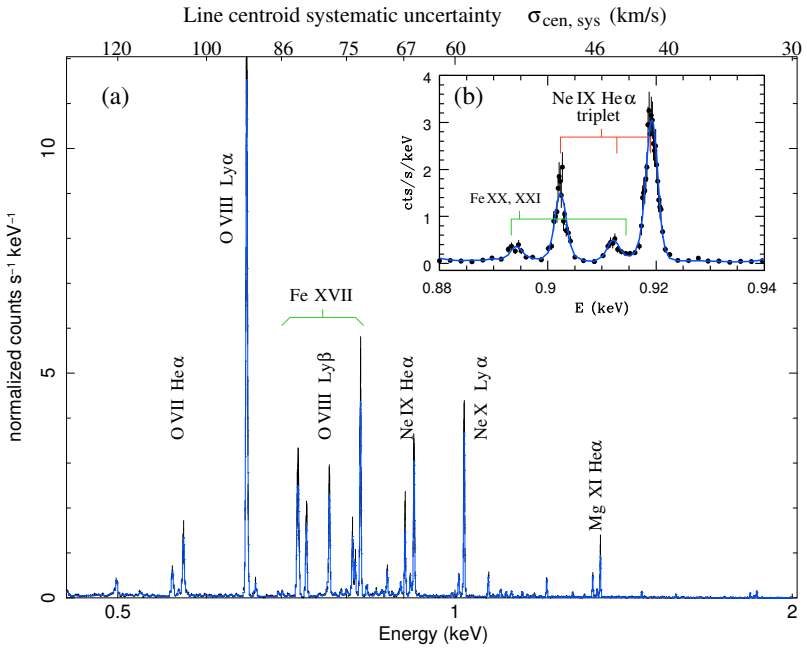

Fig. 4: (a) A simulated spectrum of a small region within a superwind based on the *IXO* XMS microcalorimeter instrument, illustrating the relative strength of the line emission. The simulation is of a supernova II-enriched $kT = 0.4$ keV thermal plasma containing ~ 16000 counts in the $E = 0.3 - 2$ keV energy band. The uncertainty in the line centroids due to the ± 0.2 eV systematic uncertainty in the absolute XMS energy scale is shown in terms of the associated velocity uncertainty. (b) A close-up of the spectrum around the energy of the Ne IX Heα triplet.

$z \gtrsim 2$ (Shapley et al. 2003). Radio and millimeter wavelength observations (e.g. *ALMA*) constrain the molecular gas budget of winds and the nature of the starburst regions where winds are launched. Nevertheless, without the X-ray spectroscopic capability to measure the "true" velocity of superwinds such progress would be futile.

4 Measuring Velocities in the X-ray-emitting Gas of a Superwind

The remainder of this White Paper discusses the experimental accuracy needed to achieve these goals, in particular velocity measurements, in comparison to the expected capabilities of the *International X-ray Observatory* (*IXO*). We consider only one of the possible observational methods of measuring hot gas velocities in superwinds with *IXO*, specifically soft X-ray emission-line spectroscopy using the X-ray Microcalorimeter System (XMS). This method is most closely related in method to traditional observational studies of the soft X-ray emitting plasmas in the halos of starbursts (e.g. Grimes et al. 2005; Tüllmann et al. 2006). The results presented here are derived and described in greater detail in the Technical Supplement[1], which also discusses alternative methods of measuring wind velocities in the soft and hard X-ray bands.

What velocities do we expect for the X-ray emitting plasma in superwinds?

- Gas motions must be comparable to galaxy escape velocities to be significant in ejecting metals, where $v_{\rm esc} \sim 2 - 3 \times v_{\rm rot}$ (the rotational velocity of the host galaxy).
- Theoretical models of superwinds predict high velocities (up to $3000\,{\rm km\,s^{-1}}$) in gas with $T \gtrsim 10^6$ K, and that this material moves significantly faster than the warm neutral and ionized medium in winds (e.g. see Fig. 2).
- Even if this existing theory is completely wrong, for a wind to exist the hot gas velocity must be comparable or higher than the sound speed in the X-ray emitting gas, for which

[1]The Technical Supplement can be accessed at `http://proteus.pha.jhu.edu/~dks/Science/DecadalWP/index.html`, or by following the links in the PDF version of this White Paper.

we have existing temperature measurements from *Chandra* and *XMM-Newton*. Thus $v_{\rm HOT} \gtrsim c_{\rm s} \sim 360(kT_{\rm X}/0.5\,{\rm keV})^{0.5}\,{\rm km\,s^{-1}}$.

- Observed line-of-sight (LOS) velocities will be lower than the intrinsic velocity, but even in the case of roughly edge-on starbursts (e.g. M82) the geometry typically only decreases the LOS velocity by a factor ~ 2 from the intrinsic velocity (see Fig. 3).

Outflows alter both the mean energy (i.e. the line centroid) and width of the strong emission lines that dominate the soft thermal X-ray emission from superwinds (Fig. 4). We expect LOS line shifts and line broadening in the range several hundred to a thousand kilometers per second, hence requiring measurements accurate to $\lesssim 100\,{\rm km\,s^{-1}}$.

We find that the *IXO* XMS is capable of obtaining high quality X-ray spectra ($> 10^4$ counts) for even the faintest currently known sub-regions of superwinds in reasonable exposures ($t_{\rm exp} \leq 100$ ks). With such spectra we can measure *individual* line centroid shifts with uncertainties $\sigma_{\rm cen} \sim 50 - 100$ km/s (68.3% confidence), and line widths with uncertainties of $\sigma_{\rm FWHM} \sim 100$ km/s (this by fitting all lines in a single spectrum). In fact it is calibration uncertainties that limit the line centroid measurement to a net accuracy of $\sigma_{\rm cen} \sim 50 - 100$ km/s. Note that both line widths and line centroids can be measured accurately to a fraction ($\sim 10\%$) of the nominal instrument resolution of $\Delta E \approx 2.5$ eV (FWHM).

The IXO XMS provides its highest spectral resolution over a 4 arcmin^2 field of view, with a spatial resolution $\sim 5''$. This would allow multiple high-quality spectra from different regions of a nearby superwind to be accumulated simultaneously. This is advantageous as it allows multiple sanity checks on the individual measurements, and the use of position-velocity diagrams to probe possible acceleration or deceleration in the wind (as done in the optical for superwinds, e.g. Shopbell & Bland-Hawthorn 1998).

Observations using *IXO* of a sample of ~ 30 local starbursts, covering a suitably broad range of galaxy mass ($8 \lesssim \log M_{\rm stellar}(\,M_\odot) \lesssim 11.5$, well matched to the local galaxy $M - y_{\rm eff}$ relationship presented in Tremonti et al. 2004), are possible with a net exposure of 1.3 Ms. Such a project will reveal whether starburst galaxies are responsible for IGM enrichment and the galaxy mass-metallicity relationship.

References

Adelberger K.L., et al., 2003. ApJ, 584, 45
Cen R., et al., 2005. ApJ, 635, 86
Chevalier R.A., Clegg A.W., 1985. Nature, 317, 44
Dalcanton J.J., 2007. ApJ, 658, 941
Efstathiou G., 2000. MNRAS, 317, 697
Ferrara A., Tolstoy E., 2000. MNRAS, 313, 291
Grimes J.P., et al., 2005. ApJ, 628, 187
Heckman T.M., et al., 1990. ApJS, 74, 833
Kauffmann G., et al., 1999. MNRAS, 303, 188
Keeney B.A., et al., 2006. AJ, 132, 2496
Lehnert M.D., Heckman T.M., 1996. ApJ, 472, 546
Martin C.L., 2005. ApJ, 621, 227
Martin C.L., et al., 2002. ApJ, 574, 663
Pettini M., et al., 2001. ApJ, 554, 981
Rupke D.S., et al., 2005. ApJS, 160, 87
Scannapieco C., et al., 2008. MNRAS, 389, 1137
Shapley A.E., et al., 2003. ApJ, 588, 65
Shopbell P.L., Bland-Hawthorn J., 1998. ApJ, 493, 129
Simcoe R.A., et al., 2006. ApJ, 637, 648
Songaila A., 1997. ApJ, 490, L1
Strickland D.K., Dinge D.C., in preparation. ApJ
Strickland D.K., Heckman T.M., 2007. ApJ, 658, 258
Strickland D.K., Stevens I.R., 2000. MNRAS, 314, 511
Strickland D.K., et al., 2004a. ApJS, 151, 193
———, 2004b. ApJ, 606, 829
Tremonti C., et al., 2004. ApJ, 613, 989
Tsuru T.G., et al., 2007. PASJ, 59, 269
Tüllmann R., et al., 2006. A&A, 448, 43
Veilleux S., et al., 2005. ARA&A, 43, 769